Active control of shimmy oscillation in aircraft landing gear
Long, Shun Hong
ProQuest Dissertations and Theses; 2007; ProQuest
pg. n/a

Active Control of Shimmy Oscillation in Aircraft Landing Gear

By

Shun Hong Long

A Thesis

In the Department of

Mechanical and Industrial Engineering

Presented in partial fulfillment of the requirements

for the degree of Master of Applied Science at

Concordia University

Montreal, Quebec, Canada

September 2006

©Shun Hong Long, 2006

Reproduced with permission of the copyright owner. Further reproduction prohibited without permission.

Library and Archives Canada

Published Heritage Branch

395 Wellington Street
Ottawa ON K1A 0N4
Canada

Bibliothèque et Archives Canada

Direction du Patrimoine de l'édition

395, rue Wellington
Ottawa ON K1A 0N4
Canada

Your file Votre référence
ISBN: 978-0-494-28942-6
Our file Notre référence
ISBN: 978-0-494-28942-6

NOTICE:
The author has granted a non-exclusive license allowing Library and Archives Canada to reproduce, publish, archive, preserve, conserve, communicate to the public by telecommunication or on the Internet, loan, distribute and sell theses worldwide, for commercial or non-commercial purposes, in microform, paper, electronic and/or any other formats.

The author retains copyright ownership and moral rights in this thesis. Neither the thesis nor substantial extracts from it may be printed or otherwise reproduced without the author's permission.

AVIS:
L'auteur a accordé une licence non exclusive permettant à la Bibliothèque et Archives Canada de reproduire, publier, archiver, sauvegarder, conserver, transmettre au public par télécommunication ou par l'Internet, prêter, distribuer et vendre des thèses partout dans le monde, à des fins commerciales ou autres, sur support microforme, papier, électronique et/ou autres formats.

L'auteur conserve la propriété du droit d'auteur et des droits moraux qui protège cette thèse. Ni la thèse ni des extraits substantiels de celle-ci ne doivent être imprimés ou autrement reproduits sans son autorisation.

In compliance with the Canadian Privacy Act some supporting forms may have been removed from this thesis.

While these forms may be included in the document page count, their removal does not represent any loss of content from the thesis.

Conformément à la loi canadienne sur la protection de la vie privée, quelques formulaires secondaires ont été enlevés de cette thèse.

Bien que ces formulaires aient inclus dans la pagination, il n'y aura aucun contenu manquant.

Canada

Reproduced with permission of the copyright owner. Further reproduction prohibited without permission.

Abstract

Active Control of shimmy oscillation in Aircraft Landing Gear

Shun Hong Long

Shimmy oscillation is an anxious concern in aircraft landing gear design and maintenance. Through related literature review, it is found that active shimmy control (suppressing) is still an open problem. In this thesis, an in-depth analysis has been carried out on aircraft landing gear shimmy dynamics and active control strategy has been developed to suppress shimmy oscillation.

Based on a nominal aircraft landing gear model, its shimmy Limit Cycle Oscillation (LCO) variation with respect to varying parameters has been studied by numerical integration. The shimmy stability variation with varying caster length and taxiing velocity has also been analyzed after linearizing the system. Due to inherent system dynamics uncertainties (such as varying taxiing velocity) and external disturbances (such as rough runway), Robust Model Predictive Control (RMPC) technology is resorted to suppress shimmy during aircraft landing. A new active control strategy has been proposed suitable for online shimmy control application by combining a RMPC control law with a LPV polytope design. The proposed RMPC has been compared with two present RMPCs both in a benchmark example and the landing gear shimmy control. It has been verified by simulation results that the proposed RMPC stabilizes the unstable parameter-varying landing gear system with guaranteed closed-loop stability, high computational efficiency and strong disturbance rejection ability. Related design parameters, mathematical proof and implementation considerations are addressed in this thesis.

Reproduced with permission of the copyright owner. Further reproduction prohibited without permission.

Acknowledgements

I would like to take this opportunity to thank everybody who has helped me during the completion of this research.

I would like to express my profound and sincere appreciation to my supervisor Dr. Wenfang Xie. It is her great patience, broad knowledge and considerable enthusiasm that helped me through the whole research. Her constructive suggestions, thoughtful insights and advices are always beneficial at every stage of my research. I also really appreciate co-supervisor Dr. Rama B. Bhat, who taught me some vibration knowledge and showed me positive research attitude.

I must acknowledge all great fellow students currently and formerly working in room EV-OS2-105 for providing a great place to work for the social and technical assistance, especially Mr. Zheng Li and Mr. Zhongyu Zhao, who helped me develop my understanding on many interesting control topics. I also thank Mr. Ming Yang and Mr. Ping Ding, who once assisted me with related information or materials. In addition, I would like to thank the faculty and stuff working at the Mechanical and Industrial Engineering Department for the excellent learning and research environment.

Finally, I am so grateful to my family. My wife Yan Cui and my lovely daughter Annie Siyu Long, who have been standing by me and always supported me in all of my research endeavors. I feel indebted to my parents, parents-in-law, and brothers, sister in spite of their being physically far from me. Without their constant care and encouragement, I could not have finished my research.

Reproduced with permission of the copyright owner. Further reproduction prohibited without permission.

Table of Contents

Reproduced with permission of the copyright owner. Further reproduction prohibited without permission.

Reproduced with permission of the copyright owner. Further reproduction prohibited without permission.

Reproduced with permission of the copyright owner. Further reproduction prohibited without permission.

List of Figures

Reproduced with permission of the copyright owner. Further reproduction prohibited without permission.

Reproduced with permission of the copyright owner. Further reproduction prohibited without permission.

Reproduced with permission of the copyright owner. Further reproduction prohibited without permission.

List of Tables

Reproduced with permission of the copyright owner. Further reproduction prohibited without permission.

List of Symbols, Abbreviations and Nomenclature

Symbol	Parameters/Variables	Value	Unit
a	Half Contact Length	0.1	m
k	Torsional Spring Rate	10000	Nm/rad
$C_{F\alpha}$	Tire Side Force Derivative	20	1/rad
$C_{M\alpha}$	Tire Aligning Moment Derivative	-2	m/rad
e	Wheel Caster Length	0.1	m
F_y	Tire Side Force		N
F_z	Vertical Force		N
I_z	Moment of Inertia about z-axis	1.0	Kgm^2
c	Torsional Damping Constant	0...100	Nm s/rad
M_1	Spring Moment		Nm
M_2	Damping Moment		Nm
M_3	Total Tire Moment about z-axis		Nm
M_4	Tire Damping Moment		Nm
M_z	Tire Aligning Moment		Nm
V	Taxiing Velocity	0...80	m/s
V_r	Tire Yaw Velocity		m/s
V_t	Tire Sideslip Velocity		m/s
y	Lateral Deflection		m
α	Slip Angle		rad
α_g	Limiting Slip Angle for		10 deg

Reproduced with permission of the copyright owner. Further reproduction prohibited without permission.

	Aligning Moment		(=π/18 rad)
β	The Minimizer in the PRMPC		N/A
γ	The Minimizer in the KRMPC		N/A
δ	Limiting Slip Angle for		5 deg
	Tire Side Force		(=π/36 rad)
κ	Tread Width Moment Constant	-270	Nm^2/rad
σ	Relaxation Length	0.3	m
ψ	Yaw Angle		rad
$\dot{\psi}$	Yaw rate		rad/s

Reproduced with permission of the copyright owner. Further reproduction prohibited without permission.

Abbreviations	Definition
ASME	American Society of Mechanical Engineering
CRMPC	F.A. Cuzzola's RMPC, [33]
DMC	Dynamic Matrix Control
Eqs.	Equations
FIR	Finite Impulse Response
GPC	Generalized Predictive Control
KRMPC	M.V. Kothare's RMPC, [34]
LCO	Limit Cycle Oscillation
LMI	Linear Matrix Inequality
LPV	Linear Parameter Varying
LQG	Linear Quadratic Gaussian
LQR	Linear Quadratic Regulator
LTI	Linear Time Invariant
LTV	Linear Time-Varying
MIMO	Multiple Input Multiple Output
MPC	Model Predictive Matrix
NASA	National Aeronautics and Space Administration
PDLM	Parameter Dependant Lyapunov Matrix
PDM	Positive Definite Matrix
PRMPC	Proposed RMPC in this Thesis
PUS	Polytopic Uncertainty system
RHC	Receding Horizon Control
RMPC	Robust Model Predictive Matrix
SISO	Single Input Single Output

Reproduced with permission of the copyright owner. Further reproduction prohibited without permission.

Nomenclature	**Definition**
A,B,C,D	matrices of continuous system
$A(\theta)$, $B(\theta)$, $C(\theta)$, $D(\theta)$	matrices of system affine on varying parameter θ
A(k),B(k),C(k),D(k)	matrices of discrete system
$Diag(x_1,\ldots x_n)$	diagonal matrix with diagonal elements equal
I_{nxn}	identity matrix(nxn)
Q_w	state weighting matrix
R_w	input weighting matrix
u	control input
u(k+1|k)	predicted next input vector at present instant
V	Lyapunov function $V=x^TPx$
x	system state
x(k)	present state vector
x(k+1)	next state vector
x(k+1|k)	predicted next state vector at present instant
y	system output
y(k)	present output vector
$(.)^T$	transpose of (.)(matrix or vector)
|.|	absolute value of (.)
$\|v\|_2$	Euclidean Norm of vector v ($=\sqrt{v^Tv}$)
$\|v\|_2^2$	Square of Euclidean Norm of vector

Reproduced with permission of the copyright owner. Further reproduction prohibited without permission.

Chapter 1
Introduction

1.1 Landing gear and shimmy history

Landing gear is the structure under an aircraft's fuselage that allows it to land or take off safely and smoothly. This structure usually has wheels and some form of shock absorbing apparatus. At landing or takeoff, the landing gear has to perform the task of absorbing the energy of vertical motion of the aircraft via the shock absorber and the kinetic energy due to horizontal motion by means of the brakes. During taxiing, the landing gear has to carry the aircraft over runways and taxiways with varying quality.

There are two configurations for wheeled aircraft landing gear: taildragger and tricycle. Conventional taildragger landing gear is set up with two wheels near the front of the plane and one smaller taildragger wheel, which is sometimes steerable, at the rear of the airplane, see Figure1-1.

Figure 1-1 Taildragger of Cessna 150 [23]

Reproduced with permission of the copyright owner. Further reproduction prohibited without permission.

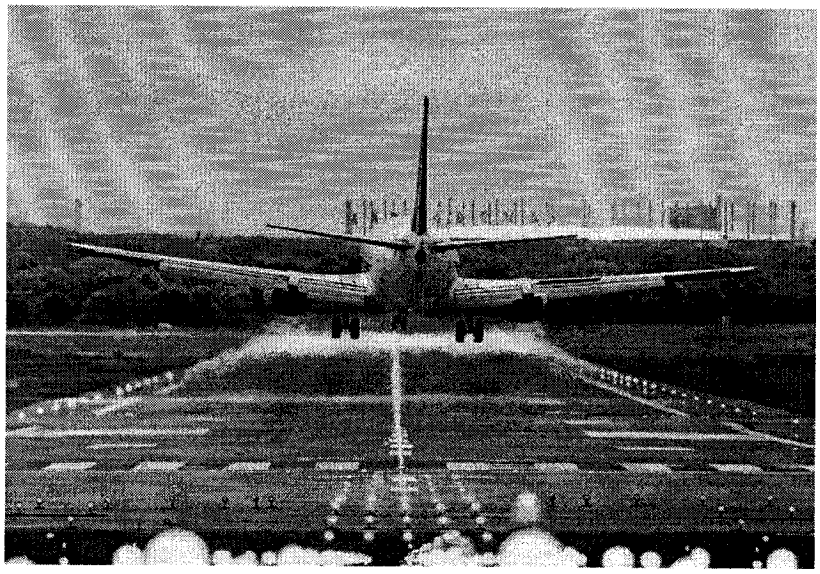

Figure 1-2 Boeing 737-200 in landing, [23]

On the other hand, tricycle landing gear has one steerable nose wheel set near the front of the plane, and a main pair of wheels set approximately under the middle of the wing, which is by far the predominant modern configuration (see Figure1-2).

Both taildragger and tricycle can be found in either a fixed or retractable subtype. An aircraft tricycle configuration consists of a nose landing gear and a left and right main landing gear. Each main landing gear includes an oleo shock strut with two or more wheel and tire assemblies that cushions the landing and keeps the plane level while landing. The main landing gears are often equipped with a brake assembly with anti-skid protection. The main landing gear is retracted forward and up into the left and right lower wing area, and each is enclosed with a single door. The nose landing gear is retractable forward and up into the lower forward fuselage (referring to Appendix G) and is enclosed by two doors located in the lower forward fuselage. In addition, the nose

Reproduced with permission of the copyright owner. Further reproduction prohibited without permission.

landing gear is steerable. The steerable nose landing gear is subject to self-induced lateral and torsional oscillations. This oscillation phenomenon is summarized as "shimmy" for all ground vehicles, especially for aircraft landing gears. In this thesis, research is only limited to nose landing gear in the tricycle configuration.

In the design and development of aircraft landing gear, shimmy test has to be conducted during aircraft taxi-test phase [1]. In extreme cases, shimmy can cause severe damage to landing gear hardware or even severe loss of the aircraft. In less extreme cases, shimmy can be nothing more than an annoyance, but it does affect customer satisfaction and can cause added maintenance expense [9].

. In a 1995 accident investigation report (Report Number A95W0202) of The Transportation Safety Board of Canada (TSB) [73], some accident details are cited as following: The left main landing gear of the Fokker F28-Mk1000 began to shimmy immediately after touchdown when landing at Calgary. Brakes were applied to slow the aircraft in an attempt to control the shimmy, but the oscillations continued until both left main wheels and brake assemblies separated from the axles. After the aircraft came to a stop, the passengers and crew were evacuated without incident through the forward main cabin door. Site examination revealed that the upper torque link failed within the first 200 feet of the landing roll, and the wheels separated about 1,450 feet from touchdown. There was substantial damage to the oleo lower sliding member, wheels, tires, brakes, and left inboard and outboard flaps. Furthermore, it is reported that this accident was the 29th occurrence of this type recorded in the aircraft manufacturer's data base up to that time.

Reproduced with permission of the copyright owner. Further reproduction prohibited without permission.

As early as in 1941, Von Schlippe analyzed the shimmy motion of an aircraft tyre and described the interaction of tyre and landing gear leg stiffness with tyre forces. A wheel is said to be shimmy when it oscillates about its caster axis. Shimmy is caused by the interaction between tyre behaviour and landing gear structural dynamics. In detail, it is caused by a lack of torsional stiffness (structural or fluidic) in the gear, excessive torsional freeplay, inadequate trail (too much or too little) and improper wheel mass balancing or worn parts. A repaired or rough runway often leads to fast parts worn and likely induces shimmy. Shimmy oscillation typically has a frequency in the range of 10 to 30 Hz [1]. The detailed analysis about shimmy formation can be found in [4] and [6].

1.2 Literature review

Aircraft landing gear is a complex multi-degree-of-freedom system. Many early researchers focused on shimmy dynamics analysis and tire modeling, which helped landing gear designers to find optimized structural configuration or search better tire physical parameters [1][10][15][17]. Unlike other system of aircraft (e.g. aircraft engine system), landing gear has been treated as a passive vibration absorber. For purposes of better performance and more comfort to the pilots and passengers, active landing gear concept recently has attracted much attention of researchers [2][3][19].

1.2.1 Shimmy phenomenon

It is found that there are limited landing gear guide books [1][2], not to mention books about landing gear shimmy. It is hard to get any literature concerning systematic

Reproduced with permission of the copyright owner. Further reproduction prohibited without permission.

shimmy analysis or shimmy suppression. Only available references are papers about landing gear dynamics analysis or shimmy analysis [5, 7, 8, 9, 10, 11, 18].

From National Aeronautics and Space Administration (NASA) Langley Research Center, Jocelyn Pritchard launched a valuable shimmy literature survey in 1999 [4], which was originated from the NASA safe air travel initiative. The initiative gained increasing interest in improving landing gear design to minimize shimmy and brake-induced vibration. The major focus of survey was to summarize and document previous works to highlight the latest efforts in solving vibration problems and to reveal a variety of analyses, testing, modeling, and simulation of aircraft landing gear.

In a doctoral dissertation [9], two analytical landing gear shimmy models were proposed: a nonlinear model and a linear Finite Element Model, which were numerically simulated and analyzed by standard eigenvalue techniques. A test running with the two models showed good correlation and illustrated the effects of changes to various parameters. W. Kruger et al [6] presented three software packages, which were used in the numerical simulation of aircraft ground dynamics and gave an overview of landing gear design requirements including shimmy stability.

In [15], a set of parameters for accurate prediction of shimmy stability of landing gears are suggested and the stability maps of a typical landing gear varying with changes in tire parameters are also shown.

Der Valk Gordon presented a mathematical model in [10] to analyze the stability of a two-wheeled landing gear and its failure. The model was validated by ground vibration

Reproduced with permission of the copyright owner. Further reproduction prohibited without permission.

tests and aircraft taxi test. Finally, it was concluded that any two-wheeled 'F.28 like' landing gear is unstable and an apex shimmy damper is needed as a remedy for shimmy oscillation. In addition, a perturbation analysis for simple landing gear shimmy model with nonlinear terms of coulomb friction and freeplay was presented by J. T. Gordon in [18] and the analysis results were shown to be in good agreement with direct numerical integration results. Other papers [5] [7][8] are focused on shimmy modeling and stability boundaries analysis.

1.2.2 Tire modeling

An important and difficult part of shimmy modeling is the tire modeling, which has a longer history compared to shimmy modeling. Strictly speaking, tire modeling may be classified into three separate categories: tire mechanical properties, tire stresses and tire temperatures [71]. In this thesis, only mechanical properties are considered.

In the 1950s, two basic analytical tire modeling theories were suggested for determining the forces on a wheel due to tire deflections: the stretched string theory by Von Schlippe-Dietrich [12] and the point contact theory by Moreland [13]. Another well-known Pacejka Model [14] is thought to be an extended string theory. In the stretched string theory, the tire is approximated by an elastic string, which is stretched about the outer edge of a wheel at the tire radius and attached to it by elastic springs. For point contact theory, tire inertia and the effect of the finite length of the contact patch are neglected. Hence the tire is thought as a single point contact with the ground. The contact point may move with respect to the ground in lateral and longitudinal

Reproduced with permission of the copyright owner. Further reproduction prohibited without permission.

directions. These two theories are still used in today's most publications about shimmy analysis. L.C. Rogers claimed in 1972 that considering the small tire deformation, these two classical tire models are equivalent and give similar results for shimmy analysis if the involved tire parameters are properly selected [17].

Based on the comparison of experimental data and the theoretical curves from string model, the equations relating ground force and torque on the tire to arbitrary angle and lateral deflection are provided in [17]. Furthermore, some objections were found in [17], such as non-agreement between the physics of Moreland model and experimental frequency response curves. In the same paper, it was thought that Pacejka's theory is too cumbersome for direct use in tire dynamic studies.

In [16], two tire equations relating tire forces to wheel yaw angle and lateral displacement were developed from tire frequency response data to calculate transient tire forces. These two tire models were said to have advantage of being more accurate than existing tire theories with relatively simple form provided that the limitation of small slip angles is not exceeded.

1.2.3 Shimmy damping

For the earlier aircrafts, there were no extra shimmy damping equipments installed. Although shimmy phenomenon was observed and analyzed, how to suppress shimmy oscillation effectively and actively remains a challenge. In France and Germany, landing gear shimmy was treated as a problem that should be dealt with early in the design stage.

Reproduced with permission of the copyright owner. Further reproduction prohibited without permission.

On the contrary, in the United States, the general tendency was to fix this problem after it had occurred [4].

Shimmy can occur in the main landing gear or nose landing gear, but nose wheel shimmy is more common. Nose wheel shimmy is an oscillatory motion that could be brought on by runway surface irregularities, non-uniformity of the tire or other factors. It is further exaggerated by worn landing gear components that allow significant play in the linkages.

Current shimmy suppressing methods are shimmy damper as in Figure1-3 (zoom-in view in Figure1-4) and structural damping in Figure1-5.

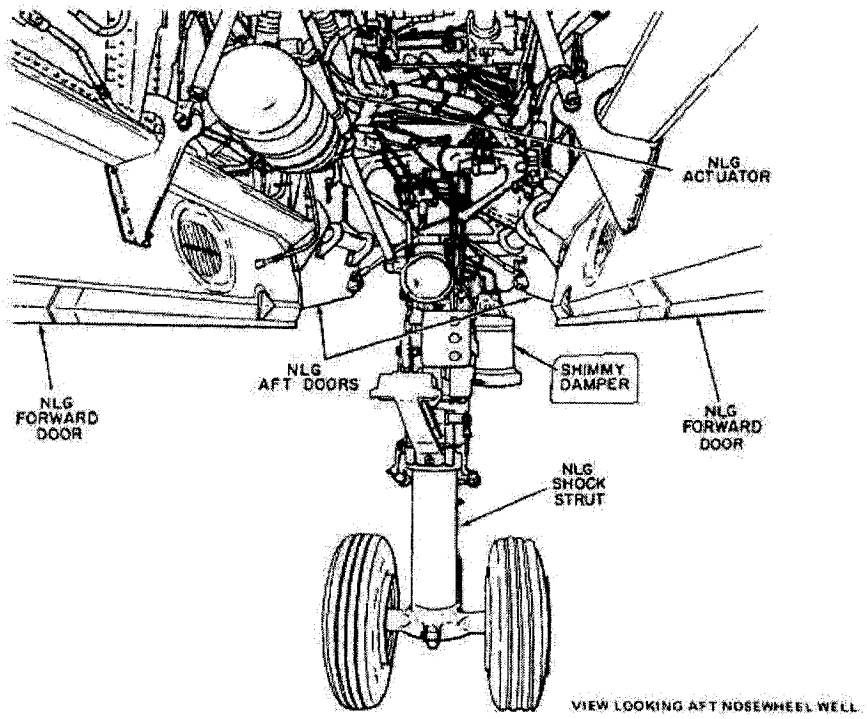

Figure 1-3 Shimmy damper in the Nose-wheel well (aft view), [68]

Reproduced with permission of the copyright owner. Further reproduction prohibited without permission.

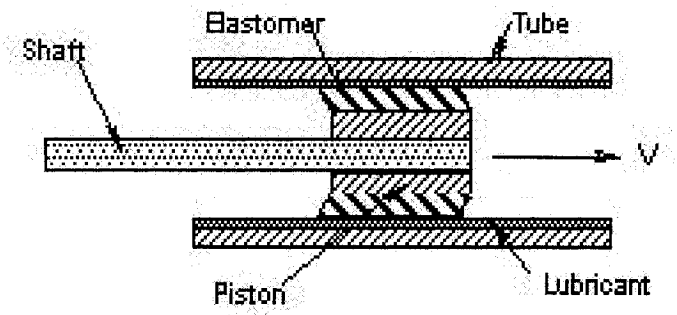

Figure 1-4 General schematic of shimmy damper

The shimmy damper is a device that is used to reduce the effects of shimmy by restraining the movement of the nose wheel, or in detail, by reducing the amplitude and/or by preventing the onset of the shimmy limit cycle. The shimmy damper allows the wheel to be steered by moving it slowly, but does not allow the wheel to move back and forth rapidly. This device consists of a hollow tube filled with hydraulic fluid with a shaft and piston that cause velocity dependent viscous damping forces to be generated when moved through the fluid, see Figure1-4.

Some disadvantages are found in the current shimmy damper. One such problem is the need for frequent maintenance. Increasing temperature causes the hydraulic fluid to expand and to leak past the seals thereby reducing the damping efficiency of the device. This problem has been known to occur even after only 100 hours of operation. Maintenance costs associated with this were sometimes found unacceptable, so were the replacement costs. It is reported that the new-generation shimmy damper uses surface-effect technology to absorb nose wheel vibration and provide consistent damping without much maintenance.

Reproduced with permission of the copyright owner. Further reproduction prohibited without permission.

On the other hand, commonly used structural damping is referred to as hydraulic shimmy damping as described in [1], and reprinted in Figure1-5. Here, shimmy damping is obtained in steering system by restricting motion in the steering actuator. The one-way restrictor ensures oil to go forward smoothly and come backward with restriction to suppress some external disturbances, which tends to induce shimmy oscillation. Check valve is a purely one-way valve. The self-centering steering actuator does help keep the wheel alignment. Other shimmy damping methods in terms of design consideration could be co-rotating wheels, an appropriate amount of trail (the distance that the wheel centers are behind the shock strut centerline) or canting the nose gear [1].

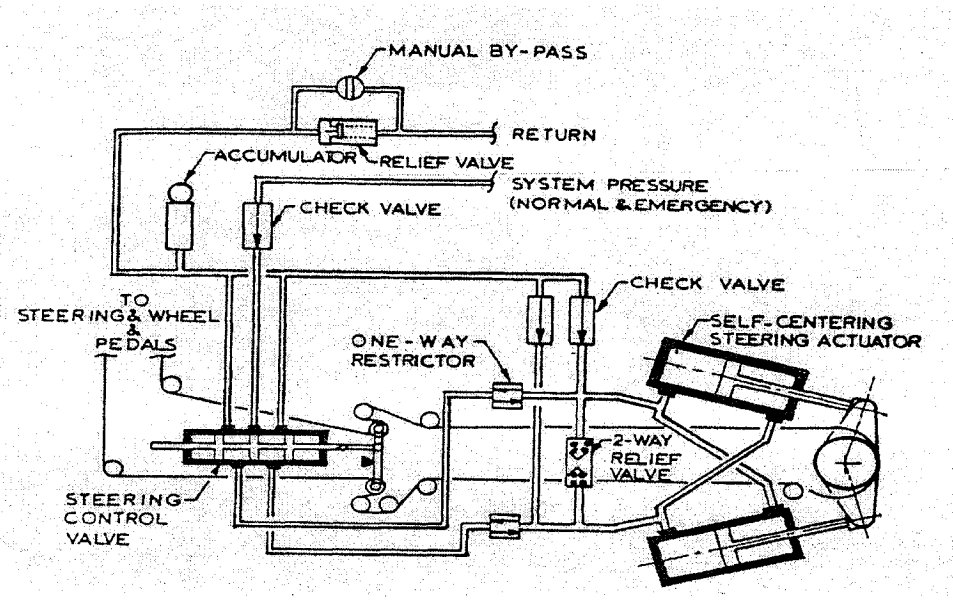

Figure 1-5 Hydraulic steering system with shimmy damping, [1]

1.2.4 Actively controlled landing gear

Although current shimmy oscillation damping of landing gear is based on passive mechanical or hydraulic shimmy damping, active control concept presents a possibility

Reproduced with permission of the copyright owner. Further reproduction prohibited without permission.

of improved control effect and widened aircraft operation range. In the last 10 years, the active or semi-active vertical vibration control for landing gear has attracted the attention of some researchers and has shown some advantages. An example of control design for aircraft landing gear vertical vibration elimination is described in dissertation [19]. In this dissertation, the active control is compared to semi-active control on aircraft suspension system and it is pointed out that semi-active landing gear does not need large external power supply and its implementation is simpler and more practical. Nevertheless, in NASA Report [3], L. G. Horta et al started from a simplified model of main landing gear of Navy A6 Intruder and implemented an external servo-hydraulic system for active control in vertical damping (Figure1-5 and Figure1-6). Because the landing gear test was time-consuming and very expensive, this kind of active control test was not found in literatures for landing gear before. The control algorithm in [3] was common PID feedback control. They successfully developed a facility to test various active landing gear control concepts and their performance and demonstrated that fuselage vertical vibration level was reduced by a factor of 4 by experiments in case of landing. However, it is not reduced to zero. This was inspiring news for those researchers who are interested in actively controlled landing gear. Although the landing gear active control was restricted to vertical damping and active suspension in [3], the extension of active concept to landing gear shimmy control is proved to be possible or at least theoretically possible in the latter chapters of this thesis.

Reproduced with permission of the copyright owner. Further reproduction prohibited without permission.

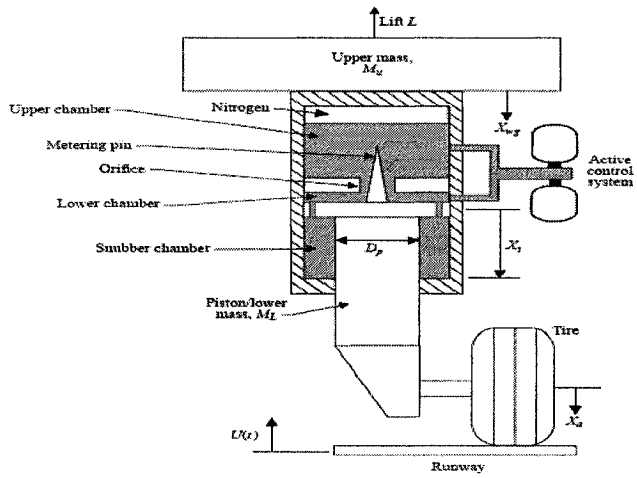

Figure 1-6 Schematic of NASA actively controlled landing gear, [3]

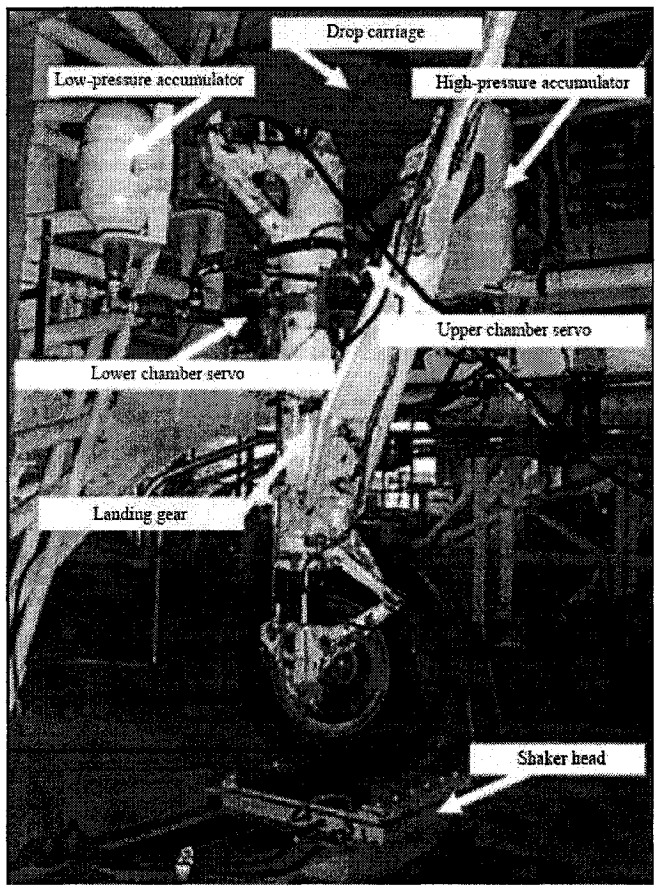

Figure 1-7 Test setup of NASA actively controlled landing gear system, [3]

Reproduced with permission of the copyright owner. Further reproduction prohibited without permission.

The problem of stabilizing a system with changing dynamics was investigated and a straight forward switching scheme by Lyapunov Function was applied to a shimmying wheel resulting from switches between sliding and rolling in [20]. W. Kruger presented a multi-body aircraft simulation model in [22], and designed three control laws for semi-active aircraft landing gears. Simulation results were compared among passive, fully active, and semi-active systems. In [21], B. Goodwine considered the design of nonlinear stabilizing controllers for a system with unstable rolling dynamics using nonlinear feedback linearization technique. Such system was suggested to be used to approximate the complex dynamics of an aircraft landing gear structure and related three controllers were designed to stabilize three different simplified models of the system.

1.2.5 MPC application to shimmy suppressing

Model Predictive Control (MPC) or Receding Horizon Control (RHC) started from the end of 1970s. MPC essentially solves standard optimal control problems and differs from other controllers in that it solves the optimal control problem online for the current state of plant, rather than determining an optimal feedback strategy offline.

MPC usually contains the following three ideas according to [26]:

- Explicit use of a model to predict the process output along a future time horizon.
- Calculation of a control sequence to optimize a performance index
- Use of a receding horizon strategy so that at each instant the horizon is moved towards the future and the first control signal of the sequence calculated at each step is applied to the plant.

Reproduced with permission of the copyright owner. Further reproduction prohibited without permission.

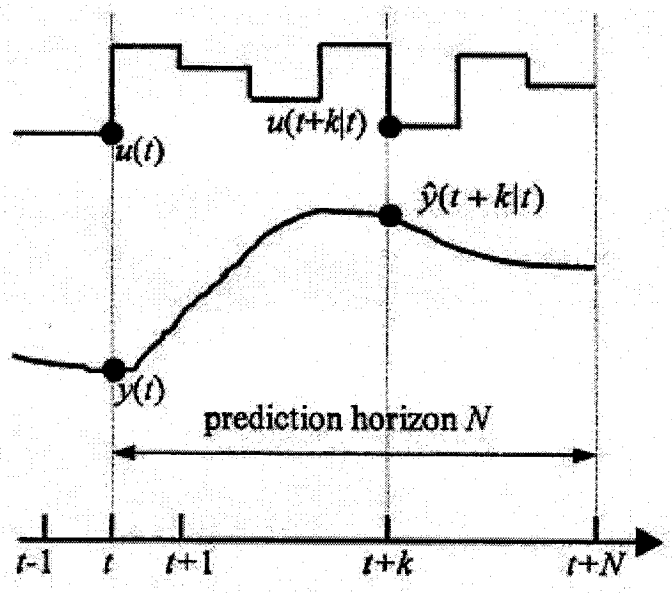

Figure 1-8 Strategy of Model Predictive Control, [26]

As illustrated in Figure1-8, the future outputs $\hat{y}(t+k \mid t)$ is predicted at each instant t using the process model. $y(t+k|t)$ means future output at instant $t+k$ predicted at current instant based on future reference and future control sequence $u(t+k|t)$ ($k=0,...N-1$, N is the prediction horizon). The future control sequence $u(t)$ $...u(t+k|t)$ is calculated by optimizing a determined criterion to keep the output as close as possible to the reference trajectory, but only the first $u(t+1)$ is sent to the plant. At next instant, the $u(t+1|t+1)$ is calculated and applied again, normally different from $u(t+1|t)$ because the new information is available. So MPC uses the receding horizon concept and it's an iterative optimization.

The most popular MPC algorithms are DMC and GPC. DMC uses an impulse response model, which is valid only for open-loop stable processes, and minimizes the variance of the error between the output and a reference trajectory. For GPC, quadratic

Reproduced with permission of the copyright owner. Further reproduction prohibited without permission.

performance function is used to calculate a sequence of future control signals in such a way that it minimizes a multi-stage cost function defined over a prediction horizon with weighting of control effort and a Controller Auto-Regressive Moving-Average (CARMA) model. GPC also provides an analytic solution for the optimal control in the absence of constraints.

Nonlinear model predictive control based on state space models and the receding horizon concept had also been developed, for example by Mayne and Michalska (1993) [34], who constructed a robust dual-mode receding horizon controller for nonlinear systems with state and control constraints.

In recent years, many commercial MPC products have been developed and available from vendors: SMOC (MDC Company), CONNOISSEUR (Simulation Sciences), DMCplus (AspenTech) and RMPCT (Honeywell), 3dMPC (ABB). Most of them are designed for the needs of the process industries, especially in the petrochemical sector.

The reason why MPC is chosen for landing gear shimmy suppressing is based on three points:

(1) MPC is a mature and advanced control technology, which has wide-spread applications in diverse industries. It was first applied in the petrochemical industry and currently is extended to different fields. According to [25], MPC is the only advanced control methodology which has made a significant impact on industrial control engineering and is more advanced than standard PID control.

Reproduced with permission of the copyright owner. Further reproduction prohibited without permission.

(2) MPC has many advantages compared to conventional control technology, such as its tunability and explicitly incorporating various constraints. MPC is said to be the only generic control technology which can deal routinely with equipment and safety constraints [25].

(3) Some related MPC research explorations have been successfully extended to application examples. MPC was applied to automobile orientation control, such as vehicle maneuvering control in [66]. Also in [69], side slip control to vehicle lateral orientation was realized by direct yaw moment, which indirectly demonstrated the possibility of direct yaw moment control to aircraft landing gear shimmy suppressing.

1.2.6 RMPC review

Normally, the standard MPC process is composed of three steps: future output prediction, objective function optimization and control signal implementation. The accuracy in these three steps is highly dependent on the model precision. Model uncertainty arises when system parameters are not precisely known, or may vary over a given range. In extreme cases, a small parameter perturbation may lead to constraint violation or system being unstable. As pointed out in [34], the primary disadvantage of current design techniques of MPC is their inability to deal explicitly with plant model uncertainty.

Robust Control is a synthesis that optimizes worst-case performance specification and identifies worst-case parameters as long as the variation of plant remains in some specified sets. In 1996, M. V. Kothare et al first developed a new RMPC using LMIs

Reproduced with permission of the copyright owner. Further reproduction prohibited without permission.

[34] (simplified as KRMPC in this thesis). The main contribution was that Min-Max robust control was reduced to a convex optimization, which dramatically decreased the computational complexity and increased the implementation efficiency. Since then, KRMPC has drawn considerable attention from robust control and MPC control research community. The works related to RMPC are summarized into three fields:

- Derivation of less conservative robust conditions [33, 38, 42, 54, 61]
- Extend RMPC into nonlinear system control [44, 47, 55]
- Extend RMPC into off-line LMIs [45, 50, 56, 63].
- Other performance improvement [32, 46, 48, 54, 59]

Despite the fact that some researchers used Min-Max robust strategy, such as A. Casavola in [43] and R. Ramirez in [64], others worked on special aspects of RMPC. For example, H. Fukushima employed closed-loop prediction to RMPC [60] ; Sheng Yunlong developed a dual-mode control scheme in [52]; D. Q. Mayne designed an output feedback RMPC in [65]. One of the shortcomings of KRMPC is the computation inefficiency if it is applied to online control according [39, 62].

1.3 Motivation and challenge

From section 1.2, it has been demonstrated that there are more shimmy analysis than shimmy active control design in the previous literatures. Although landing gear shimmy is often overlooked, shimmy can cause catastrophic damage in some extreme cases. To the author's knowledge, active shimmy control is still an open problem. Although the shimmy suppressing measures based on landing gear structural design are effective to some extent, the extension of active landing gear concept to shimmy control is very

Reproduced with permission of the copyright owner. Further reproduction prohibited without permission.

attractive in terms of the flexibility and reliability of control strategy design and effectiveness of shimmy suppressing.

As mentioned in [4], shimmy damping (mechanical or hydraulic) requirement is often in conflict with good high-speed directional control. Furthermore, once the landing gear design is done, those elaborate structural parameters for shimmy suppressing can neither be changed nor adapted to some new changes. When external disturbance (rough runway, crosswind or severe climate) or uncertain parameter variations (due to worn parts or other uncertain factors) occurs in landing gear system, it is hard to take any further actions. In such unexpected operation situations (worn parts and rough runway), active control strategy works effectively whenever shimmy occurs. With the advent of high speed and high reliable microprocessor used in controller implementation, the idea of actively controlled landing gear has gained new momentum. Landing gear shimmy dynamics varies greatly with taxiing velocity, which will be explained in Chapter 2. A velocity-dependent controller can not be obtained by the conventional constant feedback control, such as LQR control, which is often applied in LTI system.

The challenges for developing actively shimmy-suppressed landing gear are summarized in two folds.

(1) Complexity of landing gear shimmy dynamics and modeling.

Complex landing gear configuration and tire modeling, including nonlinear factors in tire and mechanical parts introduce the complexity of landing gear modeling. Aircraft landing gear normally tends to be rather heavy and bulky, so its test is time-consuming

Reproduced with permission of the copyright owner. Further reproduction prohibited without permission.

and expensive. Those physical parameters of landing gear are hard to be measured and related test data are not easy to be collected. Due to the difficult and costly landing gear test, it is hard to make shimmy dynamics analysis and build the model, or to even verify the landing gear shimmy control effects by the corresponding tests. It is reported that one of the major landing gear test facilities in United States is at NASA Langley research center.

(2) Computational load of RMPC to online shimmy suppressing application

Very limited literature is found on shimmy dynamics analysis and control. Considering the online control application, RMPC should be computation-efficient with the ensured capability of robust stability and disturbance rejection.

1.4 Thesis contributions

The main contributions of this thesis are summarized as follows:

(1) Shimmy dynamics analysis and parametric variation effects on shimmy

A landing gear shimmy model, along with a tire model is formulated and analyzed for deeper insight on shimmy dynamics. Simulation results show the existence of Limit Cycle Oscillations (LCO) in the landing gear dynamical response. The effects of torsional damping constant and taxiing velocity on shimmy dynamics variation are simulated and analyzed. Shimmy stability variation with respect to caster length and taxiing velocity are also investigated.

(2) A new active control strategy on shimmy suppressing of landing gear

Reproduced with permission of the copyright owner. Further reproduction prohibited without permission.

A theoretical exploration of applying RMPC to landing gear shimmy suppression has been carried out in this research. Through literature survey, it is found that many researchers worked on landing gear shimmy modeling and dynamics analysis, which are directly useful in landing gear design improvement. But there were few people working on active shimmy control despite there were some researches working on active suspension control. Application of RMPC to landing gear shimmy suppression is new, and it can help in the development of next-generation actively controlled aircraft landing gear. The details related to RMPC design (such as control algorithm realization, controller parameter tuning) and system implementation issues (such as integration into present control systems, conceptual choice of sensors and actuators) are also discussed.

(3)A combined LPV-RMPC synthesis procedure is proposed for LPV system

After linearizing nonlinear landing gear equations, a combined LPV-RMPC synthesis is proposed to achieve landing gear shimmy suppression during aircraft landing or taking off. By this synthesis, a taxiing velocity-dependent robust controller is designed to guarantee asymptotic stability of the closed-loop LPV system. But without introduction of LPV polytope construction in this synthesis, RMPC is not ready to be employed because the convex optimization is not guaranteed if this optimization is not executed in a convex set. After this convex polytope design, the time-varying state feedback gain is calculated online from a set of LMIs, which can be readily solved using known LMI solvers, such as Matlab LMI-Lab, YALMIP, or SeDuMi et al. Furthermore, the results are extended to the more general case of parameter varying system with

Reproduced with permission of the copyright owner. Further reproduction prohibited without permission.

external disturbance, such as rough runway. This synthesis approach can be applied to other similar systems.

(4) The proposed new RMPC algorithm improves computational efficiency

Compared with any of the present modified algorithms on RMPC, the proposed new RMPC algorithm (PRMPC) is simpler and easier to implement. This new RMPC synthesis is not only compared with two present RMPCs in the two-mass-spring example but also compared with the application of landing gear shimmy suppression. In these online control applications, the improvement on computational efficiency is significant along with guaranteed robust stability. The simulation results confirm the effectiveness of control algorithm. After the introduction of concepts of invariant ellipsoid and contracted Positive Definite Matrix (PDM), the theoretical stability is emphasized by related mathematical proof.

1.5 Thesis outline

This thesis is organized as follows. Chapter 1 introduces landing gear shimmy phenomenon and Model Predictive Control. The literature review of tire modelling, shimmy analysis and active landing gear control is given. Chapter 2 describes a typical landing gear shimmy model. Related equations for the landing gear shimmy dynamics and modeling are given. In the simulations, it has been shown what causes shimmy oscillations and how shimmy stability varies with parameters, especially its dynamics variation with respect to the taxiing velocity. A new Robust Model Predictive Control synthesis is proposed in Chapter 3. This new PRMPC is compared with two known

Reproduced with permission of the copyright owner. Further reproduction prohibited without permission.

KRMPC and CRMPC in a two-mass-spring example. Conventional LQR control is also applied and compared with these three RMPCs. In Chapter 4, active shimmy control design is described in detail, ranging from control objective, LPV polytope design, control system design, controller scheme, to simulation results. Related design parameters and implementation considerations are addressed for reference. Finally, conclusions and future work are given in the last chapter.

Reproduced with permission of the copyright owner. Further reproduction prohibited without permission.

Chapter 2
Landing Gear Shimmy Dynamics and Modeling

According to Pacejka in [70], shimmy is due to a conversion of forward motion kinetic energy to self-excitation energy. When the defective landing gear is taxiing on runway, even with little external disturbance, the oscillation tends to occur. When this oscillation grows up, the unstable landing gear experiences damage. Sometimes when the instability grows to some amplitude, the nonlinear effects limit the oscillations to remain within some response envelope. This kind of oscillation is the so-called Limit Cycle Oscillation (LCO). The shimmy LCO will be observed and analyzed in the later sections.

2.1 Landing gear shimmy modeling

Despite many attempts to employ different types of shimmy dampers for shimmy suppression, little was known about the cause of shimmy [6]. Shimmy modeling was considered to be as complex as dynamics of aircraft landing gear. In [5], Gerhard Somieski proposed a nonlinear nose landing gear shimmy model with landing gear torsional motion description and stretched string tire modeling theory. This model is a simplified model built by first-principle, which is described in [5] and redrawn in Figure2-1. In practice, this model stands for one single nose landing gear on a light aircraft, which is steerable.

Reproduced with permission of the copyright owner. Further reproduction prohibited without permission.

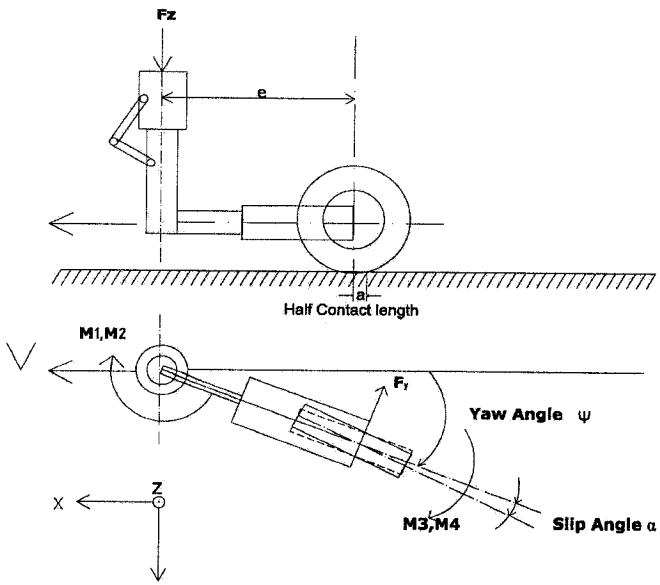

Figure 2-1 Side view and top view of landing gear model

The nonlinear shimmy dynamics equations are developed using Figure 2-1.The values and physical meanings of all parameters in equations are outlined in the List of Symbols. The related terminology of landing gear is listed in the Appendix F.

2.1.1 Torsional dynamics

The following equation (2-1) describes the torsional dynamics of the lower parts of the landing gear [5] with ψ as Yaw Angle. It is derived from Newton's Second Law for rotational motion.

$$I_z \ddot{\psi} = M_1 + M_2 + M_3 + M_4 + M_5 \tag{2-1}$$

where I_z is Moment of Inertia about z-axis.

M_1 is a linear spring torque between the turning tube and the torque link:

Reproduced with permission of the copyright owner. Further reproduction prohibited without permission.

$$M_1 = k\psi, \tag{2-2}$$

where k is torsional spring rate.

M_2 accounts for combined damping moment from viscous friction in the bearings of the oil-pneumatic shock absorber and from shimmy damper:

$$M_2 = c\dot{\psi}, \tag{2-3}$$

where c is torsional damping constant.

M_3 is tire moment and is composed of M_z (tire aligning moment about tire's center) and tire cornering moment eF_y :

$$M_3 = M_z - eF_y \tag{2-4}$$

where F_y is wheel cornering force and e is caster length (as lever arm), referring to Figure 2-1. F_y and M_z depend on vertical force F_z and side slip angle α, which shows nonlinear tire sideslip characteristics, as in following Figure 2-2 (a).

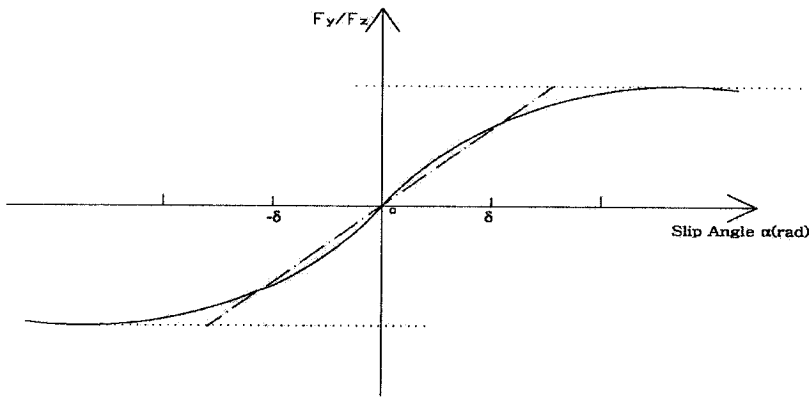

Figure 2-2 (a) Nonlinear F_y/F_z vs. side slip angle

Reproduced with permission of the copyright owner. Further reproduction prohibited without permission.

The forces F_y and F_z have the relation:

$$F_y / F_z = C_{F\alpha}\alpha, \qquad \text{for } |\alpha| \le \delta \tag{2-5}$$

$$F_y / F_z = C_{F\alpha}\delta sign(\alpha), \text{ for } |\alpha| > \delta \tag{2-6}$$

where δ is limit angle of tire force. In Equation (2-6), $sign(\alpha)$ is a sign function, which means

$$sign(\alpha) = \begin{cases} 1, & if \quad \alpha > \delta \\ -1, & if \quad \alpha \le \delta \end{cases} \tag{2-7}$$

The nonlinear tire sideslip characteristic was proposed by Pacejka in the form of following well-known "Magic Formula" [70], one of them is expressed as following.

$$F_y = D\sin[C\arctan\{B\alpha - E(B\alpha - \arctan(B\alpha))\}] \tag{2-8}$$

where variables B, C, D and E are functions of the wheel load, slip angle, slip ratio and camber. C is the shape factor; D is the peak value of the curve; B and E are coefficients related to vertical force Fz.

"Magic Formula" is widely used for both automobile tire modeling and landing gear tire modeling, such as in [5], [6] and [9]. According to "Magic Formula", the plot of F_y/F_z vs. side slip angle α is shown in Figure 2-2 (b).

Reproduced with permission of the copyright owner. Further reproduction prohibited without permission.

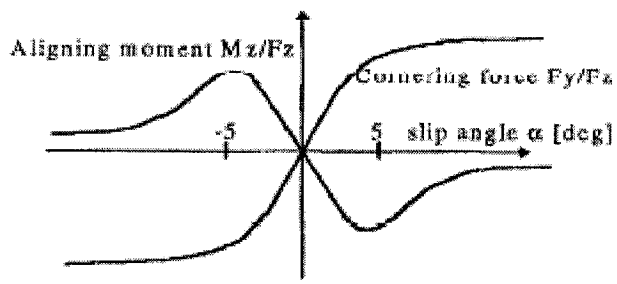

Figure 2-3 (b) Nonlinear F_y/F_z vs. side slip in "Magic Formula", [5]

It is found that both Figure 2-2 (a) and (b) share similar nonlinear side slip characteristic. Therefore, instead of complicated "Magic Formula", (2-5) and (2-6) are used as simplified approximation but still realistic [5]. As shown in the Figure2-2 (a), the function of F_y/F_z is approximated by linear function (2-5) (the blue dash-dot line in Figure 2-2 (a)) and saturation function (2-6).

M_z/F_z is approximated by a sinusoidal function and constant zero, respectively. Its mathematical expression is shown as the following equations (2-9) and the plot M_z/F_z vs. α is shown in Figure 2-3.

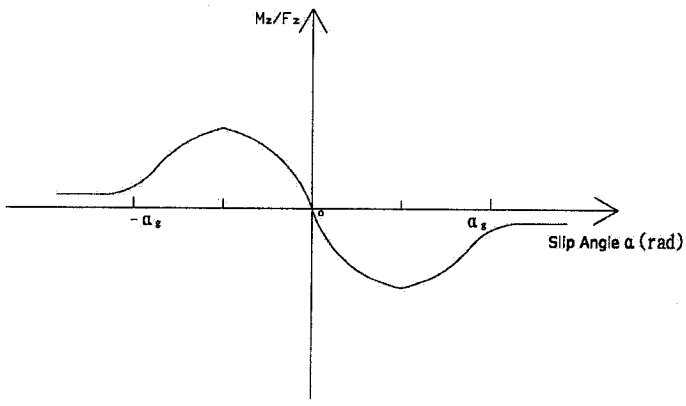

Figure 2-4 Nonlinear M_z/F_z vs. side slip angle, [5]

Reproduced with permission of the copyright owner. Further reproduction prohibited without permission.

$$M_z / F_z = C_{M\alpha} \frac{\alpha_g}{180} \sin(\frac{180}{\alpha_g}\alpha), for|\alpha| \le \alpha_g \quad (2\text{-}9)$$

$$M_z / F_z = 0, \qquad for|\alpha| > \alpha_g$$

$$M_4 = \frac{\kappa}{V}\dot{\psi} \quad (2\text{-}10)$$

where M_4 is the tire damping moment from tire tread width, which depends on taxiing velocity V and yaw rate $\dot{\psi}$, κ is tread width moment constant.

M_5 is introduced for the controller design, which is the control force/torque for shimmy elimination. It is assumed that when applying external force/torque to steer the landing gear, the landing gear will respond to some yaw angle.

$$M_5 = k_e u \quad (2\text{-}11)$$

where k_e is the moment constant related to the external control torque and u is the control signal from external actuator.

The stability analysis in the following sections is conducted based on the autonomous dynamics of landing gear (i.e. $M_5 = 0$).

2.1.2 Tire motion equation

Elastic string theory is used in modeling the tire. The equation of tire motion is given in (2-10) as in paper [5].

$$\dot{y} + \frac{V}{\sigma} y = V\psi + (e-a)\dot{\psi} \quad (2\text{-}10)$$

Reproduced with permission of the copyright owner. Further reproduction prohibited without permission.

The formation of a slip angle may result from either of two fundamental motions, i.e., pure yaw or pure sideslip. A tire rolls in pure yaw only when the yaw angle ψ is allowed to vary and the lateral deflection y is held at zero. To the contrary, in pure sideslip, the lateral deflection varies as the yaw angle is held at zero.

The deflection of tire is due to ground forces acting on the tire footprint, and these ground forces (or moments) are transmitted through the tire to the wheel. According to elastic string theory, the lateral deflection y of the leading contact point of tire with respect to tire plane can be described as a first order differential equation with time constant and $\tau = \frac{\sigma}{V}$ [5]. σ is relaxation length, which is defined as the ratio of the slip stiffness to longitudinal force stiffness. Tire sideslip velocity V_t can be expressed as (2-11).

$$V_t = \dot{y} + \frac{y}{\tau} \quad . \tag{2-11}$$

Meanwhile, the tire undergoes yaw motion, which leads to yaw velocity V_r. V_r is similar to V_t, which can be approximated as (2-12) [12] [14]

$$V_r = V\psi + (e-a)\dot{\psi} \quad . \tag{2-12}$$

When wheel rolls on the ground, the following equation should be satisfied.

$$V_t = V_r \tag{2-13}$$

Substituting (2-12) and (2-11) into (2-13), one can obtain (2-10).

Reproduced with permission of the copyright owner. Further reproduction prohibited without permission.

Furthermore, an equivalent side slip angle caused by lateral deflection is approximated as following (2-14).

$$\alpha \approx \arctan\alpha = \frac{y}{\sigma} \tag{2-14}$$

Eqs. (2-1), (2-10) and (2-14) form the full set of landing gear motion equations, in which nonlinear tire force and tire moment are included. Note that in the equation **Error! Reference source not found.**, $\kappa = -0.15a^2 C_{F\alpha} F_z$.

2.2 . Shimmy dynamics variation

In this study, a light aircraft with one nose landing gear is considered. The related parameters and values of this landing gear are shown in the List of Symbols. It is very hard to obtain the analytical solution to nonlinear differential equations (2-1) and (2-10). But if applying numerical integration to (2-1) and (2-10), the equations can be solved with respect to time.

Table 2-1 Numerical integration parameters

Integration method	Fixed-step Fourth-order Runge-Kutta
Fixed-step size	0.001
Simulation staring time	0 second
Simulation ending time	3 seconds

Reproduced with permission of the copyright owner. Further reproduction prohibited without permission.

Two initial values of disturbed yaw angle (1 rad and 0.1 rad, respectively) are compared and analyzed. Torsional damping constant is set to 10 Nm s/rad (low limit) and 100 Nm s/rad (high limit). Taxiing velocity is varying from 80 m/s to 20m/s. The numerical integration parameters are listed in the above Table 2-1.

2.2.1 Damping constant effect

Torsional damping constant c in the equation (2-3) is an important parameter in the landing gear design and also critical for shimmy oscillation analysis. In this section, the simulation parameters are set as: taxiing velocity 80 m/s, the initial disturbed yaw angle 1 radian, and torsional damping constant varying from 10, 20, 30, 50 to 100 Nm s/rad respectively and simulation time is set as 3 seconds.

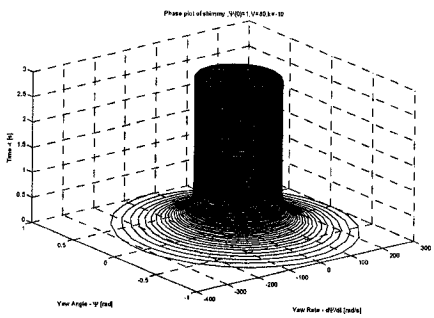

Figure 2-5 Phase plot of yaw angle

$(\psi(0) = 1rad, V = 80m/s, c = 10Nms/rad)$

As demonstrated in Figure2-4, when torsional damping constant is set to 10 Nm s/rad (weak damping), there exists obvious LCOs. But with increasing torsional damping constant, the shimmy oscillation becomes smaller and weaker in Figure2-5 to Figure 2-8. When the torsional damping constant is set to 100 Nm s/rad (very strong damping, but

Reproduced with permission of the copyright owner. Further reproduction prohibited without permission.

impossible to make it in practice), the yaw angle of landing gear quickly converges to near 0. In summary, the increase of the torsional damping constant helps suppress the shimmy.

Furthermore, a boundary torsional damping constant value 39.5 Nm s/rad is observed. When torsional damping constant is bigger than 39.5 Nm s/rad, the shimmy oscillation is not obvious in this situation, as in Figure2-9. Please note that the taxiing velocity is a constant in the below simulations.

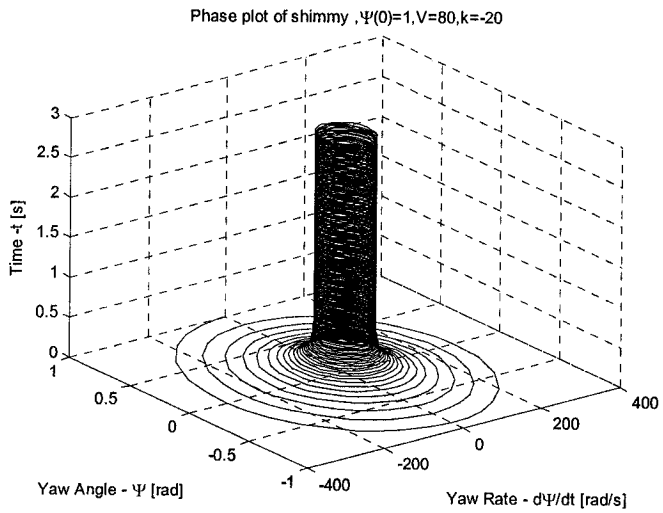

Figure 2-6 Phase plot of yaw angle

$(\psi(0) = 1rad, V = 80m/s, c = 20Nms/rad)$

Reproduced with permission of the copyright owner. Further reproduction prohibited without permission.

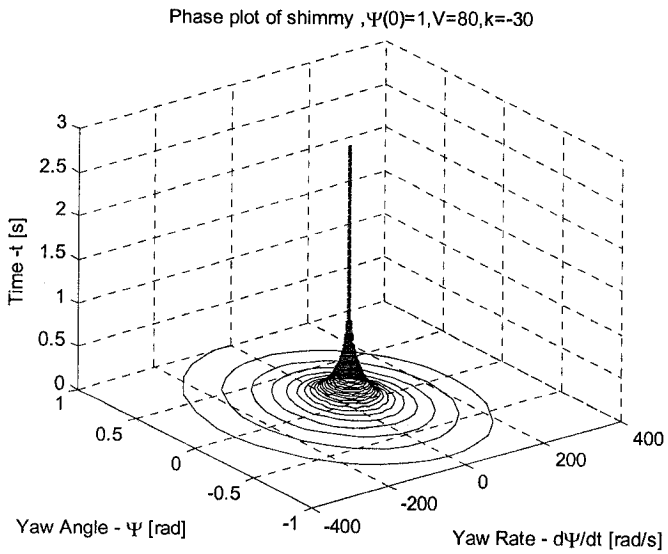

Figure 2-7 Phase plot of yaw angle

$(\psi(0) = 1rad, V = 80m/s, c = 30Nms/rad)$

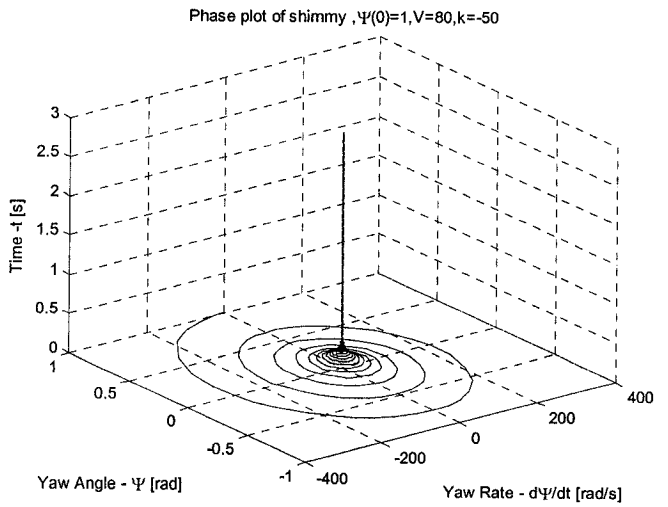

Figure 2-8 Phase plot of yaw angle

$(\psi(0) = 1rad, V = 80m/s, c = 50Nms/rad)$

Reproduced with permission of the copyright owner. Further reproduction prohibited without permission.

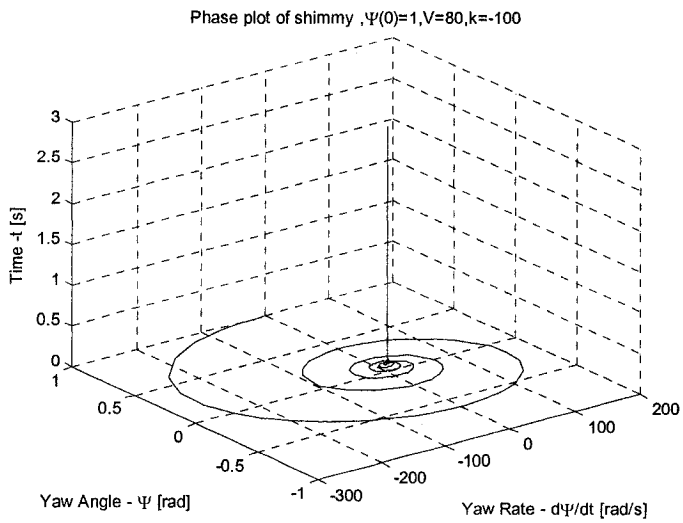

Figure 2-9 Phase plot of yaw angle

$(\psi(0) = 1rad, V = 80m/s, c = 100Nms/rad)$

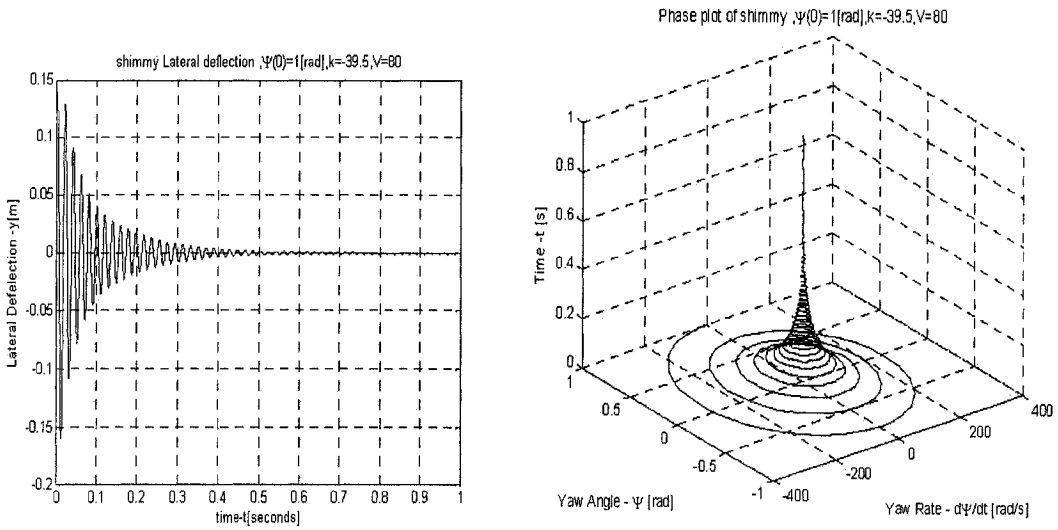

Figure 2-10 History of lateral deflection and phase plot of yaw angle

$(\psi(0) = 1rad, V = 80m/s, c = 39.5Nms/rad)$

Reproduced with permission of the copyright owner. Further reproduction prohibited without permission.

The related oscillation frequency and amplitude are collected in the following table 2-2. Note that for decreasing LCOs, these values are the final stable oscillation frequency and amplitude. $\psi(0)$ is set to 1 radian and taxiing velocity is 80 m/s.

Table 2-2 Oscillation frequency and amplitude of LCOs

Damping constant(Nm)	Frequency(H_z)	Amplitude(rad)
10	52	0.68
20	52	0.36
30	52	0.008
50	0	0
100	0	0

2.2.2 Taxiing velocity effect

The taxiing velocity is considered one of major factors introducing shimmy since it is always changing during the landing and taking-off process. Thus, it is one major parameter varying in the system model. How the taxiing velocity affects shimmy oscillation is the main topic of this section. The simulation parameters are set as follows:

Initial disturbed yaw angle is 0.1 radian or 1 radian. Torsional damping constant is 10 Nm s/rad. Taxiing velocity is descending from 80, 60 and 30 to 20 m/s respectively.

(1) Shimmy oscillation exists in the lateral direction and yaw motion as in Figure2-13 and Figure2-14, when the initial yaw angle is small (=0.1 radian in Figure2-14) or large (=1 radian in Figure2-15). At a lower taxiing velocity, the amplitude of

Reproduced with permission of the copyright owner. Further reproduction prohibited without permission.

oscillation is relatively low too. In Figure2-11, the amplitude of oscillation even tends to disappear. It is observed that when taxiing velocity is below 19.5m/s, there is no more oscillation observed with torsional damping constant.

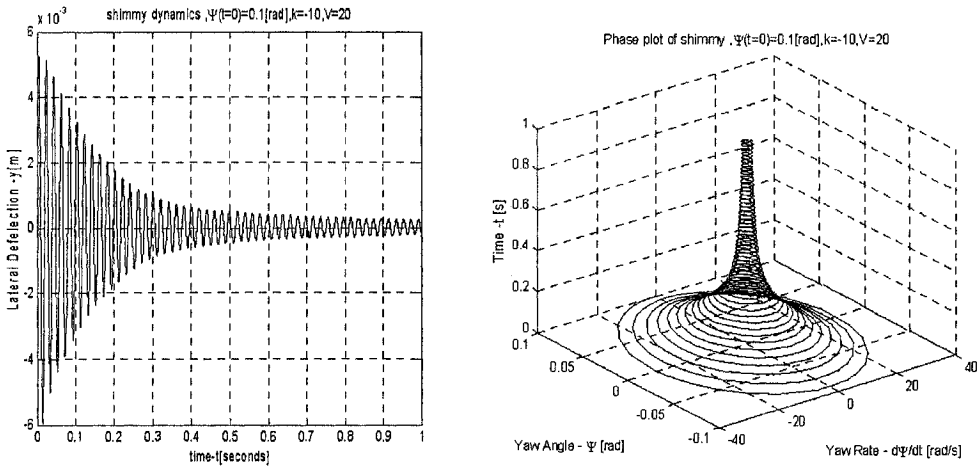

Figure 2-11 History of lateral deflection and phase plot of yaw angle

$(\psi(0) = 0.1rad, V = 20m/s)$

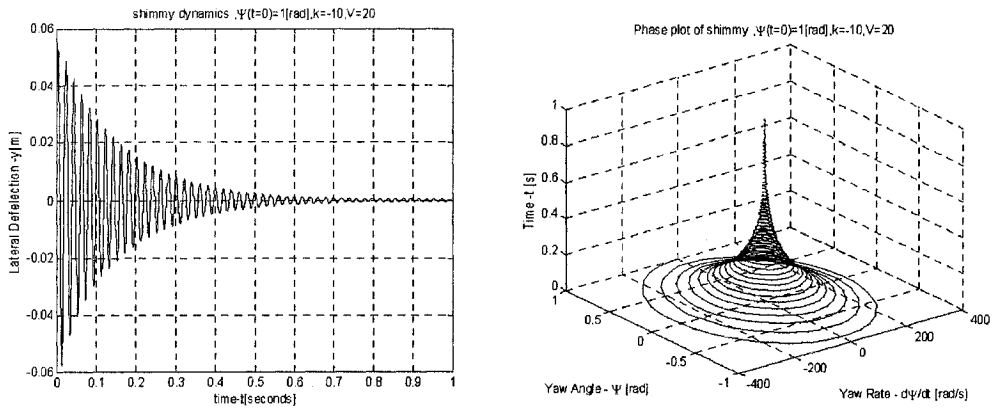

Figure 2-12 History of lateral deflection and phase plot of yaw angle

$(\psi(0) = 1rad, V = 20m/s)$

Reproduced with permission of the copyright owner. Further reproduction prohibited without permission.

(2) The amplitude of shimmy LCO is increased with taxiing velocity, which can be verified from Figure2-11, Figure2-12, Figure2-13 and Figure2-14. The amplitude of shimmy LCO is relatively small with lower taxiing velocity. It is the reason why the lower limit for taxiing velocity in the controller design is set as 20 m/s.

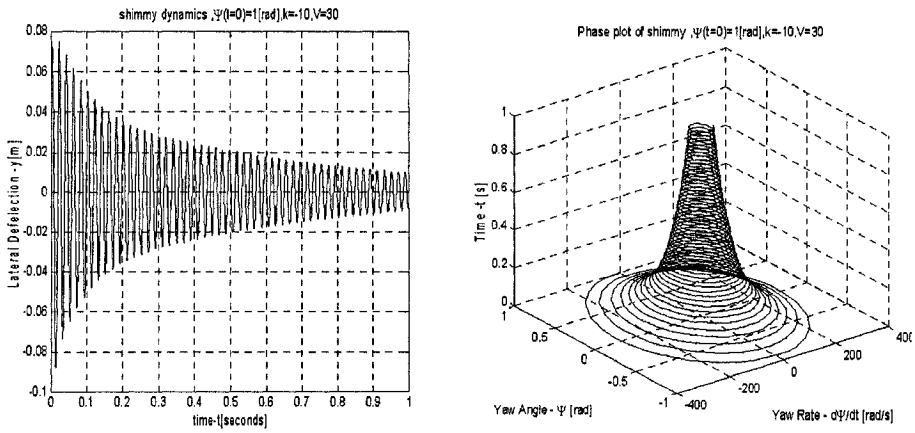

Figure 2-13 History of lateral deflection and phase plot of yaw angle

$$(\psi(0) = 0.1rad, V = 30m/s)$$

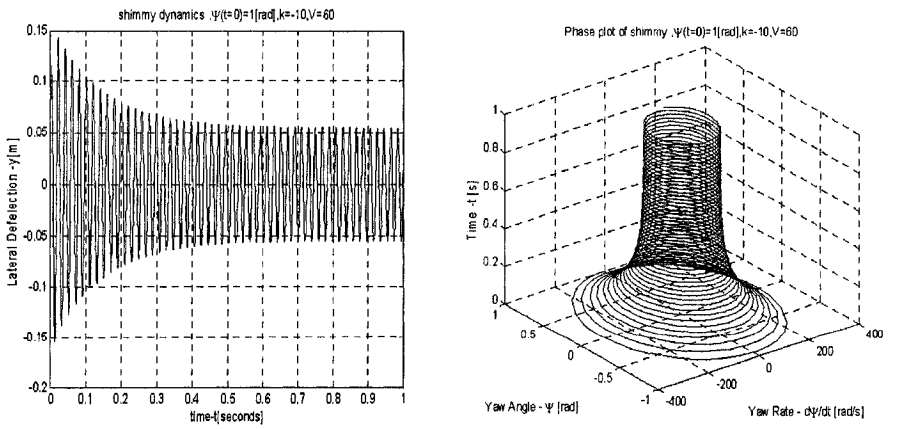

Figure 2-14 History of lateral deflection and phase plot of yaw angle

$$(\psi(0) = 0.1rad, V = 60m/s)$$

Reproduced with permission of the copyright owner. Further reproduction prohibited without permission.

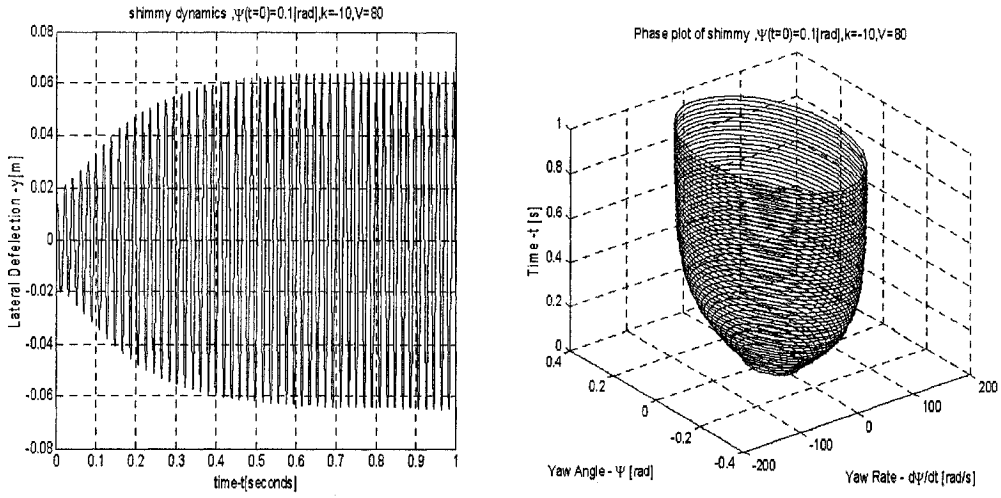

Figure 2-15 History of lateral deflection and phase plot of yaw angle

$(\psi(0) = 0.1rad, V = 80m/s)$

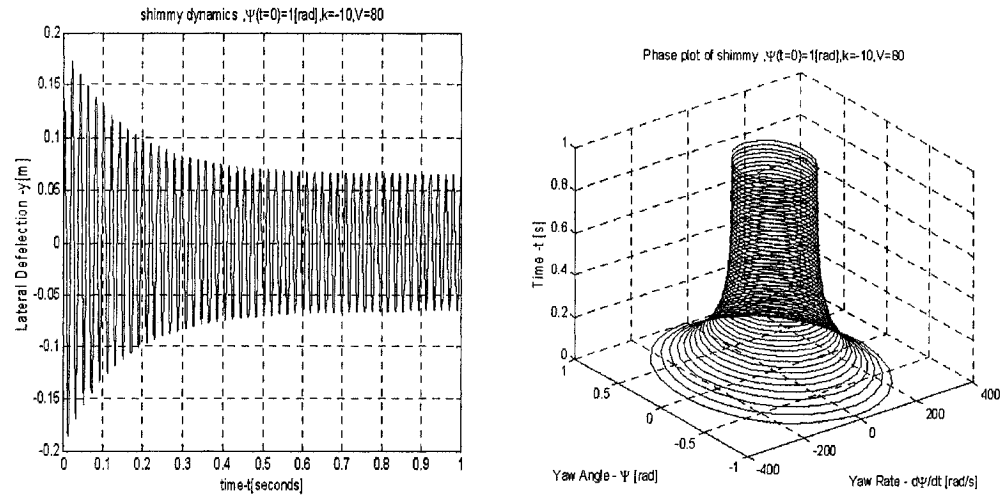

Figure 2-16 History of lateral deflection and phase plot of yaw angle

$(\psi(0) = 1rad, V = 80m/s)$

(3) The approach direction of limit cycle varies with different initial conditions. When initial yaw angle is small (ψ=0.1 radian), the stable limit cycle is approached from inside (Figure 2-14); On the contrary, when initial yaw angle is larger (ψ=1 radian), the

Reproduced with permission of the copyright owner. Further reproduction prohibited without permission.

limit cycle is approached from outside (Figure2-15). This was also observed and claimed in [5].

(4) From Table 2-2, it is found that the shimmy vibration frequency is fixed at about 52 Hertz in the simulations and it does not change with varying taxiing velocity or initial yaw angle.

(5) According to LCO theorem, if a system has a nonlinear stiffening term, in most occasions, the amplitude of oscillation will grow until the LCO is reached, such as in Figure2-11 to Figure2-14. Although the final state of LCO is bounded due to the nonlinear saturation, the system state variable--yaw angle cannot asymptotically approach its original equilibrium state as time goes by. When on the limit cycle, the rate of energy input is equal to the rate of energy dissipation, which results in a stable periodic motion as in Figure2-13 and Figure2-14.

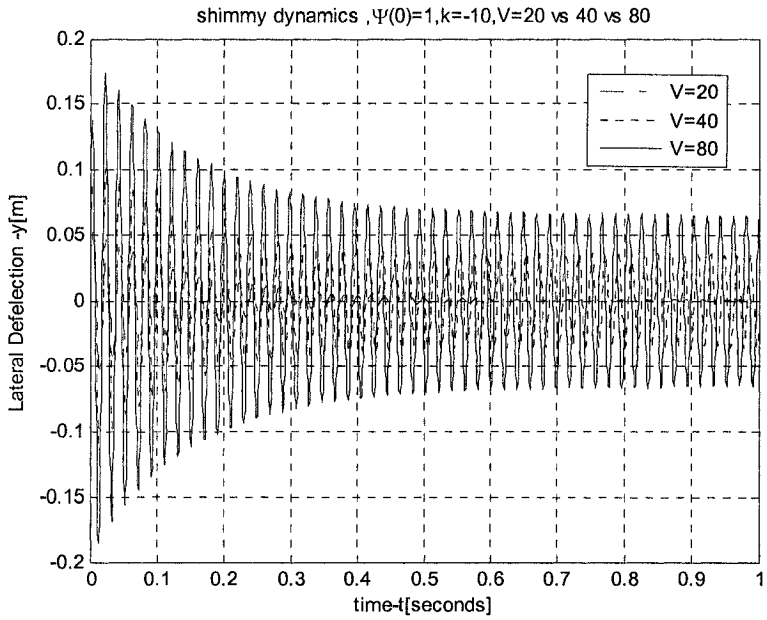

Figure 2-17 Lateral deflection $(\psi(0) = 1rad, V = 20,40,80m/s)$

Reproduced with permission of the copyright owner. Further reproduction prohibited without permission.

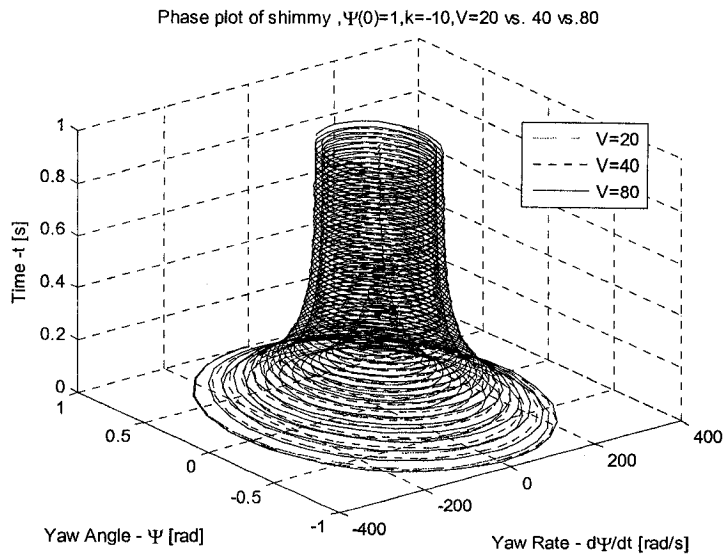

Figure 2-18 Phase plot of yaw angle $(\psi(0) = 1rad, V = 20,40,80m/s)$

For better study about how taxiing velocity affects shimmy oscillation, three groups of simulation data with different taxiing velocities are collected together and simultaneously displayed in Figure2-16 and Figure 2-17. It can be seen that the transition time from initial condition to stable limit cycle oscillation varies with taxiing velocity too. The bigger the taxiing velocity is, the shorter the transition time needed. The oscillation amplitude increases with taxiing velocity, but not proportionally increases with taxing velocity. The amplitude of yaw oscillation does not change very much when taxiing velocity goes beyond 60 m/s.

2.3 Stability variation analysis

There are many known dynamics analysis tools for linear system. In order to use these linear analysis tools, the linearization to the landing gear model has to be considered first.

Reproduced with permission of the copyright owner. Further reproduction prohibited without permission.

2.3.1 Linearization of model

From model equations (2-1), (2-10) and (2-14), before moving on to linear system stability analysis, linearization of nonlinear system is needed. Within small range of side slip angle, F_y and M_z/F_z are approximately proportional to side slip angle, as in Figure2-2 and Figure2-3. Based on this assumption, the nonlinear dynamic system is linearized using Taylor series expansion and rearranged in autonomous state-space equations as in (2-157).

$$\dot{x} = Ax \tag{2-157}$$

$$\text{where } x = \begin{pmatrix} \psi \\ \dot{\Psi} \\ y \end{pmatrix}, A = \begin{pmatrix} 0 & 1 & 0 \\ \frac{c}{I_z} & \frac{K}{I_z} + \frac{\kappa}{VI_z} & \frac{F_z}{\sigma}(C_{M\partial} - eC_{F\partial}) \\ V & e - a & -\frac{V}{\sigma} \end{pmatrix} \tag{2-18}$$

The main linearization steps are listed here. Collect equations (2-4), (2-5), (2-6) , (2-9) and (2-14)to form following (2-19) ,(2-20) and (2-21):

$$\frac{M_z}{F_z} = \begin{cases} C_{M\alpha} \frac{\alpha_g}{180} \sin(\frac{180}{\alpha_g}\alpha), & |\alpha| \geq \alpha_g \\ 0, & |\alpha| < \alpha_g \end{cases} \tag{2-19}$$

$$F_y = \begin{cases} C_{F\alpha} \alpha F_z, & |\alpha| \leq \delta \\ C_{F\alpha} \delta F_z sign(\alpha), & |\alpha| > \delta \end{cases} \tag{2-20}$$

$$M_3 = M_z - eF_y \tag{2-21}$$

Reproduced with permission of the copyright owner. Further reproduction prohibited without permission.

Substituting (2-19) and (2-20) into (2-21), one can get the complete expression for M_3 in form of (2-22) :

$$M_3 = M_z - eF_y = \begin{cases} -eC_{F\alpha}\delta F_z sign(\alpha), & \alpha \le -\alpha_g \\ F_z C_{M\alpha}\frac{\alpha_g}{180}\sin(\frac{180}{\alpha_g}\alpha) - eC_{F\alpha}\delta F_z sign(\alpha), & -\alpha_g < \alpha < -\delta \\ F_z C_{M\alpha}\frac{\alpha_g}{180}\sin(\frac{180}{\alpha_g}\alpha) - eC_{F\alpha}\delta F_z, & -\delta \le \alpha \le \delta \\ F_z C_{M\alpha}\frac{\alpha_g}{180}\sin(\frac{180}{\alpha_g}\alpha) - eC_{F\alpha}\delta F_z sign(\alpha), & \delta \le \alpha \le \alpha_g \\ eC_{F\alpha}\delta F_z sign(\alpha), & \alpha > \alpha_g \end{cases}$$

(2-22)

Substituting the expression of α (2-14) into

(2-22),

M_3 can be expressed in terms of y in the neighbourhood of $\alpha = 0$ ($y = 0$) as following.

$$M_3 = F_z C_{M\alpha}\frac{\alpha_g}{180}\sin(\frac{180}{\alpha_g}\frac{y}{\sigma}) - eC_{F\alpha}\frac{y}{\sigma}F_z \qquad (2\text{-}16)$$

Using Taylor's Series expansion, M_3 can be linearized as below.

$$\left.\frac{\partial M_3}{\partial y}\right|_{y=0} = F_z C_{M\alpha}\frac{\alpha_g}{180}\cos(\frac{180}{\alpha_g}\alpha).\frac{180}{\alpha_g}.\frac{1}{\sigma} - eC_{F\alpha}\frac{1}{\sigma}F_z\Big|_{y=0} = \frac{F_z}{\sigma}(C_{M\alpha} - eC_{F\alpha})$$

(2-24)

At last, after introducing another state variable $\dot{\psi}$, one can get the linearized state-space equation as in Eqs. (2-157) and (2-18).

Reproduced with permission of the copyright owner. Further reproduction prohibited without permission.

2.3.2 Stability variation analysis

The inherent varying parameter in landing gear system is taxiing velocity (V) during landing or taking-off. The taxiing velocity is critical in the shimmy analysis as observed in [19]: lower taxiing velocity leads to higher stability. Dynamics simulation shows the landing gear to be stable at the lower speed of 10 knots (1 knot=1.852 kilometre/hour=0.5144 metre/second). Also reported in [4], the occurrence of shimmy increases with the increasing taxiing velocity.

According to [23], in a perfect aircraft touchdown, assuming there is no crosswind, contact with the ground is made just as the forward speed is reduced to the point where there is no longer sufficient lift to remain aloft. In this thesis, the forward maximum velocity is supposed to be 155.52 knots (80 m/s) before aircraft touches down. Varying parameters is not a new concept. For landing gear designers, to get optimal design parameters, they have to try different combination of several varying design parameters. Here only two typical varying parameters, taxiing velocity V and caster length e are considered. Taxiing velocity is chosen to vary from 80 m/s to 20 m/s in 5 minutes and caster length varies between -0.5 m and 0.5 m.

According to stability theory, the method of obtaining the characteristic equation directly from the vector differential equation is based on the fact that the solution to the unforced system is an exponential function, which means that the solution to $\dot{x} = Ax$ is $x = ke^{\lambda t}$. The obtained characteristic equation is $\det(\lambda I - A) = 0$. From characteristic roots, system stability can be judged.

Reproduced with permission of the copyright owner. Further reproduction prohibited without permission.

When varying taxing velocity V, the system eigen-values vary, and consequently affects system stability, which is plotted in Figure 2-18. In Figure2-18, caster length is assumed to be constant 0.5m. It is shown that there are two repeated positive real roots and landing gear is an unstable system at the taxing velocity of 80 m/s, which means the instant of landing. Only when velocity goes below about 25 m/s, the system becomes stable. The objective of robust control design is to introduce the suitable state-feedback gain and robustly stabilize this unstable system despite varying taxiing velocity.

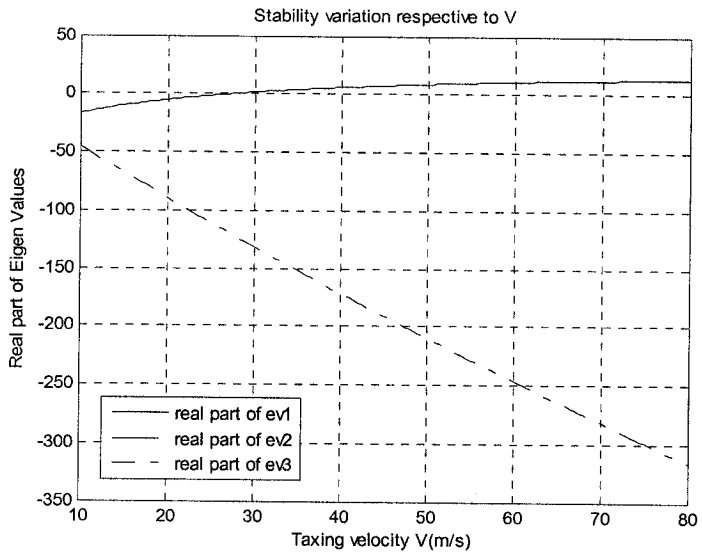

Figure 2-19 Real part of eigen-values variation vs. V

Reproduced with permission of the copyright owner. Further reproduction prohibited without permission.

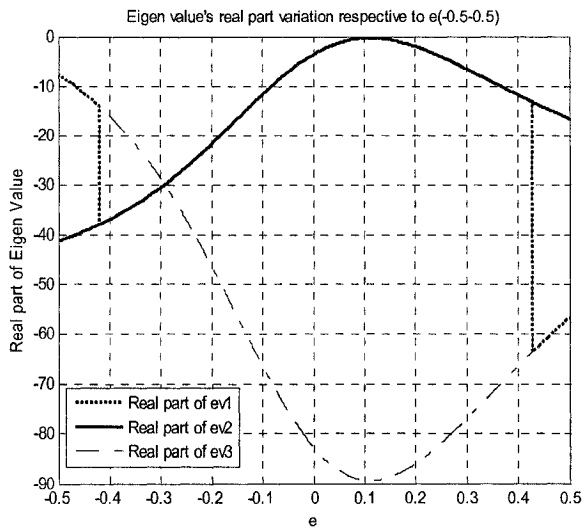

Figure 2-20 Real part of eigen-values variation vs. e

Similarly, when varying caster length e, the system eigen-values also vary, as plotted in Figure 2-19 y. It shows that when caster length varies between -0.5m and 0.5m, the real part of system eigen-values all are less than 0, so the system is stable in this situation according to the criteria of stable system.

2.4 Conclusion

From the above simulations and analysis, it is shown that LCO does exist in landing gear system and varies with varying structural parameters, such as torsional damping constant, caster length or inherent varying parameter, such as taxiing velocity. To avoid the occurrence of shimmy LCO, some structural parameters are adjusted at the landing gear design stage. However, the inherent varying parameter taxiing velocity makes nose landing gear unstable and leads to oscillation at varying amplitude and frequency. To suppress this oscillation actively and effectively, a feedback control system will be introduced in Chapter 3.

Reproduced with permission of the copyright owner. Further reproduction prohibited without permission.

Chapter 3
Robust Model Predictive Control

3.1 Modern control

Control theory can be classified into two main areas: conventional control and modern control. Conventional control covers the concepts and techniques developed up to 1950. Modern control covers the techniques from 1950 to present (Leo Rollins, "Robust Control Theory", 1999). Conventional control theory is developed based on the transfer function and the feedback theory while Modern control theory is developed with system state equations, which are realized in the form of matrix equations such that computers could efficiently solve them. Any n^{th} order differential equation describing a control system could be reduced to n 1^{st} order equations, which can be solved conveniently. The method is often referred to as the State Variable/State Space method. State-space theory is an elegant way to approach a control problem such that it is popular among academic researchers, where the system is represented by differential state equations instead of transfer functions. The state-space theory represents a paradigm shift which led to many useful system concepts and new methods for control system analysis and design. It has introduced powerful computational methods based on numerical linear algebra. Modern control methods were extremely successful because they could be efficiently implemented on computers. They could handle Multiple-Input-Multiple-Output (MIMO) systems and also they could be relatively easy to be optimized. Robust Model Predictive Control obviously belongs to modern control method which deals with the uncertainties and system constraints in a systematic way.

Reproduced with permission of the copyright owner. Further reproduction prohibited without permission.

3.2 Uncertainty and disturbance in the system

Uncertainty and disturbance are two important factors imposing fundamental limits of feedback performance in the modern robust control design. In Figure3-1, uncertainties and disturbances are shown in the system as following:

(1) There exist uncertainties in the model of the plant.

(2) Disturbances occur in the control system.

(3) Also noises often read on the sensor inputs.

Each of these uncertainties can have an additive or multiplicative component. One difficult part of designing a good control system is modeling the behaviour of the plant.

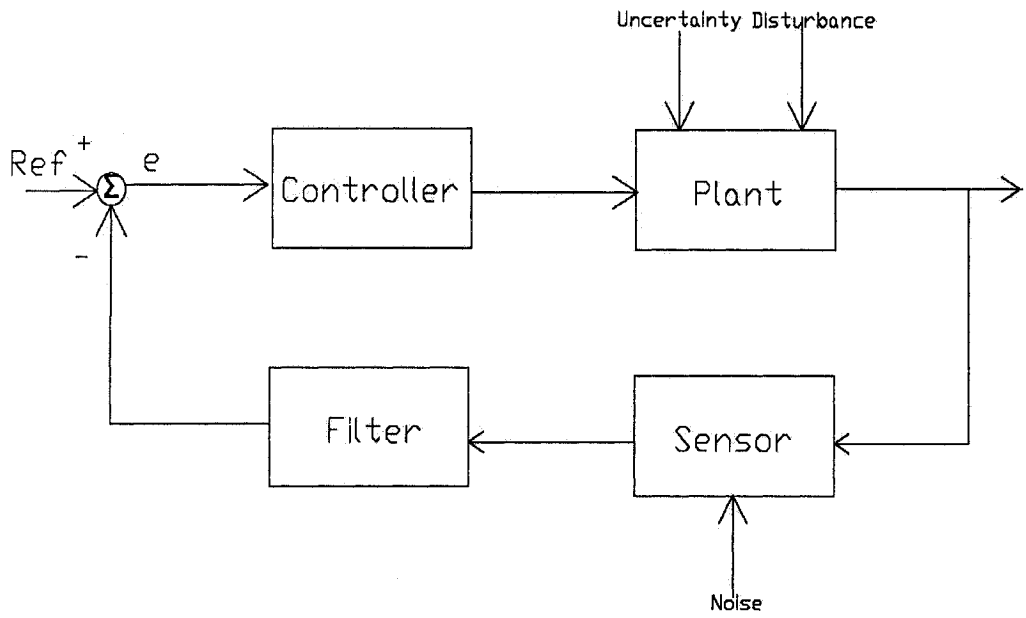

Figure 3-1 Uncertainties and disturbances in the control system

In terms of state space method, control system engineers are concerned about three main topics: observability, controllability and stability. Observability is the ability to

Reproduced with permission of the copyright owner. Further reproduction prohibited without permission.

observe all of the parameters or state variables in the system. Controllability is the ability to move a system from any given state to any desired state. Stability is often phrased as the bounded response of the system to any bounded input [27]. Uncertainties present a challenge to the control system engineer who tries to maintain these three properties using limited information. One method to deal with uncertainties in the past is stochastic control, such as LQR and LQG, in which uncertainties in the system are modeled as probability distributions and these distributions are combined to yield the control law.

Given a bound on the uncertainty, the controller is supposed to deliver results that meet the control system requirements in all cases. Therefore robust control theory might be stated as a worst-case analysis method rather than a typical case method. It must be recognized that some performance may be sacrificed in order to guarantee that the system meets certain requirements. There are many difficulties in robust control design, such as: inaccurate plant data, time-varying plant and nonlinearity. The key issue with robust control system design is the uncertainty and how the control system can deal with this problem. In this thesis, the researh focus is on linear time-varying plant. The uncertainty of system is represented by the variations in the elements of the following matrices A, B, C and D.

$$\dot{x} = Ax + Bu \tag{3-1}$$

$$y = Cx + Du \tag{3-2}$$

Reproduced with permission of the copyright owner. Further reproduction prohibited without permission.

The objective of robust control is to ensure the required performance specification be met by the designed state feedback control when the plant are subject to some uncertainties and disturbances.

3.3 LPV system and RMPC

LPV is the acronym of Linear Parameter Varying system, of which the parameters are time varying. Robust control design can normally deal with LPV system. RMPC is a powerful design tool, which is based on MPC and robust control theories.

3.3.1 LPV, LTI and LTV system

As mentioned in [25], early approaches to robust predictive control assumed that the model was defined as an FIR system of fixed order and the uncertainty was in the form of bounds on the pulse response coefficients. A more recent approach is to assume that a number of 'corner' points, which consist the so-called uncertainty polytope, as a quadrangle polytope depicted in Figure3-2, when system matrixes A and B varying within this polytope.

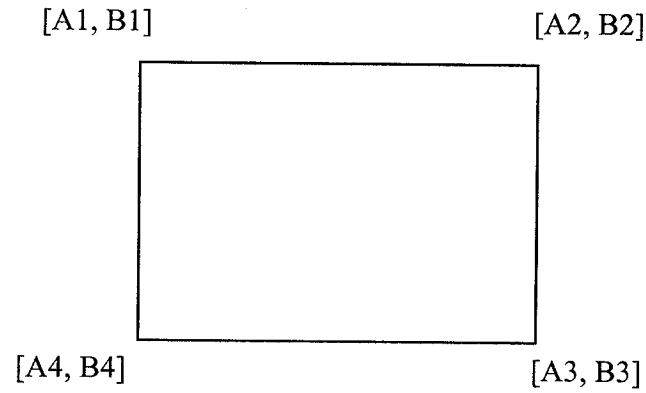

Figure 3-2 Uncertainty convex polytope of LPV system

Reproduced with permission of the copyright owner. Further reproduction prohibited without permission.

LPV system, first introduced by J.S Shamma and M. Athans, is Linear Parameter-Varying system, whose state-space description is a function of some parameter vector θ. In state-space form, a LPV system is described by Eqs. (3-3) and (3-4).

$$\dot{x} = A(\theta)x + B(\theta)u \tag{3-3}$$

$$y = C(\theta)x + D(\theta)u \tag{3-4}$$

where θ is a vector of varying parameters on which the system characteristics are assumed to depend. LPV systems can be considered in light of two other important classes of linear systems: Linear Time Invariant (LTI) system and Linear Time Varying (LTV) system. LTI system is the most common system. It is described in form of state-space if θ is constant in equations (3-3) and (3-4). LTV systems represent systems where the state-space description is completely defined by the functional time dependence of the state-space matrix, which is represented by *A(t), B(t), C(t), D(t)*. In fact, in equations (3-3) and (3-4), if θ varies with time, then it could be called LTV system, which is equivalent to a LPV system. In this thesis, LPV system is preferred in accordance with related literatures. A nonlinear system can be transformed into a LPV description. For example, the Van der Pol equation is described as:

$$\dot{x}_1 = x_2 \tag{3-5}$$

$$\dot{x}_2 = x_1 - 0.3(1 - x_1^2)x_2 \tag{3-6}$$

Reproduced with permission of the copyright owner. Further reproduction prohibited without permission.

It is known that there is limit cycle for this system. All trajectories starting outside this limit cycle diverges and all trajectories starting inside converges to zero. But it could be transformed to a LPV equation (3-7).

$$\begin{bmatrix} \dot{x}_1 \\ \dot{x}_2 \end{bmatrix} = \begin{bmatrix} 0 & -1 \\ 1 & -0.3(1-\rho^2) \end{bmatrix} \begin{bmatrix} x_1 \\ x_2 \end{bmatrix} \tag{3-7}$$

where $\rho(x) = x_1$, such that the nonlinear term of (3-7) is hidden in parameter ρ .Thus some LPV control designs can be applied to this quasi-linear system.

3.3.2 LMI optimization

For LPV system, the associated control system design for LPV model can be cast or recast as convex optimization problems that involves solving linear matrix inequalities (LMI) problems, see Appendix B for more details. Thanks to the standard efficient LMI optimization tools to solve general LMI problems; LMI-based Robust Control recently has become popular in the control community. Besides the LMI-Lab toolbox in Matlab, other LMI toolboxes have been developed, such as LMITOOL (built in Scilab software), SeDuMi(developed by the Advanced Optimization Lab of McMaster University), SDPT3(developed by K. C. Toh et al), SDPA(by K. Fujisawa et al). Most of these toolboxes are based on semi-definite programming and primal-dual interior-point method.

The LPV controller design needs some form of prediction on varying system dynamics in the sense of MPC. The linearized landing gear system is a LPV system, whose dynamics inherently depends on taxiing velocity. LPV control synthesis was

Reproduced with permission of the copyright owner. Further reproduction prohibited without permission.

studied for car yaw moment control and lateral deviation control as in [30]. Its control law is designed using the H_∞ loop-shaping method for a LPV plant, whose dynamics depends on the longitudinal speed.

3.4 RMPC control

RMPC control method can deal with LPV system with polytopic uncertainty. One important progress in RMPC design is that controller design is transformed into LMI form and then LMI optimization is executed with emerging LMI toolboxes to realize robust control objective. The algorithms available for solving LMI problems appear to be very fast, so that the formulation can be candidate for online use [25].

3.4.1 RMPC without constraints

The system considered in this thesis is a discrete time-varying linear model:

$$x(k+1) = A(k)x(k) + Bu(k) \tag{3-8}$$

$$y(k) = Cx(k) \tag{3-9}$$

Note that:

(1) The parameter matrix A is varying at every sample interval in this model while B is constant. But RMPC can handle time-varying A and B (referring to Figure3-2).

(2) Matrix A changes at each sampling interval, but it does not mean that its variation rule is known ahead of time (not a pre-defined function of c). Since their precise variations are unknown, the model dynamic behaviour is uncertain. The known

Reproduced with permission of the copyright owner. Further reproduction prohibited without permission.

parameters are the corner points described by the vertices of convex polytope Ω (about concept of convex set, see Appendix F), which means

$$A \in \Omega \tag{3-10}$$

$$\Omega = Co\{A_1, A_2, A_3, A_4, ...A_L\},$$

$$A = \sum_{i=1}^{L} \alpha_i A_i, \sum_{i=1}^{L} \alpha_i = 1, \alpha_i > 0 \tag{3-11}$$

The robust performance objective is defined as following (3-12), which means to minimize the maximum of cost function and lead to robustness against model uncertainty.

$$\min_{u(k+i|k)} \max_{[A(k+i),B(k+i)]\in\Omega} V_\infty(k) \tag{3-12}$$

where $V_\infty(k)$ is the quadratic cost functions, which is defined as:

$$V_\infty(k) = \sum_{k=0}^{\infty} [x(k+i \mid k)^T Q_w x(k+i \mid k)] + [u(k+i \mid k)^T R_w u(k+i \mid k)] \tag{3-13}$$

Suppose there exists a Lyapunov Function V(x) which satisfies

$$V(x) = x^T P x \ , \mathrm{P} = \mathrm{P}^{\mathrm{T}} > 0 \tag{3-14}$$

If V satisfies the following inequality for all $x(k+i|k)$ and $u(k+i|k,(i\geq 0)$ (predicted state variable and predicted control input at the present instant in the uncertain system model (3-8), respectively):

$$V(x(k+i+1 \mid k) - V(x(k+i \mid k))$$

Reproduced with permission of the copyright owner. Further reproduction prohibited without permission.

$$\leq -[x(k+i\mid k)^T Q_w x(k+i\mid k)+u(k+i)\mid k)^T R_w u(k+i\mid k)] \ , \quad (3\text{-}15)$$

then the system is stable. Note that P is a suitable Positive Definite Matrix (PDM, (the property of PDM, refer to Appendix A).

Inequality (3-15) is important because it leads to the upper bound formation for the cost function (3-13) as expressed in (3-16). Assuming that robust objective function is finite, $x(\infty\mid k)=0$. Thus one can infer $V(x(\infty\mid k))=0$. Summing (3-15) up from $i=0$ to $i=\infty$, one obtains:

$$\max_{A(k+j)\in\Omega} V_\infty(k) \leq V(x(k\mid k)) \qquad (3\text{-}16)$$

Then, (3-11) can be replaced by the following:

$$\min_{u(k)} V(x(k\mid k)) \qquad (3\text{-}17)$$

The above expression (3-17) is a convex optimization problem and can be solved by LMI solver. Therefore considering (3-14), the problem (3-12) is equivalent to the following (3-18):

$$\min_{\gamma,P} \gamma \quad \text{Subject to} \quad x(k\mid k)^T P x(k\mid k) \leq \gamma \quad . \qquad (3\text{-}18)$$

Define $Q=\gamma P^{-1}>0$ as a PDM. One can get $1-x(k\mid k)^T Q^{-1} x(k\mid k)\geq 0$ by using Schur Complement (referring to Appendix C), which is equivalent to following LMI:

$$\begin{bmatrix} 1 & x(k\mid k)^T \\ x(k\mid k) & Q \end{bmatrix} \geq 0 \quad . \qquad (3\text{-}19)$$

Reproduced with permission of the copyright owner. Further reproduction prohibited without permission.

Now assume that the control signal is determined by state feed-back law $u(k+i \mid k) = Fx(k+i \mid k), i \geq 0$. Substituting for *u(k+i|k)* in inequality , (3-15), one gets

$$x(k+i \mid k)^T \{[A(k+i)+B(k+i)F]^T P[A(k+i)+B(k+i)F]-P + F^T RF + Q_w\} x(k+i \mid k) \leq 0 \quad (3\text{-}20)$$

Applying property of PDM again, (3-20) holds for all $i \geq 0$ if

$$[A(k+i)+B(k+i)F]^T P[A(k+i)+B(k+i)F]-P+F^T RF+Q_w \leq 0 \quad (3\text{-}21)$$

Rearranging (3-21):

$$P-[A(k+i)+B(k+i)F]^T P[A(k+i)+B(k+i)F]-F^T RF-Q_w \geq 0 \quad (3\text{-}22)$$

Pre- and post-multiplying by Q (because Q>0, inequality still holds) and defining $Y = FQ$ and substituting $P = \gamma Q^{-1}$, one obtains another LMI by using Schur complement:

$$\begin{bmatrix} Q & (A(k+i)Q+BY)^T & Q(Q_w^{1/2})^T & Y^T(R_w^{1/2})^T \\ A(k+i)Q+BY & Q & 0 & 0 \\ Q_w^{1/2}Q & 0 & \gamma I & 0 \\ R_w^{1/2}Y & 0 & 0 & \gamma I \end{bmatrix} \geq 0 \quad (3\text{-}23)$$

where *A(k+i)* is affine in uncertain set A (referring to (3-8) to (3-10)).

If considering input and output constraints, another two LMIs should be added, which will be discussed in the next section.

Reproduced with permission of the copyright owner. Further reproduction prohibited without permission.

3.4.2 RMPC with constraints

In this thesis, the Euclidean norm constraints are considered for input and output signals at sampling instant k,

$$\left\|u(k+i\mid k)\right\|_2 \le u_{\max} \tag{3-24}$$

$$\left\|y(k+i\mid k)\right\|_2 \le y_{\max} \tag{3-25}$$

To express (3-24) and (3-25) in form of LMIs, the following derivation has to be carried out.

$$\max_{i\ge 0}\left\|u(k+i\mid k)\right\|_2^2 = \max_{i\ge 0}\left\|Fx(k+i\mid k)\right\|_2^2 = \max_{i\ge 0}\left\|YQ^{-1}x(k+i\mid k)\right\|_2^2$$

$$= \max_{i\ge 0}\left\|Y^2Q^{-1}\right\|_2\left\|x(k+i\mid k)^2Q^{-1})\right\|_2 = \max_{i\ge 0}\left\|Y^TQ^{-1}Y\right\|_2\left\|x(k+i\mid k)^TQ^{-1}x(k+i\mid k)\right\|_2$$

Using Cauchy-Schwarz inequality (If X and Y are real vectors, then following inequality holds $\left|XY\right|_2 \le \left\|X\right\|_2\left\|Y\right\|_2$), the above inequality becomes:

$$\le \max_{i\ge 0}\left\|Y^TQ^{-1}Y\right\|_2.\max\left\|x(k+i\mid k)^TQ^{-1}x(k+i\mid k)\right\|_2$$

From (3-19), One knows $1-x(k\mid k)^TQ^{-1}x(k\mid k)\ge 0$ holds for all k>0. Since $\max_{i\ge 0}\left\|u(k+i\mid k)\right\|_2^2 \le u_{\max}^2$, the following LMI holds if $U_{jj} \le u_{\max}^2$

$$\begin{bmatrix} U & Y \\ Y^T & Q \end{bmatrix} \ge 0 \quad . \tag{3-26}$$

Reproduced with permission of the copyright owner. Further reproduction prohibited without permission.

Note that $x(k+i\,|\,k)$ is a vector and belongs to state-invariant ellipsoid $\mathrm{E} = \{z \mid z^T Q^{-1} z\} = \{z \mid z^T P z \le \gamma\}$. Besides, for Matrix A and B, if $A \ge B$ then $A_{jj} \ge B_{jj}$ holds.

Similarly, for output constraint (3-22):

$$\max_{i\ge 0}\left\|y(k+i\,|\,k)\right\|_2^2 = \max_{i\ge 0}\left\|C[A(k+i)+B(k+i)F]x(k+i\,|\,k)\right\|_2^2$$

Substituting $F = YQ^{-1}$, one obtains from above equation

$$= \max_{i\ge 0}\left\|C[A(k+i)+B(k+i)YQ^{-1}]x(k+i\,|\,k)\right\|_2^2$$

$$= \max_{i\ge 0}\left\|C[A(k+i)Q+B(k+i)Y]Q^{-1}x(k+i\,|\,k)\right\|_2^2$$

Using Cauchy-Schwarz inequality, one derives:

$$\le \max_{i\ge 0}\left\|C[A(k+i)Q+B(k+i)Y]\right\|_2^2 . \max\left\|Q^{-1}x(k+i\,|\,k)\right\|_2^2$$

$$= \max_{i\ge 0}\{C[A(k+i)Q+B(k+i)Y]\}^T Q^{-1}\{C[A(k+i)Q+B(k+i)Y]^T\}$$

$$.\max\{x(k+i\,|\,k)^T Q^{-1}x(k+i\,|\,k)\}$$

Again, introducing $1 - x(k\,|\,k)^T Q^{-1}x(k\,|\,k) \ge 0$, if $\max_{i\ge 0}\left\|y(k+i\,|\,k)\right\|_2^2 \le y_{\max}^2$ holds, then the following inequality holds.

$$\{C[A(k+i)Q+B(k+i)Y]\}^T Q^{-1}\{C[A(k+i)Q+B(k+i)Y]\} \le y_{\max}^2 ,$$

which is equivalent to the following LMI using Schur complement,

Reproduced with permission of the copyright owner. Further reproduction prohibited without permission.

$$\begin{bmatrix} Q & [A(k+i)Q+B(k+i)Y]^T C^T \\ C[A(k+i)Q+B(k+i)Y] & y_{\max}^2 I \end{bmatrix} \geq 0, (i \geq 0) \quad (3\text{-}27)$$

In summary, for system (3-8) and (3-9), if there exists matrix Y and Q satisfying all the five LMIs (including robust stability condition and input, output constraints) (3-17), (3-19), (3-23) , (3-26) and (3-27) , the controller $F = YQ^{-1}$ achieves the robust control objective (3-12).

3.5 PRMPC

According to section 3.4, online step-by-step convex optimization can finally lead to asymptotically stable state evolution. However, for the online control application, the computation efficiency is still a challenging problem in the RMPC application to the online control problems. To get over this drawback, the following algorithm (called PRMPC) have been proposed.

3.5.1 Proposed algorithm description

The objective of proposed PRMPC is to find a stable but faster RMPC algorithm. The main idea is that there is only one-time running for relatively time-consuming LMIs (3-17), (3-19), (3-23) , (3-26) and (3-27) . Then the faster convex LMI computation is used to maintain state convergence process and compute suitable feedback gain matrix at every sample interval.

The proposed algorithm is described as follows. Given the system (3-8) and (3-9) with an initial feasible state *x(0)*, (that means there is feasible solution to all related five LMIs subject to *x(0)*), the following procedures are carried out:

Reproduced with permission of the copyright owner. Further reproduction prohibited without permission.

(1) Compute Q subject to (3-17), (3-19), (3-23) , (3-26) and (3-27) with initial condition $x(0)$ and polytopic vertices of A_j (i.e. A_1, A_2, A_3,... in (3-10)), then save the solution Q, Y;

(2) At time k, solve related LMIs (3-28) to (3-31) to obtain optimized $Q(k)$ from present $x(k)$;

(3) Compute feed-back gain $F(k) = YQ(k)^{-1}$ and controller is designed as $u(k)=F(k)x(k)=YQ(k)^{-1}x(k)$. Apply the current control input $u(k)$ to the system;

(4) At time $k+1$, set $Q = Q(k)$ go back to (2).

In the step (2), all involved LMIs are described as follows:

$$\min_{\beta,Q,Y,Q(k)} \beta \text{ subject to following (3-28) to (3-31).}$$

$$\begin{bmatrix} 1 & x(k)^T \\ x(k) & Q(k) \end{bmatrix} \geq 0 \tag{3-28}$$

$$\begin{bmatrix} u_{\max}^2 & Y \\ Y^T & Q(k) \end{bmatrix} \geq 0 \tag{3-29}$$

$$\begin{bmatrix} y_{\max}^2 Q(k) & C^T(A_j Q(k) + BY)^T \\ (A_j Q(k) + BY)C & y_{\max}^2 I \end{bmatrix} \geq 0 \tag{3-30}$$

$$0 < Q \leq \beta Q(k) \qquad (0 < \beta \leq 1) \tag{3-31}$$

Note that A_j means vertex point of the convex polytope.

Reproduced with permission of the copyright owner. Further reproduction prohibited without permission.

3.5.2 Mathematical proof

The proposed PRMPC is based on concepts of invariant ellipsoid and contracted positive definite matrix (PDM). Although its proof is simple and easily understandable, the saving on computational time compared with other RMPCs is profound.

Definition: Given a polytopic uncertain system (3-8) and (3-9), the subset $\varepsilon = \{x \mid x^T Q^{-1} x \le 1\}$ of the state space $x \in R^{n_x}$ is defined as an asymptotically stable invariant ellipsoidal set.

Lemma: The first PDM Q obtained from step1 is the upper bound of invariant ellipsoidal set for system with the initial state *x(0)*.

This upper bound only depends on initial state if all related LMIs have feasible solutions and convex polytope has been predefined. Related materials can be referred to [33]and [34]. Note that LMIs (3-29) and (3-30) are nothing but input and output constraints, which should be satisfied at every sample interval.

Theorem: Considering the LPV system (3-8) and (3-9), this system with state-feedback gain $F(k) = YQ(k)^{-1}$ and control input $u(k) = F(k)x(k)$ is asymptotically stable if $Q(k)^{-1}$ is asymptotically contracted.

Proof: From characteristics of Positive Definite Matrix (refer to Appendix A), for $Q(k) > 0$ and $Q(k+1) > 0$ ($k>0$), one can infer that if $0 < Q \le \beta Q(k)$ and $Q(k) < Q(k+1)$ holds, then $0 < Q(k)^{-1} - Q(k+1)^{-1}$ holds.

Multiplying the above inequality left side by *x (k)* and right side by *x (k)*^{T}, one derives:

$$0 < x(k)Q(k)^{-1}x(k)^T - x(k)Q(k+1)^{-1}x(k)^T$$

Reproduced with permission of the copyright owner. Further reproduction prohibited without permission.

According to [34], if at time k there exits $Q>0$ and $x(k \mid k)^T Q^{-1} x(k \mid k) \leq 1$ holds, then at time $k+i$, $Max\{x(k+i \mid k)^T Q^{-1} x(k+i \mid k)\} < 1$ holds. Thus if applying state-feedback control law $F(k) = YQ(k)^{-1}$ and $u(k) = F(k)x(k)$ to the controlled system, it will generate one ellipsoid inside another, which assures that the system is asymptotically stable.

Note that Q^{-1} is the upper bound of contracted $Q(k)^{-1}$. A contracted ellipsoidal set is expressed in terms of LMIs as (3-28) to (3-31), see figure 3-3.

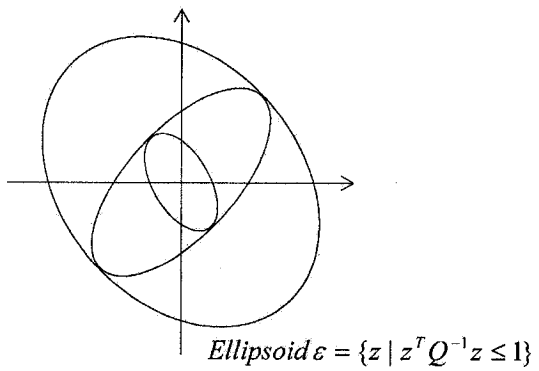

Figure 3-3 Graphical description for contracted ellipsoidal sets

3.6 CRMPC

One way for LPV control design is to find a single Lyapunov matrix, like KRMPC proposed by Kothare [34], but sometimes this is thought to be conservative (not always though). Another way is to find parameter dependent Lyapunov matrix (PDLM). PDLM involves introduction of one or more matrix variables, such as matrix G in the following (3-32), to get hopefully less-conservative controller.

Reproduced with permission of the copyright owner. Further reproduction prohibited without permission.

Based on KRMPC [34], F.A. Cuzzola in [33] and N. Wada in [32] presented improved RMPC successively by PDLM. F.A. Cuzzola's method is a typical RMPC method, which is the so-called CRMPC in this thesis.

To alleviate the repetition, only the different parts of CRMPC are listed comparing to previous RMPCs. The related proof refers to [33].

$\forall j = 1,2....L,$

$$\begin{bmatrix} G+G^T-Q_j & [A_jG+BY]^T & [Q_w^{1/2}G]^T & [R_w^{1/2}Y]^T \\ A_jG+BY & Q_j & 0 & 0 \\ Q_w^{1/2}G & 0 & \gamma I & 0 \\ R_w^{1/2}Y & 0 & 0 & \gamma I \end{bmatrix} > 0 \tag{3-32}$$

where A_j is related to vertex point of the convex polytope, such as A_1 to A_4 in Figure3-2.

The state-feedback gain is $F(k) = YG(k)^{-1}$ and control input is $u(k) = F(k)x(k)$

The input and output constraints are expressed as:

$$\begin{bmatrix} u_{\max}^2 I & Y^T \\ Y & G+G^T-Q_j \end{bmatrix} \geq 0 \tag{3-33}$$

$$\begin{bmatrix} G+G^T-Q_j & [C(A_jG+B_jY)]^T \\ C(A_jG+B_jY) & y_{\max}^2 I \end{bmatrix} \geq 0 \tag{3-34}$$

The comparison between two robust stability conditions of KRMPC and CRMPC is described in Appendix D.

Reproduced with permission of the copyright owner. Further reproduction prohibited without permission.

3.7 A RMPC application example

3.7.1 System model

To verify the proposed RMPC algorithm, a benchmark example in [34] has been adopted. The system consists of a two-mass-spring system shown in Figure3-4. Its discrete-time state-space equations are obtained by Euler first-order approximation with sampling time 0.1 second. Now the proposed PRMPC is applied to this example system and its control performance is compared with that of KRMPC, CRMPC in terms of robustness. The respective simulation results are shown in the following Figure3-5 to Figure 3-13.

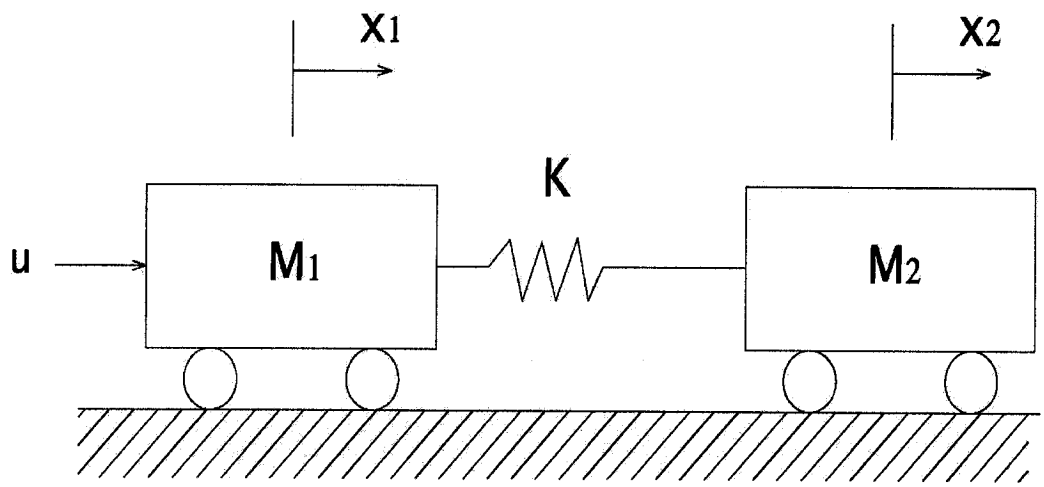

Figure 3-4 Two mass-spring system

The system model is:

Reproduced with permission of the copyright owner. Further reproduction prohibited without permission.

$$\begin{bmatrix} x_1(k+1) \\ x_2(k+1) \\ x_3(k+1) \\ x_4(k+1) \end{bmatrix} = \begin{bmatrix} 1 & 0 & 0.1 & 0 \\ 0 & 1 & 0 & 0.1 \\ -0.1K/m_1 & 0.1K/m_1 & 1 & 0 \\ 0.1K/m_2 & -0.1K/m_2 & 0 & 1 \end{bmatrix} \begin{bmatrix} x_1(k) \\ x_2(k) \\ x_3(k) \\ x_4(k) \end{bmatrix} + \begin{bmatrix} 0 \\ 0 \\ 0.1K/m_1 \\ 0 \end{bmatrix} u(k) \tag{3-35}$$

where m_1 and m_2 are the two masses and K is the spring constant , x_1 and x_2 represent the positions of these two masses, x_3 and x_4 are their velocities.

The control objective is to drive the initially disturbed four states (positions and velocities of m_1 and m_2) to equilibrium point (0, 0, 0, 0) while the spring constant K is arbitrarily varying between its maximum 10 N/m and minimum 0.5 N/m.

3.7.2 Simulation results

The simulation results of three RMPCs in the two-mass-spring example are shown below. Figure 3-5 to Figure 3-7 are the control inputs. Figure 3-8 to Figure 3-10 demonstrate the state history. Figure 3-11 to Figure 3-12 show the minimized performance index γ.

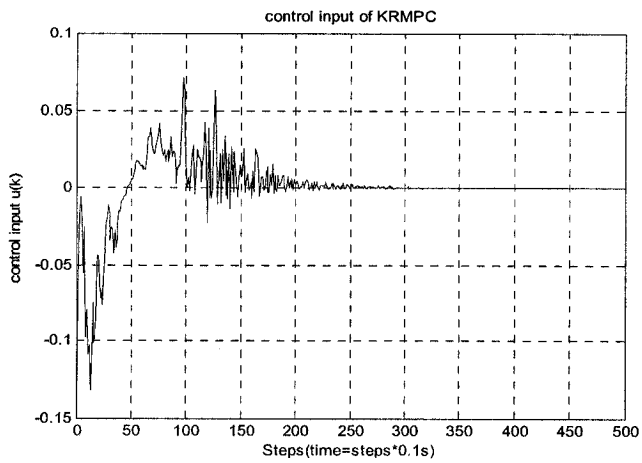

Figure 3-5 Control input of KRMPC

Reproduced with permission of the copyright owner. Further reproduction prohibited without permission.

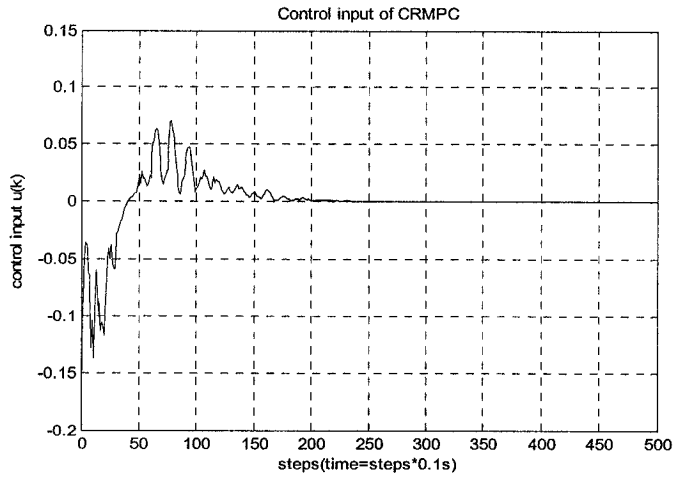

Figure 3-6 Control input of CRMPC

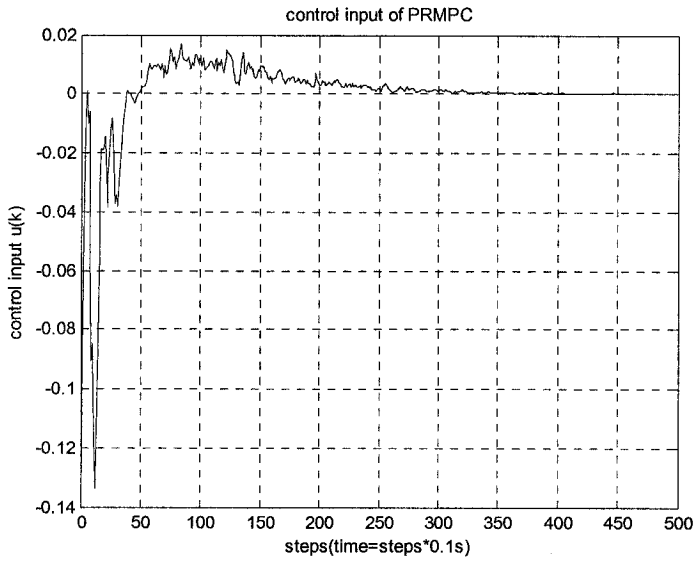

Figure 3-7 Control input of PRMPC

From above Figure3-5, 3-6 and 3-7, one can see that at the beginning, CRMPC has smoother control input evolution than KRMPC and PRMPC. But at the end (after 200 iterations), the control signals of all three RMPCs vibrate within relatively limited amplitudes. PRMPC has longer settling time than KRMPC and CRMPC, because it is

Reproduced with permission of the copyright owner. Further reproduction prohibited without permission.

designed with less computational load for application to online feedback control while sacrificing some performance of convergence speed. However, for the PRMPC, it has been mathematically proved that its robust stability property is ensured, see section 3.5.

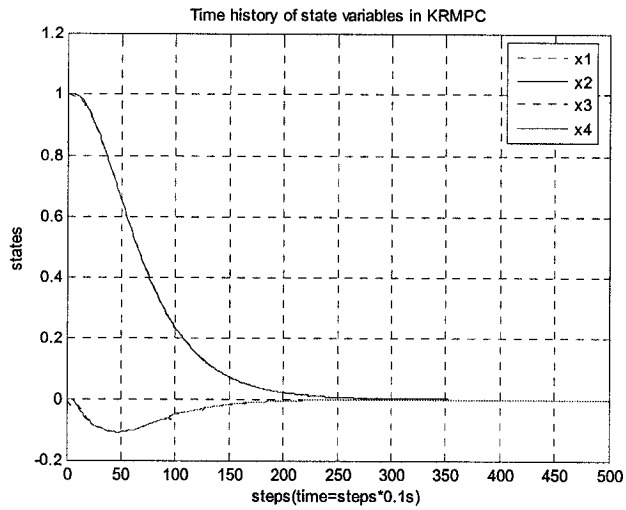

Figure 3-8 States of KRMPC

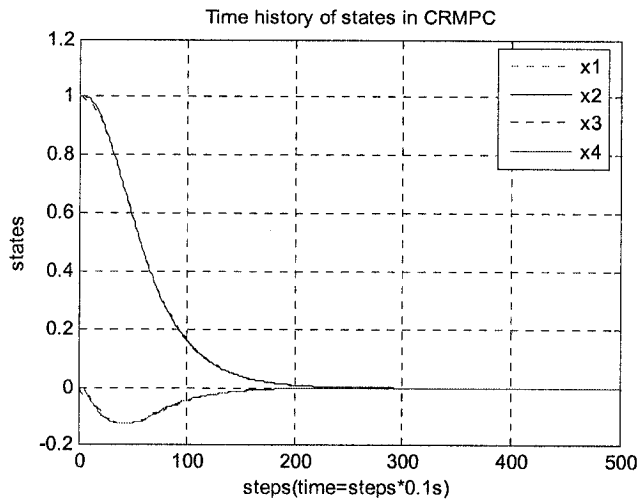

Figure 3-9 States of CRMPC

Reproduced with permission of the copyright owner. Further reproduction prohibited without permission.

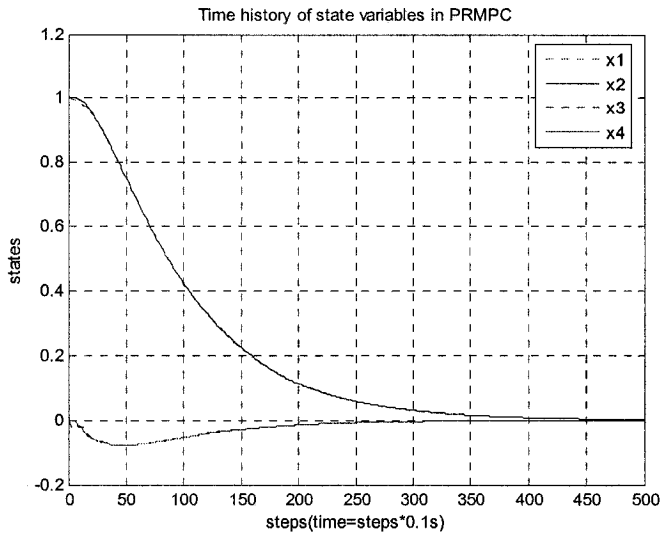

Figure 3-10 States of PRMPC

Obviously, CRMPC has faster convergence of states than KRMPC and PRMPC. PRMPC needs almost 400 steps to reach desired state in this example. Note that unit of x-axis is iteration steps. Because sampling interval is 0.1 second, time is equal to iteration step times by 0.1 second. Although CRMPC has best convergence, it suffers the heaviest computational load than other two RMPCs, which will be explained in later section.

As for the minimized performance index, only figures of KRMPC and CRMPC are shown (see Figure3-11 and Figure3-12). Because PRMPC uses different algorithm, it does not need to compute the same performance index in the step-by-step optimization. Similarly, the computation of the minimized index β is needed for PRMPC and shown in Figure 3-13. CRMPC starts from lower γ (200.43) and KRMPC from bigger γ (279.75), then CRMPC converges to near to 0 at 10 seconds (100 steps) while KRMPC at 12 seconds (120 steps).

Reproduced with permission of the copyright owner. Further reproduction prohibited without permission.

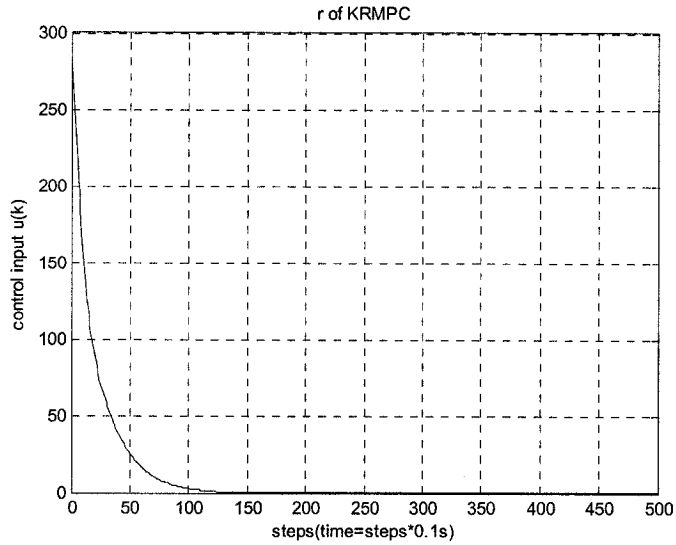

Figure 3-11 Minimized performance index (γ) of KRMPC

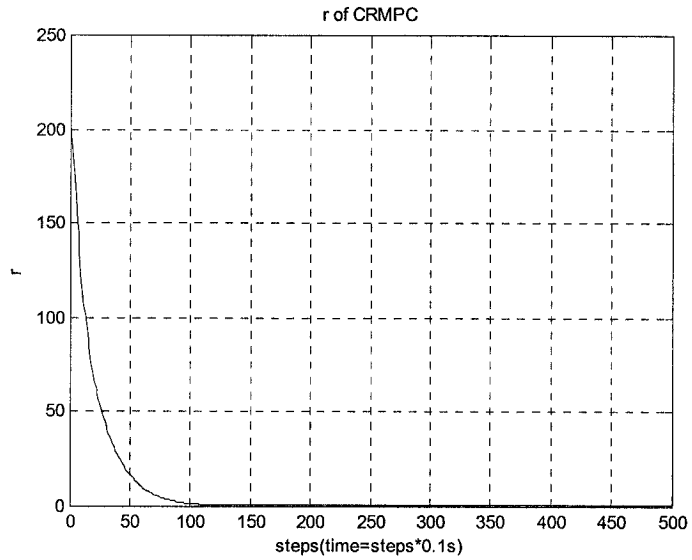

Figure 3-12 Minimized performance index (γ) of CRMPC

Reproduced with permission of the copyright owner. Further reproduction prohibited without permission.

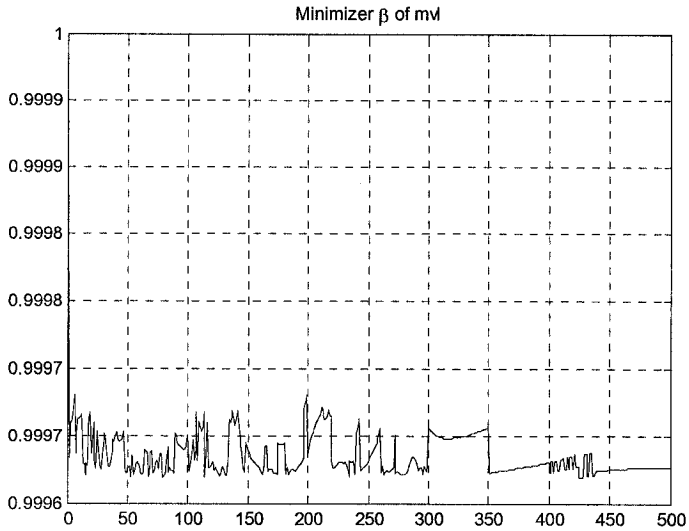

Figure 3-13 Minimized index (β) of PRMPC

3.7.3 LQR control

As mentioned section 3.2, one method to deal with limited uncertainty is the stochastic control, such as LQR and LQG, in which uncertainties in the system are modeled as probability distributions (not arbitrary distributions). In order to verify distinct characteristics of RMPC compared to stochastic optimal control LQR, LQR method has been applied in the same two-mass-spring system with same initial conditions. The simulation results are shown as following Figure 3-14 to 3-17.

Reproduced with permission of the copyright owner. Further reproduction prohibited without permission.

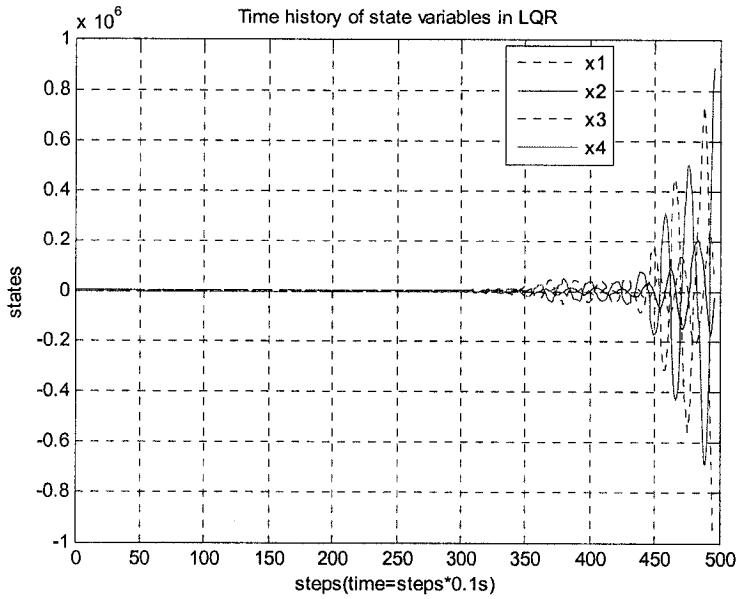

Figure 3-14 States of LQR

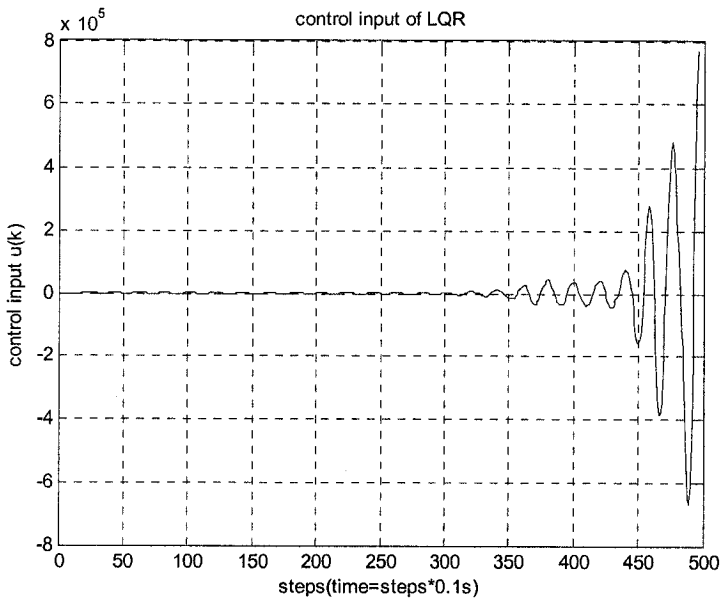

Figure 3-15 Control input of LQR

From the above simulation results, one can see both the states and control input diverge quickly as system parameter is varying. Therefore the conclusion is drawn that

Reproduced with permission of the copyright owner. Further reproduction prohibited without permission.

LQR method does not work in this two-mass-spring LPV system at all. But if simulation condition is changed, i.e., if system parameters variation is known for LQR in advance, the results are totally different with Figure 3-14 and Figure 3-15.

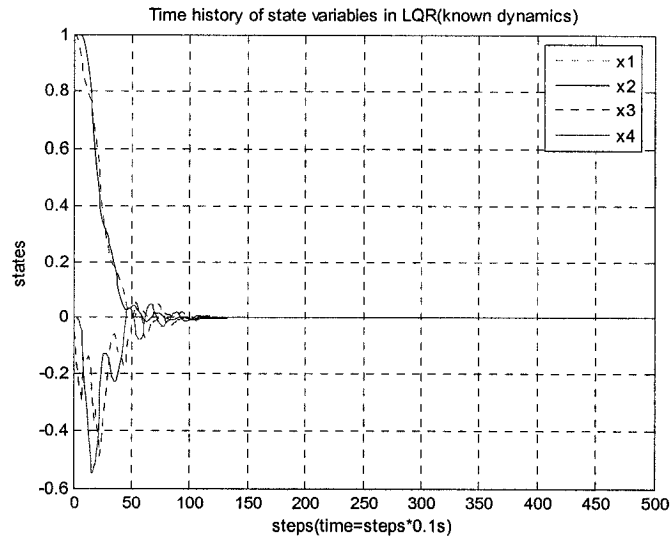

Figure 3-16 States of LQR (known variation of dynamics)

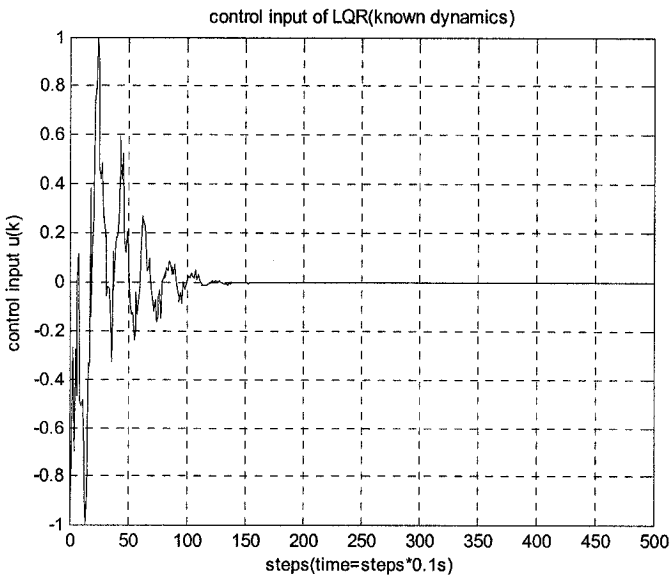

Figure 3-17 Control input of LQR (known variation of dynamics)

Reproduced with permission of the copyright owner. Further reproduction prohibited without permission.

From Figure 3-16 and Figure3-17, one can see that LQR method even has better control performance than the previous KRMPC, PRMPC or CRMPC. But note that there is a prerequisite for these simulation results. In fact, in Figure3-16 and Figure3-17, there is no uncertainty of system dynamics at all. In other words, it means if the system parameters are completely known at every sampling instant, then LQR can work well. In LQR computation, the first step is to solve the discrete-time Riccati equation [67] based on definite system model, and then obtain the optimal feedback gain, and finally apply this constant feedback gain to stabilize the controlled system.

Some characteristics of LQR are concluded here:

(1) LQR is a model-based optimization method, and hence it cannot deal with neither time-varying uncertainty nor input and output constraints systematically. The simulations have shown that for the controlled system with polytopic uncertainty (as in Figure3-14 and 3-15) or with system constraints (plots are omitted here), LQR controller makes the controlled system unstable.

(2) LQR is a faster algorithm compared to RMPC, but it can not guarantee the robust stability globally due to its inability for LPV system and deficiency for any future prediction as system dynamics varies.

All the simulation results are summarized in Table.3-1 for purpose of performance comparison. For LQR, the results are based on Figure 3-15 and 3-16. The total computation time of PRMPC is only 19% of KRMPC and 4% of CRMPC, respectively,

Reproduced with permission of the copyright owner. Further reproduction prohibited without permission.

which means 5.25 times faster than KRMPC and 24.8 times faster than CRMPC, so that the computational efficiency is greatly improved.

Table 3-1 Comparison of three RMPCs and LQR

Compared items	KRMPC	CRMPC	PRMPC	LQR
Starting value of upper bound index (γ)	279.74	200.43	279.74	N/A
Total Computation time (seconds)	1260	5947.8	239.92	61.3
Average computation time per iteration (seconds)	2.52	11.90	0.48	0.12

Note that in table 3-1, it seems that average computation time per iteration is larger than sampling time (0.1 second). For online control application, this computation time should be less than sampling time. Considerations about this are addressed as follows:

(1) The simulated programs are Matlab-based and not compiled executable programs. Thus, its computation is certainly slower than the compiled ones.

(2) The computation is executed in the computer of a student lab. In practice, improvements on both computational hardware and software are possible to express the whole computation.

Reproduced with permission of the copyright owner. Further reproduction prohibited without permission.

3.8 Trajectory tracking

The two basic control applications are regulation and tracking. The above two-mass-spring example is a regulation problem, which means that given a controlled system, controller should try to make the system states return to equilibrium point in spite of system dynamics variation or uncertainties. But for trajectory tracking problem, it starts from initial conditions (normally at equilibrium point), control system will drive the states to the required set point. Figure 3-18 shows simulation results using KRMPC algorithm, in which starting point is at [0;0;0;0] and set point is at [1;1;0;0;].

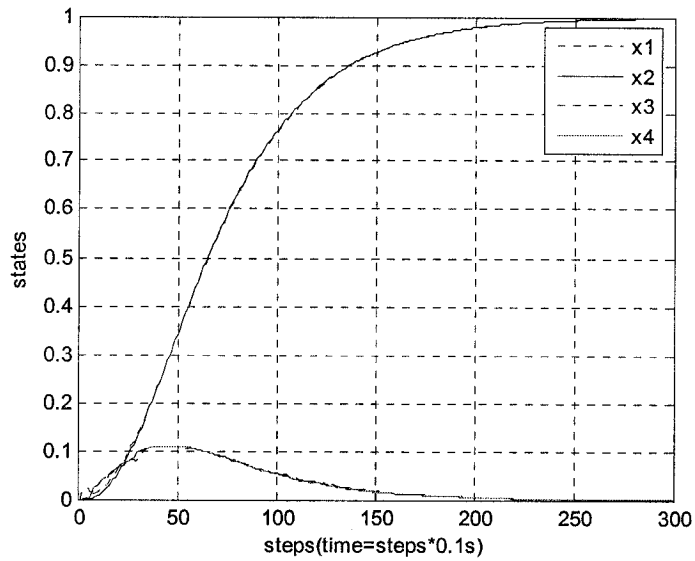

Figure 3-18 States history of tracking example

Reproduced with permission of the copyright owner. Further reproduction prohibited without permission.

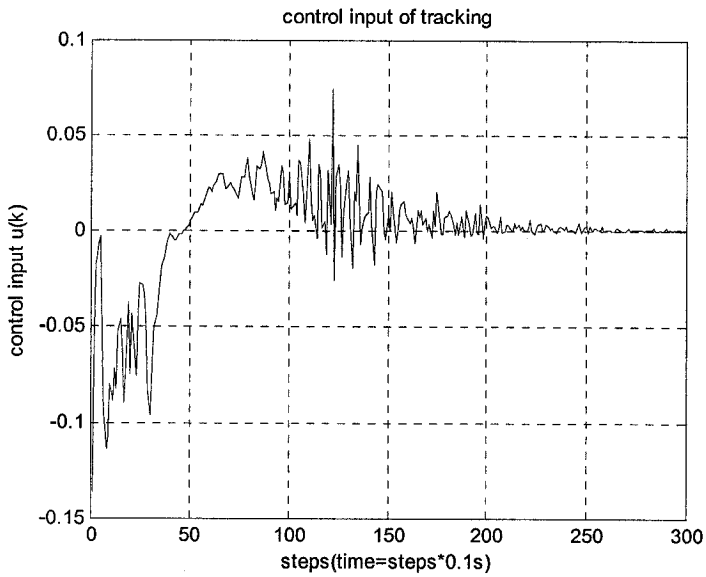

Figure 3-19 Control input of tracking example

3.9 Conclusion

This chapter starts from modern control development history and introduction of system with uncertainty and disturbance. Three different system definitions: LPV, LTI and LTV are given. And the stable and faster PRMPC has been proposed to handle LPV system with input and output constraints efficiently and effectively. Three RMPCs have been tested and compared in a benchmark example. Through simulation results, it is concluded that all of three RMPCs can work with LPV system while LQR can not deal with LPV system. The proposed PRMPC does save lots of computational time and is proved to be more practical for online control application compared to two other RMPCs.

Reproduced with permission of the copyright owner. Further reproduction prohibited without permission.

Chapter 4
Active Shimmy Control Design

As the simulation results demonstrated in section 3.7.3, LQR may be designed based on known variation of dynamics within some certain operation ranges. In practice, a more robust control design is in need for dealing with wider operation range while considering the system input and output constraints. In this chapter, the proposed PRMPC algorithm is applied to accommodate online landing gear active shimmy control. Considering the linearized shimmy dynamics Eqs. (2-17) and (2-18), one may find out that landing gear shimmy system is a typical LPV system since state matrix A changes with taxiing velocity.

4.1 Control objective

The objective of active shimmy control is to asymptotically suppress yaw vibration with less overshoot and short settling time during landing process and to robustly stabilize the system despite the taxiing velocity varying from 80 m/s to 20 m/s. The control input constraint $\|u(k+i\,|\,k)\|_2 \le 0.5$ rad/Nm and output constraint $\|y(k+i\,|\,k)\|_2 \le 1$ radian should always be satisfied. And the index β is to be minimized at every sampling interval to guarantee the robust stability with respect to the varying parameter and the external disturbance.

Reproduced with permission of the copyright owner. Further reproduction prohibited without permission.

In terms of LPV controller design, given a system described by $x_{k+1}=A(V)x_k+Bu(k)$ with initial deviation x_0, to find a feedback control law u such that the closed-loop system state x_k tends to near 0 in desired time .

4.2 LPV polytope design

In last chapter, through a two-mass-spring example, three RMPCs are demonstrated dealing with LPV system very well. Note that in the linearized landing gear state-space equations (2-157) and (2-157), there are two coupled parameters V and $1/V$. Although the involved LMIs computation in RMPC is identified as a convex optimization, taxiing velocity is not ready to be incorporated into RMPC computation because V-$1/V$ curve is not a convex set (see the definition of convex set in Appendix F).

Prior to the design control law of RMPC, a convex polytope must be constructed to cover whole range of V-$1/V$. The design criterion for constructed convex polytope is subject to maximum-minimum rule: (1) The constructed polytope should cover maximum variation range of parameters; (2) This polytope should be designed with minimum area (for two-dimension polytope) or volume (for three-dimension polytope). The first criteria is to ensure control system global stability and the second one is to ensure that this polytope is the closest to varying parameters to obtain most suitable feedback gain and less computational load.

In [31], one design technique to construct this kind of convex polytope was presented although this technique was used in H-infinity controller design.

Reproduced with permission of the copyright owner. Further reproduction prohibited without permission.

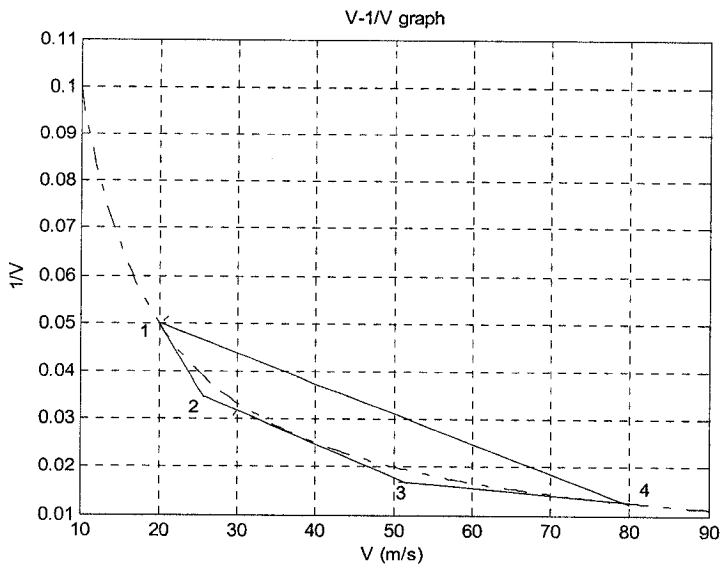

Figure 4-1 Constructed (V-1/V) convex polytope

The constructed convex polytope(1,2,3,4) in the above figure is explained as follows: Line 1-4 is the connection between maximum and minimum velocity; line1-2 tangent to hyperbola at 1; line 3-4 tangent to hyperbola at 4; line 2-3 is parallel to line1-4 and tangent to hyperbola. This polytope covers the whole range of varying parameters $(V, 1/V)$. Then according to the characteristic of convex set, any point P on the curve $(V, 1/V)$ can be expressed as the linear combination of four vertexes P_1, P_2, P_3 and P_4 of quadrangle, which means

$$P = \alpha_1 P_1 + \alpha_2 P_2 + \alpha_3 P_3 + \alpha_4 P_4$$

$$(\alpha_1 + \alpha_2 + \alpha_3 + \alpha_4 = 1, \alpha_1, \alpha_2, \alpha_3, \alpha_4 > 0) \qquad (4\text{-}1)$$

Although P can be expressed as linear combination of P_1 to P_4, the solution of real number to α_1 to α_4 in the (4-1) is not always easily obtained and sometimes it is

Reproduced with permission of the copyright owner. Further reproduction prohibited without permission.

unsolvable. Fortunately, from the derivation in Chapter 3, one can see α_1 to α_4 is not needed for the related LMIs computation. On the contrary, only four vertices value of P_1 to P_4 will be involved in that computation. Although this is conservative for the controller design, it assures robust stability globally.

4.3 Shimmy control system design

In this section, all control system design details are addressed and explained.

4.3.1 Closed-loop system parameters

The linearized landing gear system is described in open-loop state-space equations as in (2-157) and (2-157). In order to introduce state-feedback control, one needs to introduce external control force/torque and then normalize in discrete time domain in compliance with controller design as following equation (4-2) and (4-3). Note that because *A(k)* is time-varying, this is a linear discrete-time varying system.

$$x(k+1) = A(k)x(k) + Bu(k) \tag{4-2}$$

$$y(k) = Cx(k) \tag{4-3}$$

The parameters in the above system control equations are to be defined for further design:

(1) System matrix *A(x)* is known in continuous-time domain as in equation (2-18).

(2) Vector *B* is to be decided. In this thesis, it is assumed that when applying external force/torque to steer the landing gear, the landing gear will respond with some yaw angle. Referring to torsional spring rate *k* (=10000 Nm/rad) (see the List of

Reproduced with permission of the copyright owner. Further reproduction prohibited without permission.

Symbols), without loss of generality, B was chosen as $\begin{bmatrix} 0 \\ 13950 \\ 0 \end{bmatrix}$ for controller design. In practice, this coefficient matrix depends on output and input relationship of actuator.

(3) Because the output of landing gear is the yaw angle, the output vector C is chosen as $[1 \quad 0 \quad 0]$.

(4) Eqs. (2-157) and (2-18) is described in continuous-time domain. However, the robust model predictive controller is designed based on the discrete-time model. To design an active shimmy controller, the continuous-time model has to be transformed to discrete-time model. In order to transform it to discrete-time domain, the Euler first-order approximation is introduced to equations (2-157) and (2-18). The discreet-time equations are shown in form of equations (4-2) and (4-3).

4.3.2 Functional scheme of shimmy control system

The functional scheme of shimmy control system is described as Figure 4-2. Firstly, at every sample interval, the present yaw angle is measured. If it is desirable, no control action will be taken. Otherwise, we have to measure full states ($\psi, \dot{\psi}$, y) to calculate suitable control input by online RMPC algorithm. Then the computed control input is applied to landing gear steering actuator to correct yaw orientation. Because of robust

Reproduced with permission of the copyright owner. Further reproduction prohibited without permission.

stability characteristic of RMPC, the controller can stabilize the system at the equilibrium point in spite of varying dynamics and disturbance.

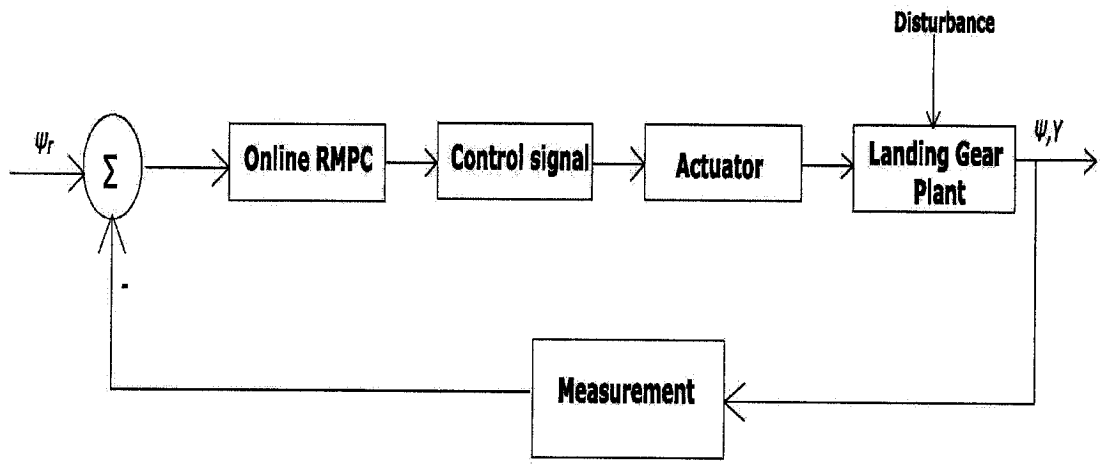

Figure 4-2 Functional scheme of shimmy control system

4.3.3 State-feedback control system configuration

A robust control system exhibits the desired performance despite the presence of significant plant uncertainties. A control system is said to be robust when it is stable over the range of parameter variations and the performance continues to meet the specifications in the presence of a set of changes in the system parameters. In this thesis, the robust control system aims at dealing with taxiing velocity variation and external disturbance, its state-feedback control system configuration is shown in Figure 4-3.

Reproduced with permission of the copyright owner. Further reproduction prohibited without permission.

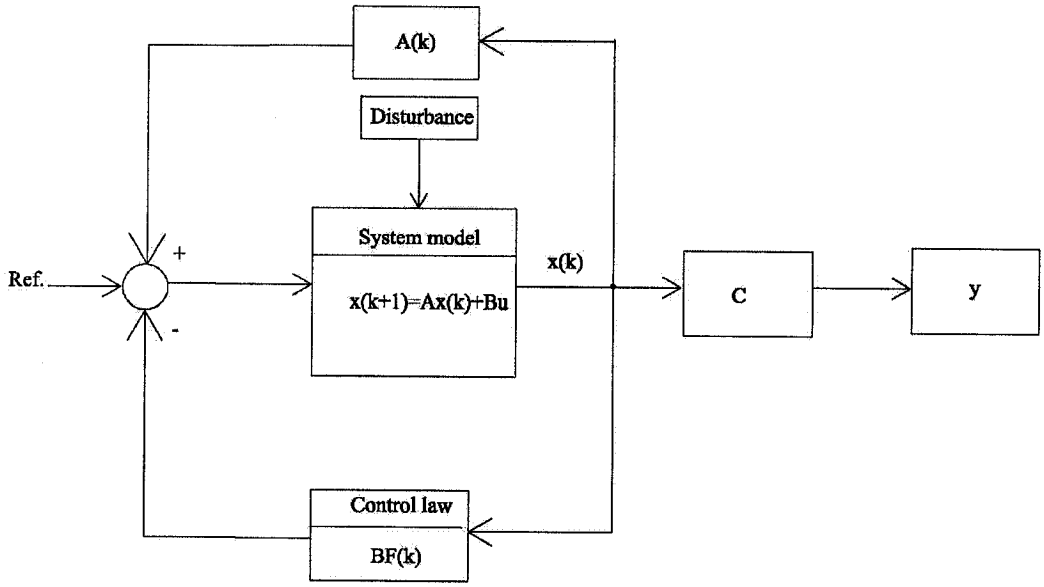

Figure 4-3 State-feedback control system configuration

4.3.4 Cost function and constraints

In the landing gear shimmy control design, the computational efficiency and the disturbance rejection ability should be emphasized due to the online control demand. RMPC is a powerful online optimal control with ability of disturbance rejection. However, its disadvantage is that computational load is too heavy to be implemented for online application. One way is to use offline RMPC to improve computational efficiency, but it is hard to handle the unexpected varying parameters or disturbance, thus PRMPC proposed in chapter 3 is chosen as active shimmy control algorithm.

The robust performance objective is chosen as

$$\min_{u(k+i|k)} \max_{[A(k+i),B(k+i)]\in\Omega} V_{\infty}(k) \tag{4-4}$$

Reproduced with permission of the copyright owner. Further reproduction prohibited without permission.

where $V_\infty(k) = \sum_{k=0}^{\infty}[x(k+i\mid k)^T Q_w x(k+i\mid k)] + [u(k+i\mid k)^T R_w u(k+i\mid k)]$; $Q_w>0$ and $R_w>0$, are two weighting matrix.

The input and output constraints are:

$$\left\|u(k+i\mid k)\right\|_2^2 = u_{\max} = 0.5 \ (i\geq 0) \tag{4-5}$$

$$\left\|y(k+i\mid k)\right\|_2^2 = y_{\max} = 1 (i\geq 0) \tag{4-6}$$

In simulation, all above LMIs are coded in Matlab software combining with YALMIP toolbox. The details about algorithm of PRMPC refer to section 3.5.

4.4 Simulation results

For online control design purpose, the simulation results are shown in real time with the sampling interval 0.005 second. Furthermore, although some disturbance rejection ability of RMPC was claimed in [34], few simulation results with disturbance were found in literature. Computational efficiency is to be verified in shimmy control application with comparisons between proposed PRMPC and other two RMPCs.

4.4.1 Simulation environment

- Hardware: Dell Workstation PWS370; Intel Pentium 4 CPU 2.80G Hz; 512 MB RAM; Hard disk 250 GB; Windows NTFS file system.
- Software: Windows XP (SP2), Matlab 7.0.1(R14) SP1, YALMIP LMI Toolbox V3 (R14SP3).

Reproduced with permission of the copyright owner. Further reproduction prohibited without permission.

4.4.2 Open-loop system response

First of all, the open-loop system response with initially disturbed states is simulated with different taxiing velocity. In Figure 4-4 and Figure 4-5, taxiing velocity is 20 m/s and initial Yaw Angle are 0.1 radian and 1 radian respectively, the system oscillates and can not get to equilibrium quickly during simulation time. In Figure 4-6 and Figure 4-7, the system becomes unstable and yaw angle diverges quickly to infinity with same taxiing velocity 80 m/s but with different initial yaw angle 0.1 radian and 1 radian respectively. The instability of the system is verified by checking the system's poles and zeros. It is found that there are two unstable poles (beyond unit cycle) in this circumstance, which are shown in Figure 4-8.

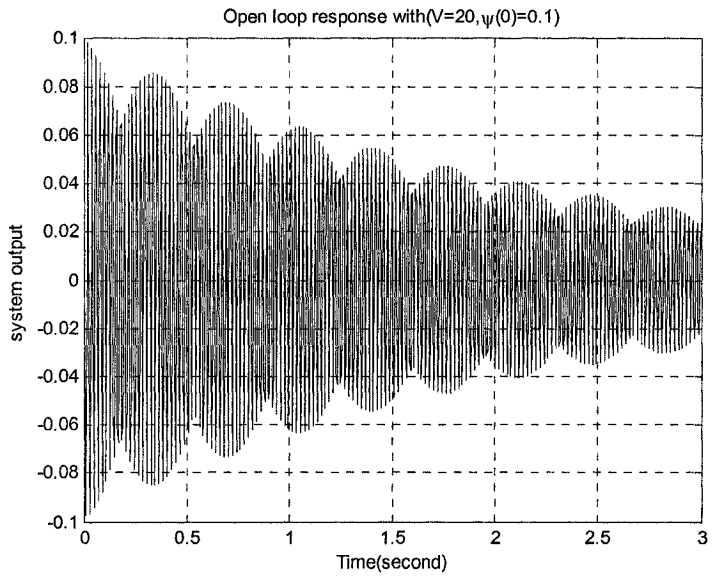

Figure 4-4 Open-loop response when V=20m/s, ψ(0)=0.1rad

Reproduced with permission of the copyright owner. Further reproduction prohibited without permission.

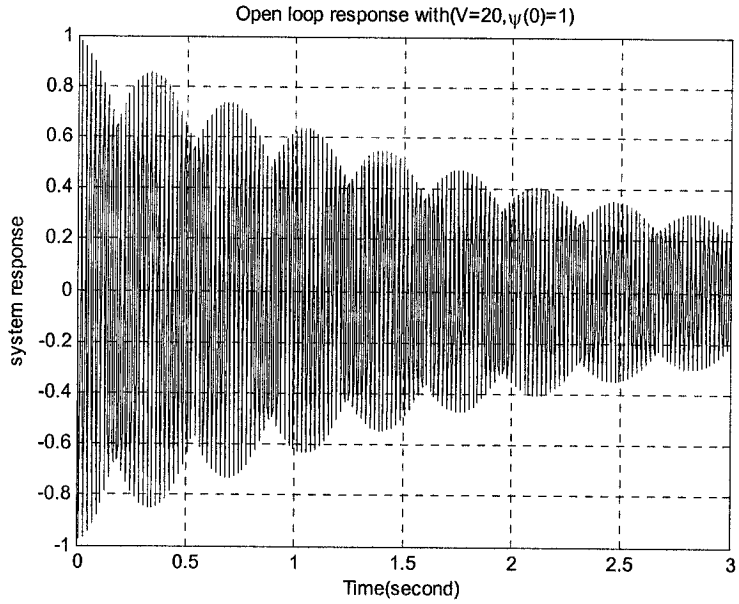

Figure 4-5 Open-loop response when V=20m/s, ψ(0)=1rad

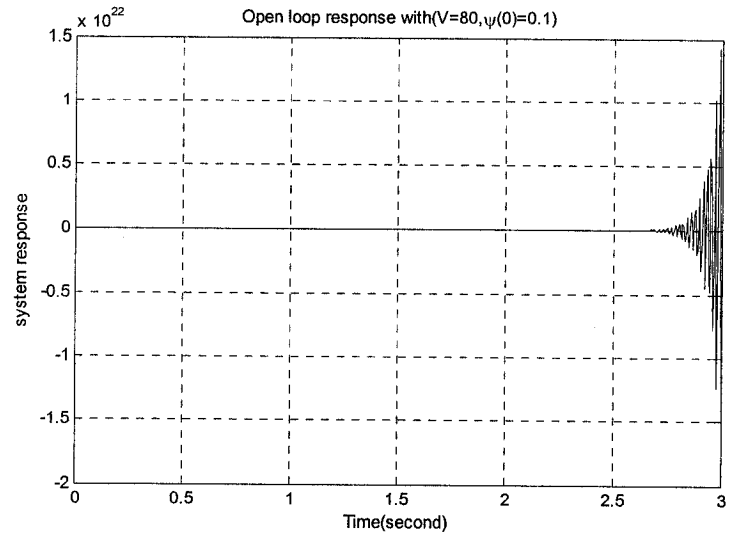

Figure 4-6 Open-loop response when V=80m/s, ψ(0)=0.1rad

Reproduced with permission of the copyright owner. Further reproduction prohibited without permission.

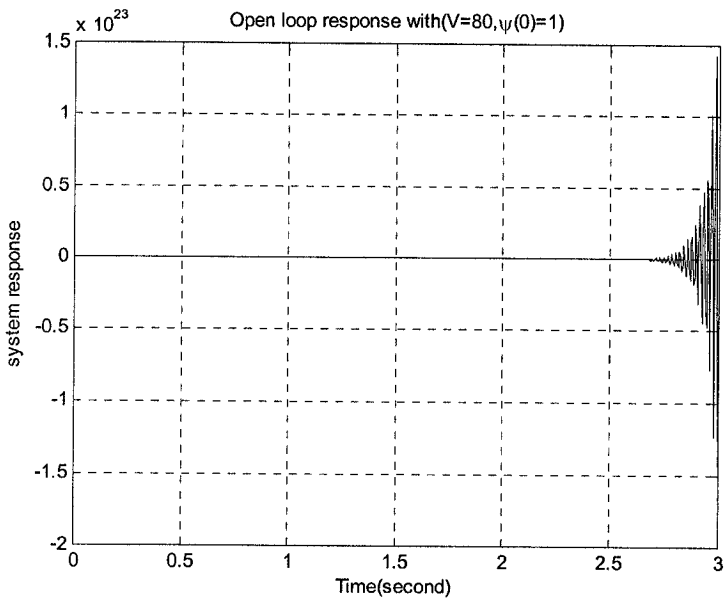

Figure 4-7 Open-loop response when V=80m/s, ψ(0)=1 rad

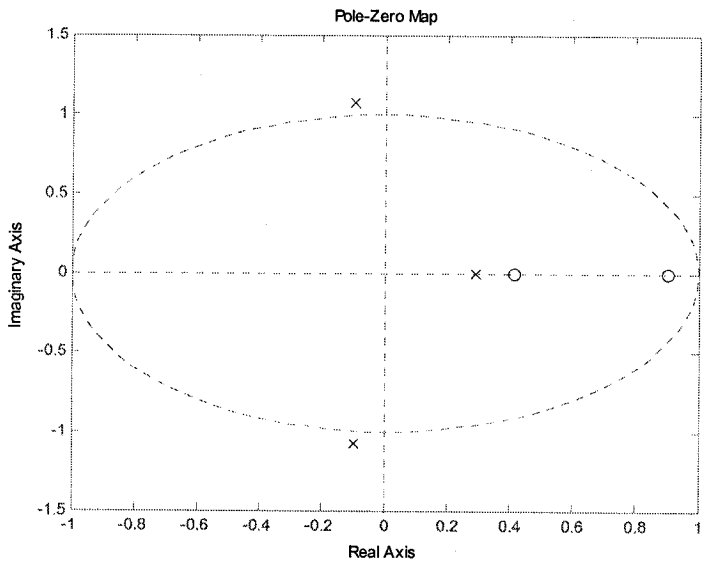

Figure 4-8 Pole-zero map when V=80 m/s

Reproduced with permission of the copyright owner. Further reproduction prohibited without permission.

4.4.3 Design parameters tuning

Tuning the design parameters to achieve better performance is important in the design stage. During parameters tuning, one trick is how to find first feasible solution of related LMIs, which is based on trial-and-error and sometimes tedious. But once the first feasible solution is found, the iterations can always carry on.

There are four important design parameters to be tuned: weighting matrixes, control input maximum, system output maximum and sampling time. Normally speaking, increasing control input weighting matrix reduces control activity and degrades feedback effect; decreasing control maximum value can lead to smoother control; sampling time is critical to solutions of LMIs, shorter sampling time assures online control reliability and global stability. According to Shannon's Sampling theorem, normally the sample rate is chosen 5 to 10 times the signal bandwidth (at least two times). All tuned parameters have to assure feasible solution to LMIs. The finally chosen design parameters are listed in the following Table 4-1.

Reproduced with permission of the copyright owner. Further reproduction prohibited without permission.

Table 4-1 Shimmy control system design parameters

Discretization method	Euler's first-order approximation
System sampling time	0.005 second
Maximum control input (rad /second Nm)	0.5
Maximum system output (radian)	1
Disturbed initial condition	Yaw Angle: 1 radian Lateral Deflection: 0.05 metre
Weighting Input coefficient R_w	1
Weighting Output Matrix Q_w	0.0001*I(3X3)

4.4.4 Simulation without disturbance

In practice, there is always disturbance into controlled system, so simulation with disturbance is always necessary. For the comparison of system response, firstly the system is simulated without disturbance. In the next section, system with disturbance will be simulated. Three RMPCs: KRMPC, CRMPC and PPRMPC are designed and simulated for landing gear shimmy suppressing based on same system model. Corresponding simulation results are collected and listed in Table 4-2. From Table 4-2, one can find out that the total computation time and average computation time per iteration of PRMPC are only 40.6% of KRMPC and 5.5% of CRMPC, which means 2.4 times faster than KRMPC and 17.9 times faster than CRMPC, respectively.

Reproduced with permission of the copyright owner. Further reproduction prohibited without permission.

Table 4-2 Comparison of three RMPCs

Compared items	KRMPC	CRMPC	PRMPC
Starting value of upper bound index (γ)	5537.6	1146.6	5537.6
Total Computation time (seconds)	63.5	465.3	25.8
Average computation time per iteration (seconds)	1.27	9.31	0.52

As claimed in Chapter 3, the PRMPC is based on the concept of invariant ellipsoid and contracted PDM. At first glance, it seems that there are more LMIs to be solved than those in KRMPC and CRMPC (total is 10 LMIs in PRMPC while KRMPC 4 and CRMPC 4), but in fact there are only 4 simpler LMIs computed in every iteration step. The LMIs (3-19), (3-23) , (3-26) and (3-27) just run once out of loop, and then solutions of Q and Y are saved. LMIs (3-28) to (3-31) are solved in loop, and a contracted $Q(k)$ can be solved at every sample interval and used for feedback-gain computation. Because LMIs (3-28) to (3-31) only run in simpler and smaller-dimension convex optimization, there is less computational load and it is the fastest algorithm among three RMPCs.

Reproduced with permission of the copyright owner. Further reproduction prohibited without permission.

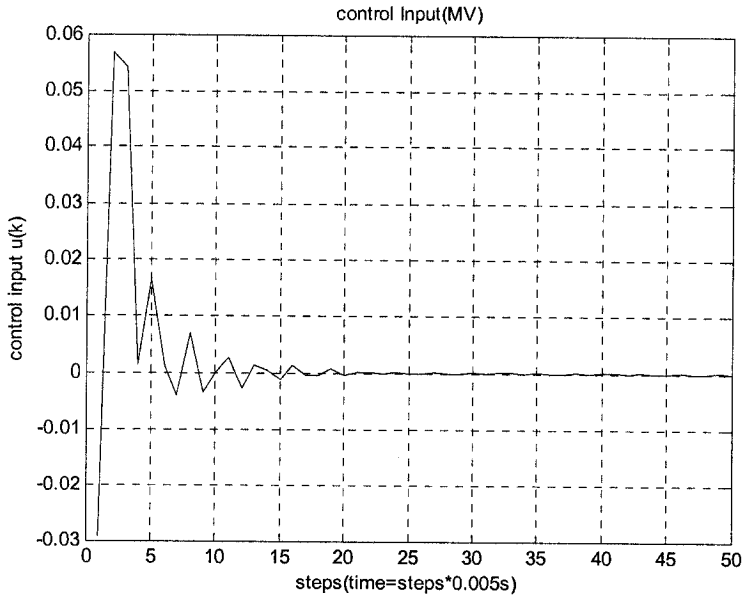

Figure 4-9 Control input of KRMPC

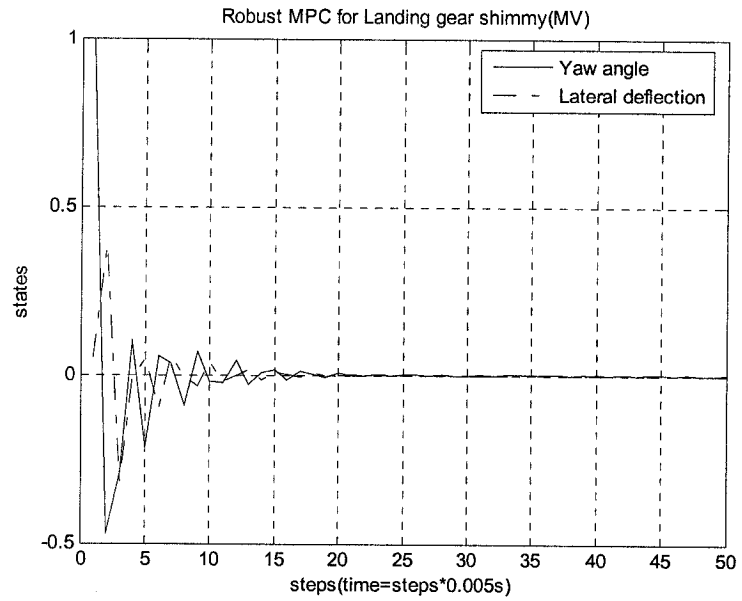

Figure 4-10 State history of KRMPC

Reproduced with permission of the copyright owner. Further reproduction prohibited without permission.

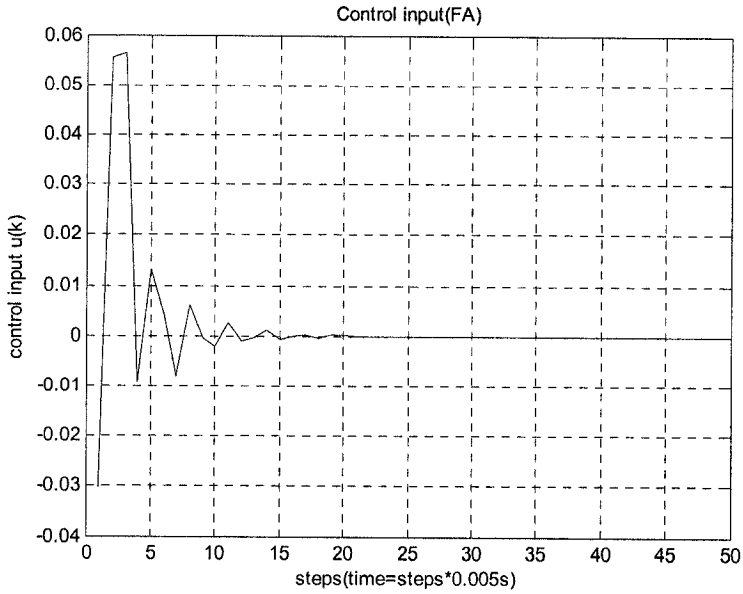

Figure 4-11 Control input of CRMPC

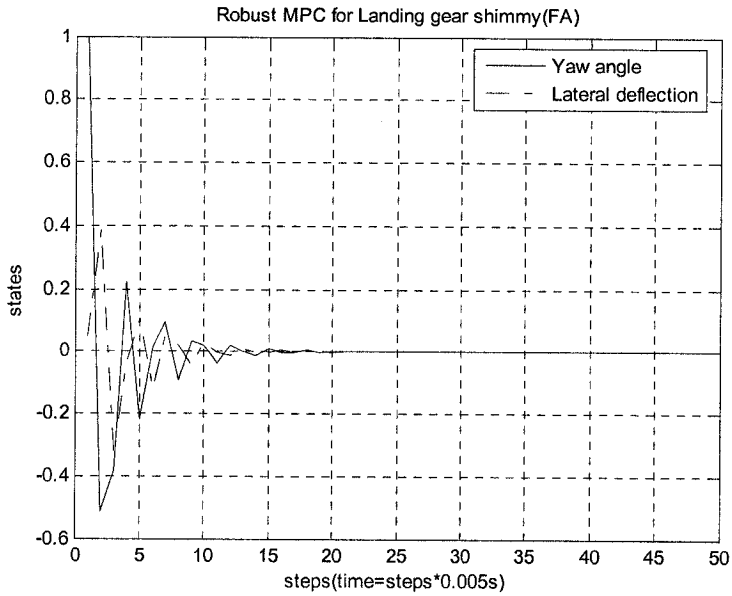

Figure 4-12 State history of CRMPC

Reproduced with permission of the copyright owner. Further reproduction prohibited without permission.

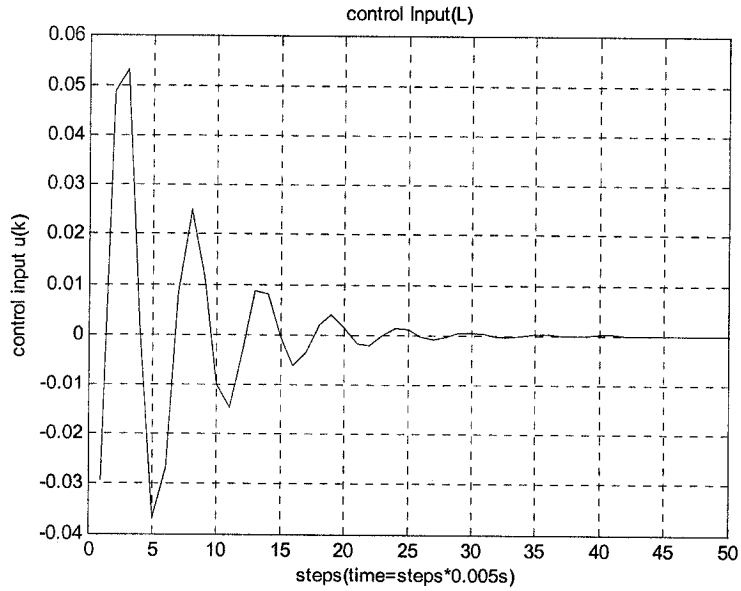

Figure 4-13 Control input of PRMPC

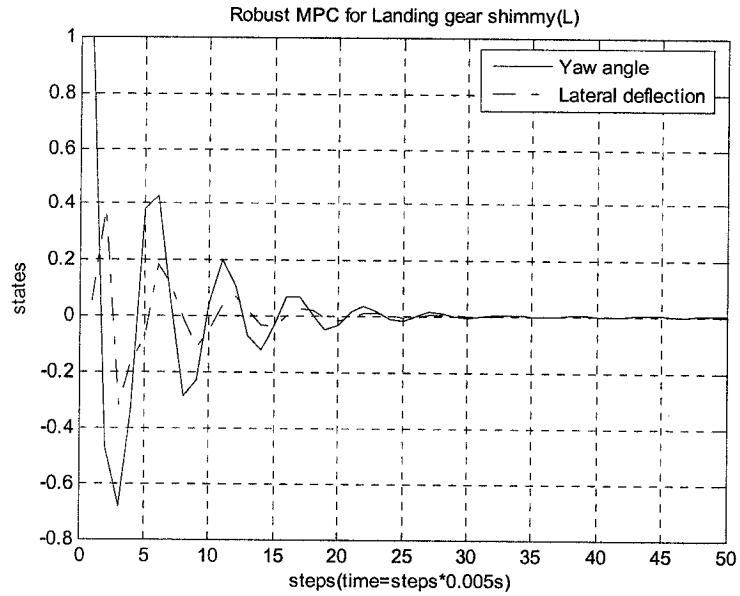

Figure 4-14 State history of PRMPC

Reproduced with permission of the copyright owner. Further reproduction prohibited without permission.

In section 4.5.2, the open-loop response of landing gear system is shown oscillatory and unstable without any control action. Figure 4-9 to Figure 4-14 show the control effect of all three RMPCs. Some points about simulation results are summarized.

(1) RMPC feasibility depends on possibility of solution of LMIs. Although the mathematical feasibility is proved in [34], but this feasibility exists only after the first feasible solution has been obtained. Otherwise, the LMIs optimization can never be carried out.

(2) The starting value of minimized index γ depends on system dynamics, initial condition and related algorithm. According to [25], the problem formulation of KRMPC tends to be somewhat conservative. From Table 4-2, CRMPC starts from a less value than KRMPC and PRMPC, but suffers heavier computational burden, which leads to longer total computational time and average computational time per loop.

(3) Obviously, the states convergence of CRMPC is a little better than KRMPC and PRMPC. Although CRMPC introduces another matrix variable (referring to [33][34]) , the control effect of CRMPC is not likely as good as claimed in two mass-spring system of Chapter 3. PRMPC is similar to KRMPC, but with less computational time.

(4) Referring to [33], because Q_j in the LMI (3-32) means four symmetric matrixes with respective to vertexes of convex polytope, 12 LMIs have to be solved to get control feedback gain $F(=YG^{-1})$ in CRMPC at every iteration step. According to LMI optimization theory [29], the fastest Interior Point algorithm's computation effort grows with (MN^3), where M is the total row size of LMIs and N is the total number of decision

Reproduced with permission of the copyright owner. Further reproduction prohibited without permission.

variables. Consequently, there are far more row sizes of LMIs and decision variables in CRMPC, thus the computational time of CRMPC is much longer than that of KRMPC and PRMPC.

(5) RMPC can deal with multi-parameter varying system. For example, one may simulate the controlled system with varying torsional damping constant c in Eqs. (2-18), and it was observed that RMPC still works (the plots are omitted here).

4.4.5 Simulation with disturbance:

Many control systems in practice tend to be disturbed. The common external disturbance signals for landing gear are crosswind and rough runway. When the aircraft experiencing any external disturbance (i.e. pot holes, cracks, and unevenness), the landing gear body should not have large oscillations and oscillations should dissipate as quickly as possible. In the following simulations, the landing gear is assumed to taxi along runway with varying taxiing velocity from 80 m/s to 20 m/s within 5 minutes (300 seconds).

The runway disturbance is assumed as a state disturbance to system. In the simulations, the runway disturbance will be approximated by a step input (Figure 4-15 and Figure 4-16) and a sinusoidal input (Figure 4-17 and Figure 4-18), respectively. These two disturbance signals last 10 seconds. The step signal could represent the landing gear coming out of a pothole. The sinusoidal signal could represent continuously uneven runway. In Figure 4-15 and 4-17, the state-feedback controller of PRMPC shows definite disturbance rejection and has less overshoot while it has shorter settling time

Reproduced with permission of the copyright owner. Further reproduction prohibited without permission.

when dealing with step disturbance (as in Figure 4-15) than with the sinusoidal disturbance (as in Figure 4-17).

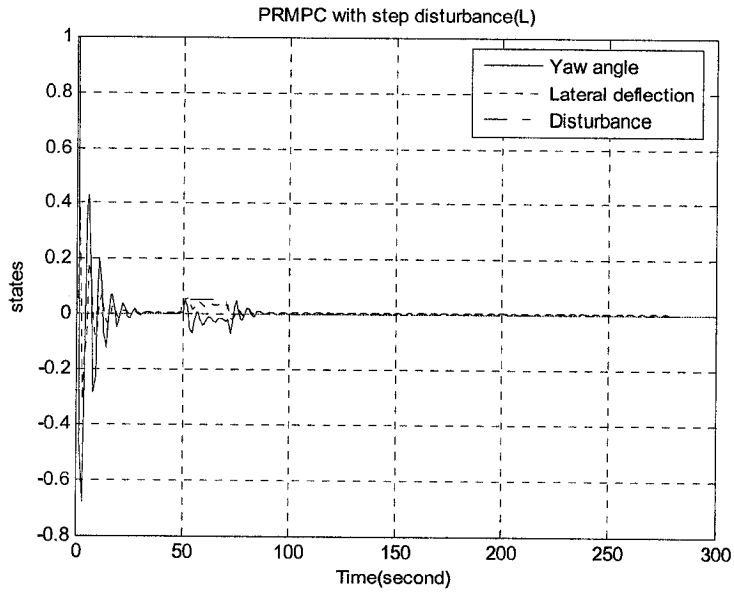

Figure 4-15 State history of PRMPC with step disturbance

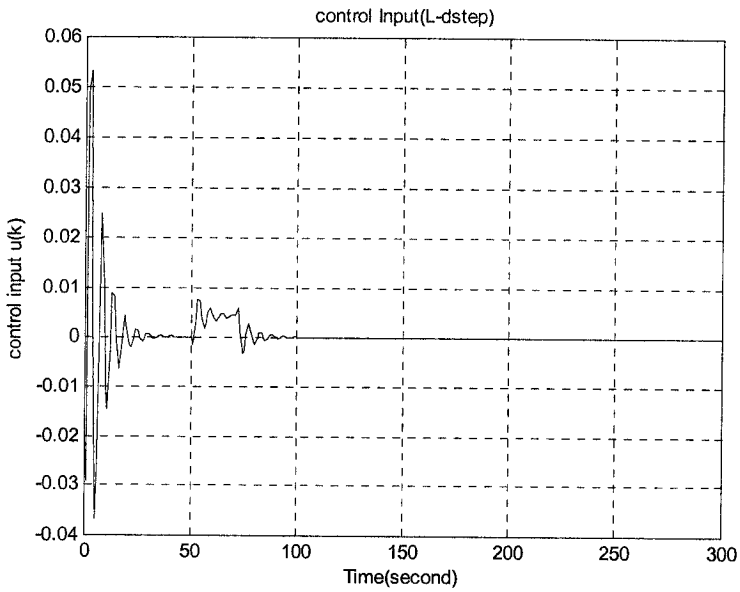

Figure 4-16 Control input of PRMPC with step disturbance

Reproduced with permission of the copyright owner. Further reproduction prohibited without permission.

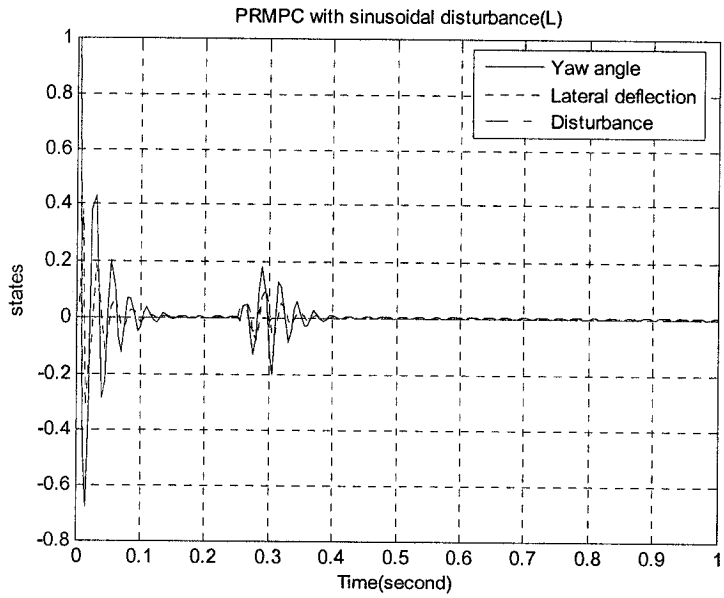

Figure 4-17 State history of PRMPC with sinusoidal disturbance

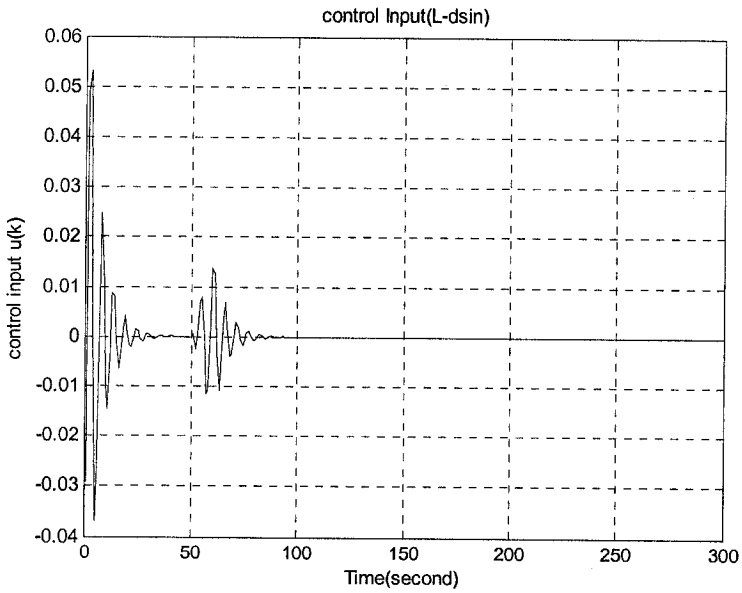

Figure 4-18 Control input of PRMPC with sinusoidal disturbance

Reproduced with permission of the copyright owner. Further reproduction prohibited without permission.

4.5 Implementation considerations

Most light aircraft accomplish nose wheel steering by some form of direct linkage between the nose-wheel and the rudder pedals that allow the nosewheel to be steered when the aircraft is on the ground. For the heavy aircrafts, the nose wheel is steered with hydraulic actuators that are controlled by the pilot, as in Figure 4-19. The proposed active shimmy control system is suggested to be used as an auxiliary-control system whenever shimmy occurs, which could be implemented with external motor drive for light aircraft or integrated into nose wheel steering control system for heavy aircrafts. In this section, I consider more implementation on heavy aircrafts.

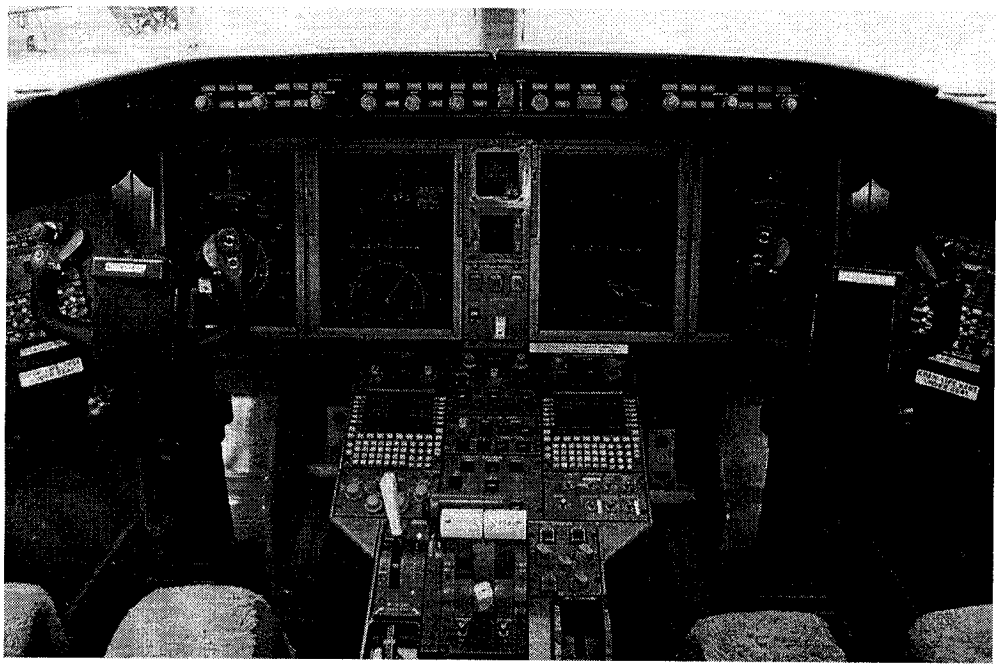

Figure 4-19 Bombardier Challenger 300 cockpit, [72]

Reproduced with permission of the copyright owner. Further reproduction prohibited without permission.

For online application, the control system has to ensure that the computer program executes and responds to plant within a reasonable time. Every control signal computation should be finished within one sample interval.

Hydraulic steering actuator of landing gear might be chosen as controller's actuator. Rotary position sensor is chosen for measuring yaw angle, which normally uses potentiometers, resolvers and a variety of magnetic and capacitive sensors. Angular speed sensor is used for yaw rate and displacement sensor is for lateral deflection. At every sampling instant, these three variables are measured by control system for state-feedback gain computation.

The conceptually chosen sensors and actuator are listed as in following Table 4-3, which are found easily in market. The considered specification of all sensors is a rough description based on assumed performance requirement of control system design. In the engineering practice, many of them may depend on aircraft part or assembly design requirements and different implementation situations.

Reproduced with permission of the copyright owner. Further reproduction prohibited without permission.

Table 4-3 Conceptual choice of sensors and actuator

Item	Type	Specification	Example model
Actuator	Push-pull hydraulic or electrical motor drive	Internal/external	N/A
Angular sensor	Rotary position sensor	Measurement range: -70 to 70 deg. accuracy: 0.5%	Model 0601-0000, Trans_tek, Inc.
Angular speed sensor	Magnetoresistive Wheel-Speed Sensor	Omnipolar, 4.5 V DC to 16 V DC supply voltage, rise time (10 % - 90 %) of 1.5 μs max.	1X Magnetoresistive, Honeywell
Deflection sensor	Linear deflection sensor	Measurement range 0.005-0.5 meter,accuracy: 0.1%, output: voltage	Vishay Model HS25,Intertechnology Inc.

In practice, landing gear design should comply with airplane design regulations, which should be seriously considered by airplane subsystem designers or by control system designers. Here some related essential regulations are cited for directional and lateral controllability for information [74].

(1) Airplane can make turns at a specified bank angle into and away from one or more inoperative engines.

Reproduced with permission of the copyright owner. Further reproduction prohibited without permission.

(2) Airplane can make sudden changes in heading while keeping the wings approximately level.

(3) These required bank angles and changes in heading angle are specified differently in each regulation, depending on the type of airplane.

4.6 Conclusion

In this chapter, the proposed PRMPC is applied to solve landing gear active shimmy suppressing problem. One significant difference between landing gear system and previous two-mass-spring system is that the constructed LPV polytope because varying coupled parameters V-1/V is not ready to be incorporated to convex computation. Through simulations and analysis, PRMPC is proved to be more computation-efficient than other two RMPCs so that PRMPC is more practical for online control application. Besides, PRMPC has been proved to have good disturbance rejection ability. For purpose of future real application, some related implementation considerations are also addressed.

Reproduced with permission of the copyright owner. Further reproduction prohibited without permission.

Chapter 5
Conclusions and Future Work

In this thesis, an active control strategy has been proposed for landing gear shimmy suppressing. From literature review, it is found that active landing gear shimmy control is still an open problem. The research started from a nosewheel shimmy model and its shimmy dynamics analysis and the variation with varying parameters. After applying numerical integration to system dynamic equations, one observed that LCO dramatically varied with parameters torsional damping constant and taxiing velocity. The system stability was found varying with parameters caster length and taxiing velocity after applying the linearization to the nonlinear system. By introducing full-state feedback RMPC controller, the landing gear system is globally stabilized and shimmy oscillation is effectively suppressed. The related state feedback gains are computed step-by-step by online LMI convex optimization. In order to reduce computation burden, a new PRMPC was proposed and proved simpler and faster without loss of robust stability and disturbance rejection ability. The important conclusions from this research are summarized as following.

(1) Linearized landing gear shimmy system is identified as an unstable and oscillating LPV system. In spite of lots of literatures about tire modeling and shimmy investigation, there are few active shimmy control strategies which have been developed. Current shimmy damper and structural hydraulic damping have some

Reproduced with permission of the copyright owner. Further reproduction prohibited without permission.

inherent drawbacks. RMPC-based active control strategy is a robust control design and has been proved effective and more suitable for online LPV system control application.

(2) RMPC can deal with LPV system very well, which are verified in both two-mass-spring system and landing gear shimmy control system by simulation results. RMPC can not only work with single-parameter varying system but also with multi-parameter varying system. Although three RMPCs (KRMPC, CRMPC and PRMPC) can work on LPV system, they have different properties. CRMPC introduces more matrix variables and starts from lower minimized stability performance index but suffers from heavier computational load. PRMPC has the least computation burden without loss of robust stability and disturbance rejection ability for online LPV application. The performance of KRMPC is between CRMPC and PRMPC. It was also proved that conventional LQR control can not work with LPV system at all.

(3) For the landing gear system with varying coupled parameters of V-1/V, in order to apply LMI-based RMPC controller design and related convex optimization, ad-hoc LPV polytope design has been introduced and is proved effective and computation-efficient. The combination of PRMPC and convex polytope design is innovative and can be extended to other similar LPV systems.

(4) Although the whole control system design for landing gear shimmy suppressing is basically a conceptual design, the real implementation has been considered. Not only landing gear shimmy control scheme and control system configurations have been proposed, but also the design parameters tuning guide and even selection of sensors and

Reproduced with permission of the copyright owner. Further reproduction prohibited without permission.

actuators have been recommended. It is expected that this control system design and related implementation considerations might be helpful for the development of next-generation actively controlled landing gear system.

It is the first-time that a conceptual design of landing gear shimmy control has been carried out, so there are certainly many improvements needed in the future work. The following are some recommendations for future work:

(1) Improvement on control algorithm

All KRMPC, CRMPC, or proposed PRMPC methods need online full-state measurement, which maybe unavailable in practice. In a more convenient way, it is better to only make use of output feedback instead of the full-state feedback. Furthermore, the measurement noise has not been considered in the controller design. One of the future researches may introduce quasi-Kalman filter or observer to suppress system noise. However the observer-based control design expressed in LMIs is still a problem. Although there is disturbance rejection ability for RMPC as observed in landing gear control simulations, the future research work could be focused on developing more robust controller which may work in larger operation range and more complicated operation environment and maybe more powerful with disturbance rejection and noise elimination in terms of LMI realization.

(2) Improvement on real landing gear control application

Although there are some implementation considerations for landing gear shimmy control as in section 4.6, the whole control system design is still in a stage of conceptual

Reproduced with permission of the copyright owner. Further reproduction prohibited without permission.

design. There maybe some unexpected problems from controller design or related control system implementation in the real case, such as the computational load of LMI for real time control and selection of control system actuator or response speed of hydraulic actuator. Despite PRMPC has shown lots of computational time saving compared to two other RMPCs, the computational load of control system and time delay of actuator might cause some real time application problems.

Landing gear vibration includes self-induced oscillations (referred to as shimmy) and brake-induced vibration. Now only nose landing gear with non-braked situation is considered in the present thesis. Integrated control system for all three landing gears (tricycle configuration) and integration with braking control system should have more practical values.

To add external hydraulic actuator is costly and tends to be impractical because of high demand for aircraft's safety and reliability to comply with strict aircraft design and operation regulation. Therefore, incorporating shimmy suppressing system with other current control systems, such as steering control system, directional control (lateral motion control) or Advanced Brake Control System (ABCS) is a suggested implementation way. For example, as mentioned in [1], ABCS aims to help the pilot by coordinating all of the systems related to directional control and by applying corrective action far more quickly than it could have been applied manually.

Reproduced with permission of the copyright owner. Further reproduction prohibited without permission.

References

[1] N. S. Currey, "Aircraft Landing Gear Design: Principles and Practices", AIAA Education Series, 1988.

[2] J. A. Tanner et. al., "Emerging Technologies in Aircraft Landing Gear", Society of Automotive Engineers, Inc., 1997.

[3] L. G. Horta et al, "Modeling and Validation of a Navy A6-Intruder Actively Controlled Landing Gear System", NASA/TP-1999-209124.

[4] J. I. Pritchard et al, "An Overview of Landing Gear Dynamics", NASA/TM-1999-209143/ARL-TR-1976, May 1999.

[5] G. Somieski, "Shimmy Analysis of a simple aircraft nose landing gear model using different mathematical methods", Aerospace Science and Technology, Vol.8, pp.545-555, 1997

[6] W. Kruger et al, "Aircraft Landing Gear Dynamics: Simulation and Control, Vehicle system dynamics", Vol.28 ,pp.119-158, 1997

[7] J. T. Gordon Jr. et al , "An Asymptotic Method for Predicting Amplitudes of Nonlinear Wheel Shimmy", Journal of Aircraft,Vol.15 No.3,pp.155-159,1978

[8] G. X. Li, "Modeling and analysis of a dual-wheel nose gear: shimmy instability and impact motions", SAE technical paper series, No. 931402, pp129-143, 1993.

[9] J. Baumann, "Aircraft landing gear shimmy", Ph.D. Dissertation, Missouri University, Rolla, USA, 1992.

[10] R. V. DerValk, et. al., "An analysis of a Civil Aircraft Main Gear Shimmy Failure", Vehicle System Dynamics, Vol. 22, PP. 97-121., 1993

Reproduced with permission of the copyright owner. Further reproduction prohibited without permission.

[11] J. X. Zhou, L. Zhang, "Incremental Harmonic Balance Method for Predicting Amplitudes of a Multi-D.O.F. Non-linear Wheel Shimmy System with Combined Coulomb and Quadratic Damping", Journal of Sound and Vibration, Vol. 279, No. 1-2, pp. 403-416, 2005

[12] B. von Schlippe, R. Dietrich, "Shimmying of a Pneumatic wheel", NASA/ TM-1365, pp.125-147, 1954.

[13] W. J. Moreland, "The Story of Shimmy", Journal of Aeronautical Sciences, Vol.21, No.12, pp.793-808, 1954.

[14] H. B. Pacejka, "The Wheel Shimmy Phenomenon", a theoretical and experimental investigation with particular reference to the non-linear problem, Ph.D. Dissertation, Delft University of Technology, Delft, The Netherlands, 1966.

[15] R. L. Collins et al, "Tire Parameters for Landing Gear Shimmy Studies", Journal of Aircraft,Vol.6 No.3, pp.252-2258,1968

[16] L.C. Rogers et al, "Synthesis of Tire Equations for Use in Shimmy and Other Dynamic Studies", Journal of Aircraft,Vol.8 No.9, pp689-697,1971

[17] L. C. Rogers, "Theoretical Tire Equations for Shimmy and other Dynamics Studies", Journal of Aircraft,Vol.9 No.8,pp585-589,1972

[18] J. T. Gordon, "Perturbation Analysis of Nonlinear Wheel Shimmy", Journal of Aircraft, Vol.39 No.2, pp.305-317, 2002.

[19] K. T. Vu, "Advances in Optimal Active Control Techniques for Aerospace System", Ph.D. Dissertation, University of California, Los Angeles, 1989.

Reproduced with permission of the copyright owner. Further reproduction prohibited without permission.

[20] M. Zefran et al, "Stabilization of Systems with Changing Dynamics by means of Switching", Proceedings of the 1998 IEEE International Conference on Robotics& Automation, Leuven, Belgium, pp.1090-1095, May 1998

[21] B. Goodwine, M. Zefran, "Feedback stabilization of a class of unstable non-holonomic systems, Journal of Dynamic Systems", Measurement and Control, Transaction of the ASME, Vol. 124, No.1, pp. 221-230, 2002.

[22] W. Kruger, "Design and Simulation of Semi-active Landing Gears for Transport Aircraft", Mechanics of Structures and Machines, Vol. 30, No. 4, pp. 493–526, 2002

[23] http://en.wikipedia.org/wiki/Conventional_landing_gear

[24] http://www.airliners.net/

[25] J. M. Maciejowski, "Predictive Control :with Constraints", Prentice Hall Press: Great Britain, 2002

[26] E.F Cammacho, C. Bordons, "Model Predictive Control", Springer Press, London; New York , 2004

[27] R. C. Dorf, R. H. Bishop, "Modern Control Systems", Pearson Prentice Hall, Upper Saddle River, NJ , 2005

[28] R.A. Horn, C. R. Johnson, "Matrix Analysis", Cambridge University Press, Cambridge [Cambridgeshire] ; New York , 1985

[29] S. Boyd, L. El Ghaoui, E. Feron, V. Balakrishnan, "Linear Matrix Inequality in systems and Control Theory", SIAM Studies in Applied Mathematics, SIAM press, Philadelphia, PA, 1994

Reproduced with permission of the copyright owner. Further reproduction prohibited without permission.

[30] S. Boyd, L. Vandenberghe, "Convex Optimization", Cambridge University Press, The Edinburgh Building, Cambridge, CB2 2RU, UK 40 West 20th Street; New York, NY 10011-4211, USA, 2004

[31] L. Palladino, G. Duc and R. Pothin, "LPV Control for μ-split braking assistance of a road vehicle", Proceedings of the 44th IEEE Conference on Decision and Control, and the European Control Conference, Seville, Spain, December 12-15, pp.2664-2669,2005

[32] N. Wada, K. Saito and M. Saeki, "Model Predictive Control for Linear Parameter Varying Systems using Parameter Dependent Lyapunov Function", the 47th IEEE International Midwest Symposium on Circuits and Systems, Hiroshima, Japan, 2004

[33] F. A. Cuzzola; J. C. Geromel, M. Morari, "An improved approach for constrained robust model predictive control, Automatica Vol.38 (2002) , pp.1183 – 1189, 2002

[34] M.V. KOTHARE, V. BALAKRISHNAN and M. MORARIS, "Robust Constrained Model Predictive Control using Linear Matrix Inequalities", Automatica Vol. 32, No. 10. pp. 1361-1379, 1996

[35] H. Michalska and D. Q. Mayne, "Robust Receding Horizon Control of Constrained Nonlinear Systems", IEEE Transactions on Automatic Control, Vol. 38. No. 11 , pp.1623-1633,1993

[36] Fen Wu, "LMI-based Robust Model Predictive Control Evaluated on An Industrial CSTR Model " , Proceedings of the 1997 IEEE International Conference on Control Applications Hartford, Hartford, CT October 5-7, pp.609-614,1997

Reproduced with permission of the copyright owner. Further reproduction prohibited without permission.

[37] Y. Lu and Y. Arkun, "A Scheduling Quasi-MinMax MPC for LPV Systems", Proceedings of the American Control Conference, San Diego, California, June 1999

[38] M.C. de Oliveiraa, J. Bernussoub, J.C. Geromel, "A New Discrete-time Robust Stability Condition", Systems & Control Letters Vol. 37, pp.261-265, 1999

[39] B. Kouvaritakis, "Efficient Robust Predictive Control", Proceedings of the American Control Conference, San Diego, California , pp.4283-4287,1999

[40] J.A. Rossiter, "Reducing the Computational Burden in Predictive Control" , The Institution of Electrical Engineers, UK, printed and published by the IEE, Savoy Piace, London WCPR 06L UK., 1999

[41] D. Q. Mayne, J. B. Rawlings et al, "Constrained Model Predictive Control: Stability and Optimality" , Automatica 36 , pp.789-814, 2000

[42] D. C. W. Ramos, P. L.D. Peres, "A Less Conservative LMI Condition for the Robust Stability of Discrete-time Uncertain Systems" , Systems & Control Letters 43 , pp.371-378 ,2001

[43] C. M. Giannelli, E. Mosca, "Min-max Predictive Control Strategies for Input-saturated Polytopic Uncertain Systems" , Automatica 36 , pp.125-133, 2000

[44] F. Wu, "LMI-based Robust Model Predictive Control and its Application to an Industrial CSTR Problem" , Journal of Process Control 11, pp.649-659, 2001

[45] Z. Wan and M. V. Kothare, "Robust Output Feedback Model Predictive Control Using Off-line Linear Matrix Inequalities" , Proceedings of the American Control Conference , Arlington, VA. ,June 25-27, 2001

Reproduced with permission of the copyright owner. Further reproduction prohibited without permission.

[46] J. Daafouza, J. Bernussou, "Parameter Dependent Lyapunov Functions For Fiscrete Time Systems with Time Varying Parametric Uncertainties " , Systems & Control Letters 43 , pp.355–359, 2001

[47] Z. Wan and M. V. Kothare, "Computationally Efficient Scheduled Model Predictive Control for Constrained Nonlinear Systems with Stability Guarantees", Proceedings of the American Control Conference Anchorage, Anchorage, AK., pp.4487-4492, May 8-1 02002

[48] L. Hu, H. SHAO, "An LMI Approach to Robust Model Predictive Sampled-data Control for Linear Uncertain Systems", Proceedings of the American Control Conference Anchorage, Anchorage, AK., pp.628-633, May 8-1 0, 2002

[49] S. Kaneva, B. De Schutterb, M. Verhaegenb, "An Ellipsoid Algorithm for Probabilistic Robust Controller Design", Systems & Control Letters 49, pp.365-375, 2003

[50] Z. Wan, M. V. Kothare, "An Efficient Off-line Formulation of Robust Model Predictive Control using Linear Matrix Inequalities", Automatica 39, pp.837-846, 2003

[51] H. Fukushima, R. R. Bitmead, "Robust Constrained Model Predictive Control using Closed-loop Prediction" , Proceedings of the American Control Conference Denver, Colorado, June 46,2003

[52] Y. Sheng, B. Liu et al, "Robust Model Predictive Control for Constrained Linear Systems Based on Contractive Set and Multi-parameter Linear Programming" , IEEE 0-7803-7952-7/03/, 2003

Reproduced with permission of the copyright owner. Further reproduction prohibited without permission.

[53] B. Ding, P. Yang and H. Sun, S. Li, "Synthesizing On-line Constrained Robust Model Predictive Control Based-on Nominal Performance Cost" , Proceedings of the 5Ih World Congress on Intelligent Control and Automation, Hangzhou, P.R. China, June 15-19, 2004

[54] B. Ding, Y. Xi, S. Li, "A Synthesis Approach of On-line Constrained Robust Model Predictive Control", Automatica 40, 163 – 167, 2004

[55] Z. Wan and M. V. Kothare, "Efficient Scheduled Stabilizing Output Feedback Model Predictive Control for Constrained Nonlinear Systems", IEEE Transactions on Automatic Control, Vol. 49, NO. 7,pp.1172-1177,July 2004

[56] L. Feng, J. Wang et al, "Off-line Formulation of Robust Model Predictive Control based on Several Lyapunov Functions " , 2004 8th International Conference on Control, Automation, Robotics and Vision , Kunming, China, 6-9th December , pp.1705-1710, 2004

[57] D. M. de la Pena, A.Bemporadb and C. Filippi, "Robust Explicit MPC Based on Approximate Multi-parametric Convex Programming " , 43rd IEEE Conference on Decision and Control Atlantis, Bahamas, pp.2491-2496, 2004

[58] R. S . Smith, "Robust Model Predictive Control of Constrained Linear Systems" , Proceeding of the 2004 American Control Conference Boston, pp.245-250, 2004

[59] Xu Cheng and Dong Jia, "Robust Stability Constrained Model Predictive Control" , Proceeding of the 2004 American Control Conference, Boston, pp.1580-1585, June 30-July 2,2004

Reproduced with permission of the copyright owner. Further reproduction prohibited without permission.

[60] H. Fukushima, R. R. Bitmead, "Robust Constrained Predictive Vontrol using Comparison Model" , Automatica 41 , pp.97-106, 2005

[61] S.W. Kaua, Y.S. Liu et al, "A new LMI Condition for Robust Stability of Discrete-time Uncertain Systems", Systems & Control Letters 54, pp.1195-1203, 2005

[62] L. Feng, J. L. Wang and E. K. Poh,, "Computational Complexity Reduction for Robust Model Predictive Control " , 2005 International Conference on Control and Automation (ICCA2005), Budapest, Hungary, pp.522-527, June 27-29, 2005.

[63] Y. I. Lee, M. Cannon, B. Kouvaritakis, "Extended Invariance and Its Use in Model Predictive Control " , Automatica 41 , pp. 2163 – 2169, 2005.

[64] D. R. Ramirez, T. Alamo, E.F. Camacho, D. M. de la Pena, "Min-Max MPC based on a Computationally Efficient Upper Bound of the Worst Case Cost" , Journal of Process Control 16, pp.511–519, 2006.

[65] D.Q. Mayne, S.V. Rakovic, R.Findeisen, F. Allgower,, "Robust Output Feedback Model Predictive Control of Constrained Linear Systems ", Automatica , v 42, NO.7, pp. 1217-1222 , July, 2006.

[66] Richards1and J.P. How, "Robust Variable Horizon Model Predictive Control for Vehicle Maneuvering " , Int. J. Robust Nonlinear Control 16, pp.333–351, 2006

[67] Matlab help files (Version 7.0.1.24704(R14) Service Package 1), The Mathworks, Inc., September 13,2004

[68] http://www.b737.org.uk

Reproduced with permission of the copyright owner. Further reproduction prohibited without permission.

[69] M. Abe, Y. Kano, K. Suzuki, Y. Shibahata, Y. Furukawa, "Side-slip Control to Stabilize Vehicle Lateral Motion by Direct Yaw Moment", JSAE Review 22, pp. 413–41, 2001

[70] H. B. Pacejka , "Tyre and Vehicle Dynamics", Oxford Press, Butterworth-Heinemann, 2002

[71] S.K. Clark et al, "Structural Modeling of Aircraft Tires", Journal of Aircraft,Vol.9 No.2, pp.162-167,1972

[72] http://www.airliners.net

[73] http://www.tc.gc.ca/air/menu.htm

[74] J. Roskam, "Airplane design Part VII", Ottawa, Kansas : Roskam Aviation and Engineering Co., 1989

Reproduced with permission of the copyright owner. Further reproduction prohibited without permission.

Appendix A
Positive Definite Matrix

Definition A-1: The matrix $A \in R^{nxn}$ is a positive definite matrix if

$$x^T Ax > 0 \tag{A-1}$$

for all nonzero vector. $x \in R^n$

Example 1: The matrix $A = \begin{bmatrix} 2 & 1 \\ 1 & 1 \end{bmatrix}$

is a positive definite one since for $\forall x = [\xi_1 \quad \xi_2]^T \in R^2$

$$x^T Ax = [\xi_1 \quad \xi_2] \begin{bmatrix} 2 & 1 \\ 1 & 1 \end{bmatrix} \begin{bmatrix} \xi_1 \\ \xi_2 \end{bmatrix} = [\xi_1 \quad \xi_2] \begin{bmatrix} 2\xi_1 + \xi_2 \\ \xi_1 + \xi_2 \end{bmatrix}$$

$$= 2\xi_1^2 + 2\xi_1\xi_2 + \xi_2^2 = \xi_1^2 + (\xi_1 + \xi_2)^2 > 0$$

Similarly, the matrix $A = \begin{bmatrix} 3 & 2 & 1 \\ 2 & 2 & 1 \\ 1 & 1 & 1 \end{bmatrix}$ is positive definite.

Main characteristics of PDM are collected here. Some are from R.A. Horn et al [28].

(1) A Hermitian (or symmetric) matrix is Positive definite iff all its eigen values are positive.

(2) A complex (or real)matrix is positive definite iff its Hermitian(or symmetric) part has all positive eigen values.

(3) If a matrix is PDM, then all its submatrices obtained by deleting the rows and columns of this matrix with the same numbers are positive definite and all the elements on the leading diagonal of the matrix are positive.

(4) The determinant of a PDM is always positive, so it is always non-singular.

(5) The inverse of a PDM is also a PDM.

(6) The principle minors of PDM are still positive.

(7) A PDM can be decomposed as $A=U^TU$ (Cholesky decomposition), U is an upper triangular matrix.

Reproduced with permission of the copyright owner. Further reproduction prohibited without permission.

Appendix B
Linear Matrix Inequality

A linear matrix inequality or LMI is a matrix inequality of the form

$$F(x) = F_0 + \sum_{i=1}^{l} x_i F_i \geq 0 \qquad \text{(B-1)}$$

where $x_1, x_2 \ldots x_l$, are the variables, $F_i = F^T$ is a symmetric matrix. x_i is scalar variable. and $F(x) > 0$ means that $F(x)$ is Positive Definite. Multiple LMIs $F_1(x) > 0$, $F_2(x) \ldots F_n(x) > 0$ can be expressed as the single

$$\text{diag}\,(F_1(x), F_2(X), \ldots, F_n(x)) > 0 \qquad \text{(B-2)}$$

The importance of LMIs is in that optimization problems of the kind

$$\min_x c^T x \quad \text{Subject to } F(x) > 0 \qquad \text{(B-3)}$$

F is a symmetric matrix that depends affinely on the optimization variable x, and k is a real vector. This is an convex optimization problem and there are very efficient algorithms for solving this problem.

In the control engineering, we often encounter problems in which the variable is matrix, for example, looking for Positive Definite Matrix in robust control(refer to Section 3.5.2 and Appendix D).

According to [34], the LMI-based optimization is most relevant to control problem is that LMI problems are tractable. LMI problems have low computational complexity: from a practical standpoint, there are effective and powerful algorithms that rapidly compute the global optimum, with non-heuristic stopping criteria. Numerical simulation shows that these algorithms solve LMI problems with extreme efficiency. LMI-based optimization is well suited for on-line implementation, which is essential for MPC.

For more details about LMI problem and convex optimization, refer to Boyd et al. (1994) [29] and Boyd et al (2004) [30], respectively.

Reproduced with permission of the copyright owner. Further reproduction prohibited without permission.

Appendix C
Schur Complement

In linear algebra and the theory of matrices, the Schur Complement (named after Issai Schur) is defined as a block of a matrix within the larger matrix. When converting convex quadratic inequalities to LMI, Schur Complement is often used.

Let $Q(x)^T = Q(x)$, $R(x)^T = R(x)$, and $S(x)$ depends affinely on variable x.

Then the LMI

$$\begin{bmatrix} Q(x) & S(x) \\ S(x)^T & R(x) \end{bmatrix} > 0 \qquad \text{(C-1)}$$

(C-1) is equivalent to the matrix inequality:

$$R(x) > 0,\ Q(x) - S(x)^T R(x)^{-1} S(x) > 0 \qquad \text{(C-2)}$$

or equivalently,

$$Q(x) > 0,\ R(x) - S(x)^T Q(x)^{-1} S(x) > 0 \qquad \text{(C-3)}$$

Reproduced with permission of the copyright owner. Further reproduction prohibited without permission.

Appendix D
Two Similar Conditions of
Discrete-time Lyapunov Stability

The linear discrete-time uncertain system defined as (3-5), is copied to here as:

$$x(k+1) = A(k)x(k) + Bu(k) \tag{D-1}$$

where A(k) belongs to a convex polytopic set defined as

$$A = \{A(k) = \sum_{i=1}^{L} \alpha_i A_i, \sum_{i=1}^{L} \alpha_i = 1, \alpha_i > 0\} \tag{D-2}$$

Theorem D1: System (D-1) is robustly stable in the uncertainty domain (D-2) if there exits a matrix $P(k) = P(k)^T > 0$ such that $A(k)^T P(k)A(k) - P(k) < 0$ for all $A(k) \in A$.

Proof:

Because $P(k) = P(k)^T > 0$, so $V(x(k)) = x(k)^T P(k)x(k) > 0$

$$V(x(k+1)) - V(x(k)) = [A(k)x(k)]^T P(k)[A(k)x(k)] - x(k)^T P(k)x(k)$$
$$= x(k)^T [A(k)^T P(k)A(k) - P(k)]x(k)$$

If $A(k)^T P(k)A(k) - P(k) < 0$, then $V(x(k+1)) - V(x(k)) < 0$

According to Lyapunov stability theorem, the system is asymptotically stable.

P is called parameter-dependent Lyapunov matrix.

Theorem D2: System (D-1) is robustly stable in the uncertainty domain (D-2) if there exists a matrix $P(k) = P(k)^T > 0$ and a matrix G such that

$$\text{LMI} \begin{bmatrix} G + G^T - P & [GA]^T \\ GA & P \end{bmatrix} > 0 \quad \text{holds for all } A(k) \in A \ .$$

Proof:

(The index k is ignored hereafter for purpose of simplicity)

From P>0, so $P^{-1} > 0$ and $(P-G)^T P^{-1}(P-G) \geq 0$

$$(P-G)^T P^{-1}(P-G) = (P^T - G^T)P^{-1}(P-G)$$
$$= P - (G + G^T) + G^T P^{-1} G \geq 0$$

Reproduced with permission of the copyright owner. Further reproduction prohibited without permission.

So get first inequality: $G+G^T-P \le G^T P^{-1} G$

From $P - A^T PA > 0$,

$$0 < P - A^T PA = P - GA(G^T P^{-1} G)^{-1}(GA)^T > P - GA(G+G^T - P)^{-1}(GA)^T$$

Using Schur complement, then it is equivalent to LMI $\begin{bmatrix} G+G^T-P & [GA]^T \\ GA & P \end{bmatrix} > 0$.

Note that if $G=G^T=P$, then it is the case of Theorem D1.

Reproduced with permission of the copyright owner. Further reproduction prohibited without permission.

Appendix E
Stability Condition's Comparison

Considering LPV system such as in (3-8) and (3-9), an interesting comparison of stability conditions between CRMPC and PRMPC is made, which will reveal some insightful points. As mentioned in literature, such as in [38] [46] [61], for discrete-time Robust Control, the following two inequalities are equivalent.

A LPV system is stable if following condition is satisfied:

(1)There exists a PDM P, such that

$$A^T PA - P < 0 \tag{E-1}$$

(2)Or : there exists a PDM Q and another matrix G such that

$$\begin{bmatrix} G + G^T - Q & [AG]^T \\ AG & Q \end{bmatrix} > 0 \tag{E-2}$$

The proofs about the above two robust stability conditions are referred in Appendix D.

Remark 1: We can track the following change in LMI parameters and help understand difference between above two stability conditions.

$$AG \xrightarrow{closed-loop} AG + BY \overset{Y=FG}{\rightarrow} AG + BFG \overset{times\ by\ x}{\rightarrow} G(Ax + BFx) \xrightarrow{u=Fx} G(Ax + Bu)$$

which means that after introducing state-feedback $u(k) = F(k)x(k)$, A is changed to A+BF. So if (E-1)**Error! Reference source not found.** holds for uncontrolled system (3-

Reproduced with permission of the copyright owner. Further reproduction prohibited without permission.

8) and (3-9), then following (E-3) certainly holds for controlled close-loop system, which is exactly the left-top sub-matrix of (3-32).

$$\begin{bmatrix} G+G^T-Q & [AG+BY]^T \\ AG+BY & Q \end{bmatrix} > 0 \qquad \text{(E-3)}$$

Remark 2: If $G=G^T=Q$ in (3-32), which is exactly the same as LMI (3-23). In this way, we can say (3-32) stability condition is the extended stability condition of (3-23) and hopefully less conservative than condition (3-23).

Reproduced with permission of the copyright owner. Further reproduction prohibited without permission.

Appendix F

Concept of Convex Set

A linear matrix inequality in canonical form is:

$$F(x) = F_0 + x_1F_1 + ...x_nF_n > 0 \qquad \text{(F-1)}$$

where F(x) is an affine function of the real vector $x=[x_1\ x_2\ \ ...x_n\ \ ]^T$. F0, F1,..., Fn are real symmetric matrices, and x is a vector of decision variables.

The feasible solution set of (F-1) {x | F(x)>0} is a convex set. This is an important property since powerful numerical solution techniques are available for the problems involving convex solution sets, details refer to "Convex optimization" (S. Boyd et al).

Convex set: A set S in a vector space over R is called a convex set if the line segment joining any pair of points of S lies entirely in S.

$$x_1, x_2 \in R, 0 < \alpha < 1, \Rightarrow \alpha x_x + (1-\alpha)x_2 \in R \qquad \text{(F-2)}$$

Examples of convex:

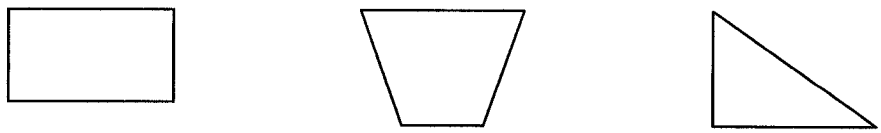

Examples of non-convex:

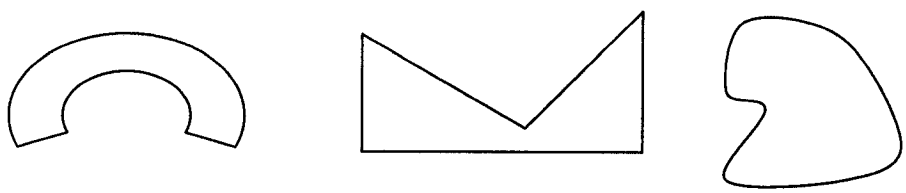

Convex combination: any point x of the form $x = \alpha_1x_1 + \alpha_2x_2 + ...\alpha_nx_n$

$(\alpha_1, \alpha_2, ...\alpha_n > 0, \alpha_1 + \alpha_2 + \alpha_n = 1)$

Convex hull: set of all convex combinations of points in S

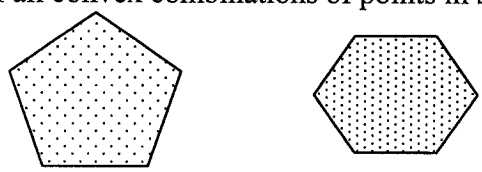

Reproduced with permission of the copyright owner. Further reproduction prohibited without permission.

Appendix G

Landing Gear Terminology

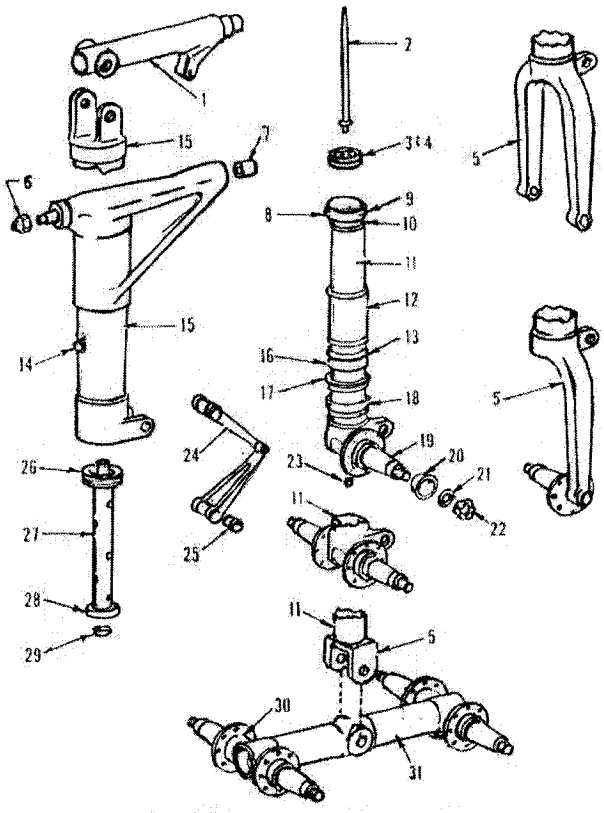

Fig. 4.1 Landing gear terminology.

1) Beam, trunnion
2) Rod, metering
3) Diaphragm, piston
4) Base, metering rod
5) Fork, landing gear
6) Nut, castellated, hexagon
7) Bearing sleeve
8) Bearing sleeve
9) Set screw
10) Valve, snubber
11) Piston, landing gear
12) Stop, piston extension
13) Packing, preformed
14) Adapter, aircraft mooring/towing
15) Cylinder, landing gear
16) Bearing, sleeve
17) Retainer, packing
18) Packing nut
19) Axle, landing gear
20) Spacer, wheel bearing
21) Washer, key
22) Nut, slotted, hexagon
23) Adapter, aircraft jacking point
24) Torque arm, landing gear
25) Bearing, sleeve or bushing
26) Base, restrictor support tube
27) Tube, support restrictor
28) Adapter, restrictor
29) Restrictor
30) Adapter, axle
31) Beam, axle

Figure G-1 Landing gear Terminology,[1]

Reproduced with permission of the copyright owner. Further reproduction prohibited without permission.